KFKI 2/2008

Z. Hózer
P. Windberg
I. Nagy
L. Matus
N. Vér
M. Kunstár
A. Vimi
M. Horváth
T. Novotny
E. Perez-Feró
A. Pintér
M. Balaskó

CODEX-CT-2 EXPERIMENT: LONG TERM TREATMENT IN HIGH TEMPERATURE HYDROGEN AND WATER QUENCHING OF A FUEL BUNDLE

CENTRAL
RESEARCH
INSTITUTE FOR
PHYSICS

BUDAPEST

CODEX-CT-2 EXPERIMENT: LONG TERM TREATMENT IN HIGH TEMPERATURE HYDROGEN AND WATER QUENCHING OF A FUEL BUNDLE

Z. Hózer, P. Windberg, I. Nagy, L. Matus, N. Vér,
M. Kunstár, A. Vimi, M. Horváth, T. Novotny, E.Perez-Feró, A. Pintér, M. Balaskó
Hungarian Academy of Sciences
KFKI Atomic Energy Research Institute
H-1525 Budapest, P.O.Box.49, Hungary

Abstract

Z. Hózer, P. Windberg, I. Nagy, L. Matus, N. Vér, M. Kunstár, A. Vimi, M. Horváth, T. Novotny, E.Perez-Feró, A. Pintér, M. Balaskó: CODEX-CT-2 EXPERIMENT: LONG TERM TREATMENT IN HIGH TEMPERATURE HYDROGEN AND WATER QUENCHING OF A FUEL BUNDLE

The simulation of the Paks-2 incident was carried out in the frame of an experimental programme in the CODEX facility with electrically heated fuel rod bundles. The main boundary conditions for the CODEX-CT-2 were similar to the previous CODEX-CT-1 test. The most significant difference between the two tests was the operation of the air let down valve that was open in the first test and closed in the second one. In the second test the hydrogen produced in the Zr-steam reaction could not escape from the test section and it prevented the access of steam to the Zr surfaces and caused much less oxidation than was observed in the first tests. The final quench by water led to temperature excursion in the bundle and in the shroud. The final state of the bundle was very brittle, the fuel rods and the shroud were cracked and fragmented.

Kivonat

Hózer Z., Windberg P., Nagy I., Matus L., Vér N., Kunstár M., Vimi A., Horváth M., Novotny T.,E.Perez-Feró E., Pintér A., Balaskó M.: A CODEX-CT-2 KÍSÉRLET: FŰTŐELEMEK HOSSZÚ IDŐTARTAMÚ KEZELÉSE MAGAS HŐMÉRSÉKLETŰ HIDROGÉNBEN ÉS VIZES ELÁRASZTÁSA

A Paks-2 üzemzavar szimulációjára a CODEX kísérleti program keretében elektromosan fűtött fűtőelem kötegekkel került sor. A CODEX-CT-2 mérés határfeltételei hasonlóak voltak a CODEX-CT-1 méréshez. A legfontosabb különbség a két mérés között az volt, hogy az első esetben a légtelenítő szelep nyitva volt, míg a második kísérletben be volt zárva. A második mérésben a Zr-vízgőz reakció során keletkező hidrogén nem tudta elhagyni a mérőszakaszt és így gátolta a vízgőz és a cirkónium felületek érintkezését, ami sokkal kisebb mértékű oxidációt eredményezett, mint amit az első mérésben lehetett tapasztalni. A mérés végén alkalmazott vizes elárasztás során hőmérséklet megszaladás lépett fel mind a kötegben, mind a kazettafalon. A köteg a mérés után nagyon rideg állapotban volt, a fűtőelemek és a kazettafal repedezett volt és széttöredezett.

Contents

List of tables

List of figures

1. INTRODUCTION

The cleaning tank incident at the unit 2 of Paks NPP on 10th April 2003 resulted in severe fuel damage of 30 assemblies. The fuel rods heated up due to insufficient cooling. The zirconium components suffered heavy oxidation. The final quenching of the assemblies led to fragmentation of brittle zirconium components. Due to the poor instrumentation there were many open questions concerning the course of the incident and the behaviour of fuel assemblies. In 2004 a new experimental programme was launched with the following objectives:

- Better understanding of the phenomena that took place during the Paks-2 incident.
- Improving knowledge on the behaviour of NPP fuel under accident conditions.
- Supporting model development, paying special attention to the effect of hydrogen uptake on cladding embrittlement.

The test programme included small scale tests (the COHYRA programme [1]) and large scale tests with electrically heated 7-rod bundles in the CODEX facility. The results of the first test (CODEX-CT-1) indicated that the release of hydrogen from the cleaning tank led to further oxidation of the bundle. However there was no reliable information on the operation of the air let down (gas off) valve in the cleaning tank. For this reason in the second bundle test (CODEX-CT-2) the produced hydrogen was not released from the cleaning tank model. The results of the CODEX-CT-2 test are summarised in the present report.

2. THE CODEX FACILITY

The CODEX (COre Degradation EXperiment) facility was originally built for severe accident studies. Several experiments have been carried out with VVER and PWR bundles. Behaviour of fuel rods in high temperature steam, quenching at high temperature, phenomena related to air ingress scenarios and the role of control rods were addressed in the earlier tests [2,3].

In the CODEX-CT (Cleaning Test) test series the original arrangements have been significantly changed. It was a basic requirement to the facility to withstand high temperature conditions for several hours. Due to the small size of the facility it was clear that only part of the cleaning tank can be simulated. Since the thermal hydraulic events were well understood from numerical analysis, the main purpose of the CODEX-CT tests was the simulation of fuel behaviour during the Paks-2 incident. The main conditions of the incident had to be reproduced in the facility and the full scenario of the Paks-2 incident was simulated. It was a great challenge to reach ≈1200-1300 °C in the facility, while the bottom of the bundle was cooled by water.

	Paks-2 cleaning tank	CODEX-CT facility
Number of fuel rods	3870	7
Total flow rate	21 t/h	106 l/h
Total volume of coolant	6 m^3	9.2 l
Volume of steam	4 m^3	6 l
Total surface of Zr	300 m^2	0.44 m^2
Ratio of total Zr surface/total volume	50 m^{-1}	48 m^{-1}
Total power	241 kW	2.3 kW

Table 1. Main parameters of the Paks cleaning tank and the CODEX-CT facility

In the design of the facility the ratio of Zr surface to the total volume was kept as a main parameter providing the similarity for fuel oxidation process (see Table 1). The relative power of the facility was much more than the decay heat of the original assemblies, since the heat losses are much higher in the case of a small scale facility.

The facility was equipped with extensive instrumentation including the measurement of temperatures, flowrates, pressures and power. Two special devices were applied for the monitoring of hydrogen: one measured the concentration in the cleaning tank, while the other recorded the integral volume of release hydrogen from the system. The scheme and the main components of the CODEX-CT facility are shown in Fig. 1. The main parameters of the Paks-2 cleaning tank and of the CODEX-CT facility are compared in Table 1.

There were no internal heaters applied inside of the fuel rods in the reconstructed facility. External heaters were used to reach high temperature in the test section. The fuel bundle was longer than in the previous tests and several technological systems were connected to the test section.

The test section with the electrically heated VVER type bundle represented the cleaning tank. Inlet and outlet junction were connected to the bottom section and perforation were used to facilitate the formation of by-pass flow. The external heater rods surrounded the bundle.

The spent fuel storage pool was simulated with an expansion tank with internal pressurisation that was connected to the test section. Special condenser unit was applied to receive coolant from the test section during the quenching phase.

2.1. FUEL ASSEMBLY

In the CODEX-CT experiment the fuel rods were filled with alumina pellets and pressurised inside. The bundle included seven rods and it was covered by hexagonal shroud made of Zr2.5%Nb alloy. Original E110 (Zr1%Nb) type VVER cladding material was used in the fuel rods. The spacer grids were manufactured from E110 (Zr1%Nb) alloy as well. The fuel rods were arranged on a hexagonal lattice with the typical parameters of the VVER-440 bundle. The main parameters of the bundle are summarised in Table 2 and the scheme and the cross-section of the bundle are shown in Figures 2 and 3.

Number of fuel rods in the bundle	7
Cladding material	Zr1%Nb
Length of fuel rods	1000 mm
External cladding diameter	9.1 mm
Internal cladding diameter	7.8 mm
Material of pellets	Al_2O_3
External diameter of pellets	7.7 mm
Diameter of internal hole in the pellets	3 mm
Height of pellets	10 mm
Number of spacer grids	5
Material of spacer grids	Zr1%Nb
Height of spacer grids	10 mm
Thickness of spacer grids	0.4 mm
Pitch size	12.2 mm
Material of shroud	Zr2.5%Nb
Thickness of shroud	2 mm
Material of header	SS

Table 2. Main characteristics of fuel rod bundle

The original UO_2 pellets were replaced by Al_2O_3 pellets in the tests, for the interaction between UO_2 and other core materials was not foreseen in the planned temperature range. Similarly to VVER-440 type pellets the Al_2O_3 pellets had internal holes, which were used for the thermocouples in the tests.

The internal pressurisation of the fuel rods was important feature in these experiments, since ballooning and burst played important role in the degradation of fuel bundle. The fuel rods were pressurised individually and this solution made possible the pressurisation of each rods to different initial value. The fuel rods were filled up by argon and were closed in cold state of the bundle.

The upper part of the bundle included a small stainless steel header that simulated the top nozzle of the fuel assembly.

The fuel bundle had perforations on each side of the hexagonal shroud at elevation 15 mm. The diameter of perforations was 6 mm, their total number was 6. It made possible the bypass flow from the bundle similarly to the original assembly design.

2.2. HEATERS

There were no internal heaters applied inside of the fuel rods, but external heaters were used. It made possible the establishment of a more uniform temperature distribution along the fuel rods that characterises the long term radiation heat transfer conditions. Furthermore the internal heaters could have stabilised the structure of the fuel rods and so could have prevented fragmentation of fuel rods.

Twelve heaters were placed around the bundle. Their active length was 1 m. The heater wire was made of 3 mm diameter Kanthal APM material. It was covered by stainless steel cladding. There was Al_2O_3 insulation between the central wire and the cladding. The heater wires and the cladding were parallel connected. A special flange was used for the connection to the electric supply system, which could provide ≈3 kW maximum power in the facility.

The heaters were welded into the bottom plate of the test section. The other ends of the heaters were not fixed. This solution eliminated the formation of a stresses associated with the thermal expansion of the heaters. The schematic view of the heaters and a picture of the flange are shown in Fig. 4 and the main parameters are summarised in Table 3.

Number of heaters	12
Length of heaters	1000 mm
Cladding material	stainless steel
External/internal diameter of cladding	10 mm / 8 mm
Material of heater wire	Kanthal APM
Diameter of heater wire	3 mm
Material of insulation	Al_2O_3
External/internal diameter of insulation	8 mm / 3 mm
Max. total power of all heaters	3 kW
Voltage	0-10 V
Current	0-300A
Electrical resistance at 20 °C	17.08 mOhm
Electrical resistance at 1300 °C	17.76 mOhm

Table 3. Main characteristics of heaters

2.3. CLEANING TANK MODEL

In the cleaning tank the coolant entered the fuel assemblies from the bottom, flowed up inside of the VVER-440 type assemblies that are covered by shroud and turned back in the upper plenum. Then flowed down between the assemblies and left the volume through a junction that was placed just above the bottom plate. This flow path was simulated in the CODEX-CT facility with the help of a stainless steel tube around the fuel bundle and heaters (Fig. 5). The water flowed up inside of the tube, turned back at the top of the tube and flowed down to the outlet junction in the annular space between this tube and the wall of the test section.

There were six perforations with 6.4 mm diameter on the tube at the elevation of 25 mm. The bypass flow was established through these perforations in the test. There were six perforations with 6 mm diameter on the shroud at 15 mm elevation.

There were two possibilities for the formation of bypass flows in the cleaning tank:

a) Through the perforations of the shroud. This flow was simulated with the holes in the shroud of the bundle.
b) Through the gap between fuel assembly bottom nozzle and the bottom plate of the cleaning tank due to the imperfect seating of the assemblies. In the tests this path was simulated so that part of the coolant was injected directly outside of the bundle and flowed out through the perforations of the steel tube.

The coolant in the cleaning tank was circulated with the help of a pump. The coolant was injected into the lower chamber of the cleaning tank model. The bottom plate of the test section had several perforations. There were 12 perforations inside of the assembly shroud with 5 mm diameter. 12 perforations with 5 mm diameter were between the heaters and the shroud. The plate had 12 perforations with 7 mm diameter between the heaters and the steel tube.

The cleaning tank model with the bundle was connected to another vessel that simulated the water volume of the spent fuel storage pool. The outlet junction of the cleaning tank model was located at 15 mm elevation (Fig. 6). The zero level corresponded to the elevation of the bottom plate in the test section.

The temperature of the inlet flow was maintained using a heat exchanger that was cooled on the secondary side by tap water. There was an air let-down valve located on the top of the tank that made possible the release of gas-steam mixture from the tank.

2.4. EXPANSION TANK

In the Paks incident the cleaning tank was surrounded by the water of the spent fuel storage pool and the water of the pool was circulated in an open loop through the tank. In the CODEX-CT tests the spent fuel pool was simulated with a special expansion tank. The volume of the tank was 28.9 l, the internal diameter of the cylindrical vessel was 320 mm (Fig. 7).

The expansion tank was pressurised inside by argon and the internal pressure was established so that it was close to the hydrostatic pressure of a ≈13 m high water column. The expansion tank was equipped with relief cock and safety valve as well. The pressure in the facility was regulated through this gas system.

The expansion tank was connected to the outlet junction of the cleaning tank model through a tube. This connection line was open during the tests and made possible the transfer of water from the cleaning tank to the expansion tank. In the quench phase of the tests this line provided water injection to the bottom of the tank. Another line was connected to the top of the cleaning tank model. During the tests it was closed by a valve that was opened only in the quench phase for the injection of water to the top of the bundle.

2.5. CONDENSER TANK

The elements of the CODEX-CT facility accumulated about ≈8 MJ energy during the long time experiments. Since the final phase of the tests included water quench of this system, it was necessary to take care of the released steam. For this reason a 100 l volume condenser tank was connected to the cleaning tank model (Fig. 8). It contained ≈20 ^{o}C water and it was connected to the top of the cleaning tank model (Fig. 1). The tank was made from Plexiglas. The water in condenser warmed up to ≈60 ^{o}C during the tests.

When the quench phase started this connection was opened and the steam-hydrogen mixture was released through a ceramic filter into the condenser tank. The non-condensable gas (hydrogen) from the mixture was collected in a 40 l gas tank. The volume of the released hydrogen through the condenser tank was determined using the pressure measurements of this gas tank.

2.6. INSTRUMENTATION

In order to understand the main processes in the tests extensive instrumentation was applied in the CODEX-CT tests. Large part of the preparatory work was devoted to connections of instrumentation, their calibration and testing. The temperature, pressure, water level, flowrate and electric power measurement are described here (Tables 4, 5 and 6), while the hydrogen measurements are summarised in the next two chapters.

Temperature measurements were taken at the following places:

- in each fuel rod at two different elevations,
- on the shroud at two different positions,
- on the heaters at one position,
- in the gap between the steel tube and the vessel wall of the cleaning tank model in five positions,
- inlet and outlet of the coolant,
- pyrometer was positioned on the top of the cleaning tank and indicated the temperature at the top of the bundle.

Temperature measurement	Thermocouple type	Placement	Position (mm)
TFR136	K	Rod No. 1	360
TFR183	R	Rod No. 1	830
TFR229	K	Rod No. 2	290
TFR276	R	Rod No. 2	760
TFR322	K	Rod No. 3	220
TFR355	R	Rod No. 3	550
TFR415	K	Rod No. 4	150
TFR462	R	Rod No. 4	620
TFR536	K	Rod No. 5	365
TFR583	R	Rod No. 5	825
TFR643	K	Rod No. 6	430
TFR690	R	Rod No. 6	900
TFR755	R	Rod No. 7	550
TSH8	K	Shroud	80
TSH27	K	Shroud	270
TSH70	R	Shroud	700
TSH75	R	Shroud	750
THR75	R	Heater	750
TG5	K	Gap	50
TG27	K	Gap	270
TG74	K	Gap	740
TG97	K	Gap	970
TCIN	K	Inlet	
TCOUT	K	Outlet	
TXT	K	Expansion tank	

Table 4. Temperature measurements

Pressure was measured at the following places:

- in each fuel rod,
- in the expansion tank.

Water level was measured as pressure difference for the following levels:

- expansion tank,
- cleaning tank model (test section with fuel bundle).

Electric power was measured with a power meter connected to the transformer unit.

There was a video camera connected to the top of the cleaning tank model. It provided useful visual information on the heat up of the bundle during the experiments.

Thermocouple type	K	R
material	Ni-CrNi	Pt-Pt13%Rh (R)
insulation	MgO	MgO
sheath material	Inconell	Inconell 600
external diameter (mm)	0.8	1.6

Table 5. Thermocouple characteristics

Parameter	Device	Placement	Comment
system pressure	pressure transducer	expansion tank	0-6 bar (ABS) 4-20 mA
test section level	DP transducer	test section	0-75 mbar 4-20 mA
quench tank level	DP transducer	quench tank	0-75 mbar 4-20 mA
coolant flowrate	calibrated flowmeter	coolant inlet junction	resolution: 1 imp./ 1 liter
fuel rod pressure	pressure transducer	fuel rods	0-100 bar (ABS) 4-20 mA
hydrogen flowrate	gas measuring system with "U"-pipe	expansion tank junction	charging volume: ≈0,8 liter / 1cycle
hydrogen concentration	system with TCD	gas off junction	
power	choppered transformator		output: 0-3000 W
	video camera	test section vessel	

Table 6. Measurement of system parameters

2.7. HYDROGEN FLOWRATE MEASUREMENT

The hydrogen production was a key factor in the Paks incident and for this reason two independent systems were applied in the CODEX-CT tests to collect data on hydrogen production and release from the tank. The hydrogen produced during the oxidation of Zr in high temperature steam accumulated in the upper volume of the cleaning tank.

In the CODEX-CT-1 test the operation of the air letdown valve was simulated and part of the produced hydrogen was released from the tank. The flowrate of release was manually regulated so that the system pressure remained constant. The released hydrogen-steam mixture first entered a condenser unit, where the steam was condensed. The remaining non-condensable gas (only hydrogen) was collected in a large U tube. Initially the U tube was filled with water. The hydrogen was injected into one leg of the U tube and the water level in the other leg moved up. The accumulated gas was released when its volume reached 0.8 l. It took place before the water level reached the bottom of the U tube. After the release the hydrogen accumulation started again in one leg of the tube in the next cycle. During the most intense period of the test the U tube was opened almost every minute (Fig. 9). The volume of released hydrogen was calculated using the number of cycles and the water level in the U tube.

In the CODEX-CT-2 test the U tube system was connected to the expansion tank. It was intended to keep the system pressure constant in the facility with the help of this device. Hydrogen could be evacuated through this system if the pressure would have reached high value and some gas would have passed from the test section to the expansion tank. In the CODEX-CT-2 such conditions did not take place and so there was no hydrogen release during the oxidation phase of the experiment.

2.8. HYDROGEN CONCENTRATION MEASUREMENT

The concentration of hydrogen gas in steam was a substantial factor during the processes; it reflected the extent of zirconium-steam reaction, the amount of formed and released hydrogen during the pressure reduction, moreover it was necessary for assessment of the rate of steam-zirconium reaction and for the embrittlement of cladding. Thermal conductivity method was used for the measurements.

Pressure in the cleaning tank was 2.6 bar at CODEX-CT-1 and 2.0 bar at CT-2 test. Steam-hydrogen mixture containing 0-100 % v/v H_2 was expected, the detector facility was planned to work in this range. Because only steam and hydrogen were in the gas phase to be investigated thermal conductivity detectors (TCD) of gas chromatographs seemed to be satisfactory as basic sensors. The scheme of analyser unit can be seen in Fig. 10. At CODEX-CT-2 experiment an additional TCD unit was applied to measure the H_2 concentration at 760 mm elevation between the shroud and the heater rods (TCD2). The other TCD unit (TCD1) was placed above the bundle similarly to the CODEX-CT-1 test.

Our previous experiences with the same detectors proved, that an argon stream with $\approx$1 cm^3/sec with about 20-30 vol% hydrogen added to this stream is a range, where good reproducible results can be achieved after a proper calibration. The intensity of gas stream from the bundle has to be adjusted to this concentration range.

The TCD detectors had pure argon streams on the reference sides and those were added to the steam-hydrogen mixtures coming from the bundle area. The measuring sides of TCDs had argon or argon-hydrogen mixtures flow with constant water vapour content (saturated at 0^oC), determined by ice-water bath. This solution had some advantages: at deep cooling the vessels should be tightened by ice, absorbers would need to large volume and the

time resolution would be poor. The present solution resulted in a time resolution not more than some seconds.

The TCDs were attached into Wheatstone bridges. The data collection was performed by computer equipped with analogous-digital converter. TCDs signals, time, temperatures of TCDs, temperature of capillary tubes were also registered. TCD temperatures were adjusted to about 140 ^{o}C to avoid water condensation and reduce the amount of adsorbed water. Calibration of TCDs were performed by argon-H_2 mixtures modelling exactly the conditions at the experiments.

As inlet device between the bundle and TCDs capillary tubes have been used and they determined the flow rate of steam-hydrogen mixtures coming from the bundle. It has the advantage of a well reproducible flow compared to that of needle valves. Capillaries were 8.5 m long stainless steel tubes originally intended to be liquid chromatograph columns. Their inner diameters were 0.236 mm. These tubes were also heated to 140 ^{o}C for avoiding steam condensation. The streaming intensity of gas in capillary tube has been calculated by the Poiseuille's law.

$$p_1^2 - p_2^2 = \frac{16 \cdot \eta \cdot G}{r^4 \cdot \pi} \cdot \frac{k \cdot T}{m} \cdot l \qquad (1)$$

or

$$p_1^2 - p_{21}^2 = \frac{16 \cdot \eta}{r^4 \cdot \pi} \cdot \frac{V}{T_F} \cdot \frac{273.16}{22410} \cdot R \cdot T \cdot l$$

where
G mass of gas streamed through during time unit,
p_1 and p_2; pressure at inlet and outlet of capillary, respectively,
η dynamic viscosity,
k Boltzmann constant,
T temperature of capillary in K,
T_F temperature of gas measuring unit in K,
R gas constant,
l length of capillary tube,
r inner radius of capillary,
m mass of gas atoms,
V gas streaming rate measured at temperature T_F.

This formula has been used for determination of capillaries' length, both for the diluting argon and argon-hydrogen mixtures coming from the bundle. Calibrations of TCDs were performed with argon-hydrogen mixtures. On TCDs reference sides pure dry argon was applied at the calibrations as well. Like at real experiments hydrogen was mixed in between the reference and measuring side and also saturated with water vapour at 0 ^{o}C. Streaming of argon was constant (1 cm^3/s) and the hydrogen was added at different rate. The results of calibrations can be seen in Fig. 11. In the figure equations are presented to calculate hydrogen concentrations in gas streaming through the TCDs measuring cells from the voltage signals of Wheatstone bridges. The formulas resulted from fitting for

CODEX-CT-1

$C(H_2\ v/v\%)=0.287\cdot V_{TCD}(mV) - 3.098\cdot 10^{-4}\cdot [V_{TCD}(mV)]^2 + 7.86\cdot 10^{-5}[V_{TCD}(mV)]^3$

CODEX-CT-2 TCD1

$C_1(H_2\ v/v\%)=0.4244\cdot V_{TCD1}(mV)$

CODEX-CT-2 TCD2

$C_2(H_2\ v/v\%)=0.0742\cdot V_{TCD2}(mV)+0.00107\cdot [V_{TCD2}(mV)]^2$ (2)

where $V_{TCDx}(mV)$ is the TCDx bridge signal in mV at our experimental arrangement.

The evaluation of results demanded the flow intensity of hydrogen component leaving the capillary tube. It is

$$\frac{dV_{H_2}}{dt} = \frac{dV_{Ar}}{dt} \cdot \frac{c_{H_2}}{1 - c_{H_2}} \qquad (3)$$

where

$\frac{dV_{H_2}}{dt}$ the intensity of hydrogen flow from the capillary,

$\frac{dV_{Ar}}{dt}$ intensity of argon flow in the reference side and mixing,

c_{H_2} hydrogen concentration from TCD signal.

To estimate the hydrogen concentration in bundle area hydrogen component from capillary was compared with the total amount of gas streaming through the capillary. The later was calculated by using equation (1) and the appropriate parameters as follows:

P_1	pressure in bundle;	2.6	bar (CT-1)
		2.0	bar (CT-2)
P_2	outer pressure;	1.0	bar
r	inner radius of capillary,	0.118	mm
l	length of capillary	8.5	m
T	temperature of capillary	400	K
η	dynamic viscosity of gas	$13.5\cdot 10^{-6}$	Pa·s
T_F	ambient temperature.	300	K

The viscosity of steam - hydrogen mixture had been calculated according to the method published by C.R.Wilke [4]. Results are plotted in Fig. 12. The original method of calculation would be too complicated for evaluation of results with some thousands of values, therefore a polynomial formula had been fitted for the values calculated according to Wilke method. It resulted for the dynamic viscosity

$$\eta = 13.385 - 1.4668 \cdot c(H_2) + 9.4329 \cdot c(H_2)^2 - 10.321 \cdot c(H_2)^3$$

The capillary temperature was 400 K, on large part of its 8.5 m length. Up to about 70 % v/v H_2 component the η is constant with an error not larger than accuracy of other parameters and TCD measurements.

As was mentioned earlier the concentration of hydrogen in the bundle can be achieved by comparing of escaping hydrogen and the total escaping gas volume rate. Because of the total escaping gas volume rate leaving the bundle is depending on hydrogen concentration and pressure at the evaluation can be made only by iterative calculation method. According to our experience the evaluation of every single measured point needed up to 0.1 v/v% accuracy was achieved after 10-21 iteration steps.

3. THE CODEX EXPERIMENTAL PROGRAMME

In AEKI an experimental programme was initiated focusing on the high temperature behaviour of VVER fuel and core materials. The interactions of Zr1%Nb cladding with UO_2 pellet, stainless steel spacer and boron steel absorber were studied in small scale separate effect tests [5]. On the basis of the experience gained in these tests the CODEX integral test facility was constructed to continue this work under more prototypic conditions.

First the capabilities of the facility were demonstrated carrying out the CODEX-1 experiment with Al_2O_3 pellets. The test section was heated up with argon, and then the electric power was increased. When bundle degradation was indicated by temperature measurements, the power was switched off and the section was cooled down by argon. The post-test examination showed that the bundle partially damaged, the further melting was stopped in due time. So the facility proved to be applicable to the experimental modelling of controlled core degradation processes.

In the second experiment similar procedures were taken, but the Al_2O_3 pellets were replaced with UO_2 [2]. The CODEX-3/1 and CODEX-3/2 experiments were performed with fast water cooling [2]. Air ingress conditions were simulated in the AIT-1 and AIT-2 tests with PWR fuel rods [3,6,7]. The B4C test was devoted to the examination of control rod degradation and gas production during a severe reactor accident [2]. The main parameters of the test matrix are given in Table 7.

After significant reconstruction of the CODEX facility special tests have been carried out with the main conditions of the Paks-2 cleaning tank incident. First a preliminary test was carried out with empty cladding tubes and sheets of assembly shroud. The CODEX-CT-1 test was performed with 1 m long seven-rod bundle and simulated the whole scenario of the incident. The CODEX-CT-2 test simulated the Paks-2 incident, too. In this test the produced hydrogen was not released from the cleaning tank.

Test	Bundle type	Pellet	Year	Test type
CODEX-1	7-rod VVER	Al_2O_3	1995	scoping test
CODEX-2	7-rod VVER	UO_2	1995	escalation and slow cooling down
CODEX-3/1	7-rod VVER	UO_2	1996	water quench at 1150 ^oC
CODEX-3/2	7-rod VVER	UO_2	1997	water quench at 1500 ^oC
CODEX-AIT-1	9-rod PWR	UO_2	1998	air ingress
CODEX-AIT-2	9-rod PWR	UO_2	1999	steam oxidation and air ingress
CODEX-B4C	7-rod VVER	UO_2,B_4C	2001	control rod degradation
CODEX-CT-1	7-rod VVER	Al_2O_3	2006	long term oxidation and quench
CODEX-CT-2	7-rod VVER	Al_2O_3	2006	treatment in hydrogen and quench

Table 7. Main parameters of CODEX test matrix

4. THE CODEX-CT-2 EXPERIMENT

In order to simulate the Paks-2 incident special conditions were applied in the CODEX facility. The pressurised fuel bundle included seven rods with pellets inside surrounded by E110 cladding tubes. The CODEX-CT-2 experiment was carried out on the 18th December 2006.

The test started with several technological actions. The test section was filled with water and the initial water level was established in the expansion tank. The cleaning tank model and the expansion tank were connected through the outlet junction of the cleaning tank located at 15 mm above the bottom plate by opening the valve. The upper connection between the top of cleaning tank and the expansion tank was closed. Water circulation with ≈70 g/s flowrate was established. The electrical power of the heaters was set to 2.6 kW. The fuel rods were pressurised in the beginning of the test to different values between 5 and 11 bars in cold state. Under these conditions most of the power of the heaters was removed by the coolant. The main temperature in the room was 21 ºC.

The CODEX-CT-2 experiment was performed in three main phases:

0-2700 s – formation of steam volume

- During the first phase of the test water was evaporated from the upper part of the cleaning tank model and a water level was established at the elevation of by-pass. The water level in the test section dropped from the original 110 cm to 10 cm between 2410-2700 s (Fig. 46). In the same time the water released from the cleaning tank model resulted in the increase of coolant level in the expansion tank (Fig. 47).
- The flowrate was reduced from ≈70 g/s to ≈40 g/s by the regulating valve after 1380 s (Fig. 48).
- The secondary side heat exchanger was put into operation at 2220 s.
- The decrease of coolant flowrate led to heat up of the water and formation of steam volume as a result of by-pass flow (Figures 13-33).

2700-27720 s – high temperature treatment in hydrogen

- The low water level was kept for seven hours with low coolant flow and constant electric power (Figures 46 and 52). The temperatures monotonously increased and the maximum temperature reached 1234 ºC (Fig. 24). Figures 13-24 show fuel rod temperatures in the seven rods at different elevations. The hottest part of the rods was in the central-upper section at about 700 mm elevation. The bottom part of the rods was cooled by water and the temperatures remained low in that section (Fig. 25).
- The heat-up of the bundle led to oxidation of Zr components. The hydrogen content in the atmosphere started to increase after 5300 s and it indicated the beginning of the oxidation process (Figures 50 and 51) .
- Some blockage of coolant flow was observed at 7200 s and it was avoided with manipulating the valve position (Fig. 48).
- Three out of the seven rods lost their integrity due to burst between 800-900 ^{o}C. (Rod No. 3 at 9115 s, rods no. 4 and 7 at 9330 s). The pressure increase reached a maximum during the test and before burst their value slightly decreased (Figures 40, 41 and 44). It

was a result of plastic deformation that increased the internal gas volume and had larger effect on the pressure change, than the temperature increase.

- Rod No. 1 was leaking and did not burst (Fig. 38).
- Rod no. 2 failed at 14300 s probably due to crack formation in the brittle cladding (Fig. 39).
- Rod no. 5 was leaking, its pressure stabilised at 6 bars after 10000 s and the rod failed only during quench (Fig. 42).
- Rod no. 6 failed at 23350 probably due to crack formation in the brittle cladding (Fig. 43).
- The hydrogen produced in the oxidation process was not released from the test section (fig. 49). The accumulation of hydrogen in the tank did not lead to pressure increase (Fig. 45).
- The pressure slowly decreased in the system and was increased from 1.91 bar to 2.1 bar by adding argon into the expansion tank at 16140 s (Fig. 45).
- The coolant flowrate was slightly increased at 27420 s (Fig. 48).
- The maximum fuel rod temperature reached 1286 ºC before quench (Fig. 24).

27720-29090 s – water quench

- Finally the bundle was quenched from the bottom and the top simulating the opening of the cover of cleaning tank. The quench process included several technological steps:
  - The connecting line between the cleaning tank model and the expansion tank was closed at 27696 s.
  - The pressure in the expansion tank was increased to 4 bars, for it was intended to carry out faster quench than in the previous test (Fig. 45).
  - The connecting tube between the cleaning tank model and the condenser tank was open at 27960 s and the blowdown process was initiated (Figures 46 and 47).
  - The lower connection between the expansion tank and the cleaning tank model were open at 28008 s.
  - Electrical power was switched off at 28009 s (Fig. 52).
  - The upper connection between the expansion tank and the cleaning tank model were open at 28064 s and it resulted in top flooding of the bundle.
- Quenching of the hot surfaces of the fuel bundle resulted in temperature excursion in some positions of the bundle and of the shroud (Figs. 14, 20 and 27).
- The release of steam + hydrogen mixture led to pressure decrease in the system, but the evaporation of injected water on the hot surfaces of the fuel rods produced a second pressure peak that was above 4 bars (Fig. 45). This peak was followed by fast pressure decrease that took place parallel to temperature increase in the bundle.
- The cool down of the facility took relatively long time because of the large thermal inertia of the structural materials and insulation. (Temperature of the external surface of the thermal insulation layers increased up to 250 °C, see Table 9.)
- The water level in the condenser tank increased by 135 mm. The volume of the collected gas (hydrogen) in the tank was 80 l. The temperature of the condenser tank increased from 20 to 31 °C.

The main events and actions of the CODEX-CT-2 test are summarised in Table 8.

Time (s)	Event
0	Initial conditions established (2600 W power, 70 g/s flowrate)
1380	Flowrate reduction to 40 g/s
2220	Secondary side heat exchanger in operation
2410	Start of water level decrease
2700	Low water level established
5300	Beginning of Zr oxidation (indicated by hydrogen measurement)
7200	Temporary blockage of coolant flow path
9115	Burst of fuel rod No. 3
9330	Burst of fuel rod No. 4
9330	Burst of fuel rod No. 7
14300	Burst of fuel rod No. 2
16140	System pressure increased to 2.01 bar
23350	Burst of fuel rod No. 6
27720	1286 ºC temperature reached
27696	Connection line between test section and expansion tank closed
27700	Pressure in expansion tank increased to 4 bar
27960	Opening of gas release to condenser tank
28008	Beginning of quench from the bottom
28009	Power switched off
28064	Start of quench from the top
28085	1384 ºC temperature reached
29094	End of test

Table 8. Main events and actions of the CODEX-CT-2 test

Time (s)	Inlet temp. (ºC)	Outlet temp. (ºC)	Temperature on the thermal insulation (ºC)				
			bottom		center		top
7200	63	66	25	27	31	35	32
9000	35	38	27	32	38	46	35
10800	33	37	31	39	52	62	41
12780	36	40	33	53	76	93	51
14400	39	43	35	62	95	125	61
16260	43	46	38	73	111	145	67
18120	38	41	42	88	132	165	79
20400	39	42	43	94	158	181	103
21960	32	36	44	108	175	228	127
23400	39	43	46	113	191	230	138
25760	42	45	47	120	196	244	146
27000	40	44	50	122	200	253	148

Table 9. Measured temperatures on the external surface of the facility

5. EXPERIMENTAL RESULTS

The CODEX-CT preliminary test, CODEX-CT-1 and CODEX-CT-2 tests well illustrated the probable scenarios of the Paks-2 cleaning tank incident. The main differences between the two tests are summarized in Table 10.

The operation with high flowrate led to stable conditions, since the electrical power and heat removal with the coolant were in balance. The flowrate decrease (simulating the operation of the small pump in the incident) quickly led to the stratification of water in the cleaning tank model and rapid formation of steam volume in the vessel. The water level was established according to the elevation of by-pass holes in the facility. This period was very similar in the CODEX-CT-1 and CT-2 experiments.

The dry period of the CODEX-CT-1 and CT-2 tests lasted about seven hours, like in the incident in 2003. This period was characterized by monotone temperature increase in the dry section of the fuel rods. Plastic deformation of cladding tubes took place and the high pressure rods suffered burst at about 800 ºC. Only one fuel rod survived the period of plastic deformation without burst in the CODEX-CT-1 test. In the CODEX-CT-2 experiment the initial pressure in the fuel rods was lower, but six out of seven rods failed before the quenching phase in this test, too.

Parameter	CODEX-CT-1	CODEX-CT-2
System pressure (bar)	2.6	2.0
Electrical power (W)	2300	2600
Fuel rod No. 1. initial pressure (bar)	30.3	5.9
Fuel rod No. 2. initial pressure (bar)	9.9	6.5
Fuel rod No. 3. initial pressure (bar)	12.5	11.1
Fuel rod No. 4. initial pressure (bar)	16.3	9.3
Fuel rod No. 5. initial pressure (bar)	20.9	8.1
Fuel rod No. 6. initial pressure (bar)	24.5	6.2
Fuel rod No. 7. initial pressure (bar)	6.2	10
Number of fuel bursts before quench	6	6
Duration of dry phase (h)	7	7
Max. temperature before quench (°C)	1245	1286
Max. temperature during quench (°C)	1245	1384
Hydrogen release before quench (l)	270	0
Hydrogen release during quench (l)	7	80
Mass of hydrogen in Zr (g)	10	7
Total hydrogen production (g)	33	13
Average degree of oxidation (%)	33	13

Table 10. Comparison of CODEX-CT-1 and CT-2 experiments

The oxidation of zirconium produced high amount of hydrogen in all tests. In the preliminary test 196 l and in the CODEX-CT-1 277 l was released from the tank under

controlled conditions. In the CODEX-CT-2 test the produced hydrogen was not released from the cleaning tank model during the dry phase of the experiments, but during the quenching phase 80 l was collected. In the CT-2 test the Zr oxidation was limited by the high hydrogen concentration in the tank. In the same time large amount of hydrogen was absorbed by the Zr metal.

The maximum temperature reached 1245 ºC in the CODEX-CT-1 test. In the CODEX-CT-2 test 1384 ºC was measured during quench that was accompanied with local temperature excursion. The temperature profile (Fig. 53) similarly to CT-1 test showed that the bottom of the bundle was intensively cooled by water, while the upper part heated up to very high temperatures. The temperatures at the top of the bundle were not as high as in the central part because of radiation heat losses to the top of the test section in both CT-1 and CT-2 tests.

The molar fraction of hydrogen in the test section exceeded 80% before quench The temporary peaks in hydrogen content took place the same time, when the coolant flowrate was manually increased to avoid blockage. (See Figs. 48 and 50 at 8000 s and 20000 s.) The hydrogen concentration above the bundle was lower than in the other measured position at 760 mm between the bundle and heater rods (Figs. 50 and 51). The decrease of hydrogen concentration was clearly the result of hydrogen uptake by the Zr components, since no gas was released from the system.

The quench of fuel was initiated after a long term oxidation in hydrogen rich steam. The scenario included both quench from the bottom and the top, similarly to the cleaning tank incident. The fragmentation and failure of the brittle fuel took place obviously during this period.

The oxidized cladding and shroud in CODEX-CT-2 test were very brittle. The fragmentation of the fuel continued during the handling and post-test examination procedures. The fragmentation during these actions was similar to the behaviour of damaged fuel assemblies during their removal from the cleaning tank.

After the experiment the fuel bundle rods showed similar view to the samples observed at the Paks NPP after the incident. The upper part of the rods was severely damaged, while the bottom part – cooled by water during the experiment – remained intact. The middle and upper sections were broken into several pieces. The material was very brittle, further fragmentation took place during the handling of fuel rods.

6. BUNDLE POST-TEST EXAMINATION

The examination of the bundle started with visual examination. The inspection of the internal structure was performed with X-ray radiography. Cross sections were prepared for detailed examination of the bundle by optical microscopy and SEM. Destructive methods were applied for the determination of hydrogen content in the materials.

6.1. VISUAL EXAMINATION OF THE CODEX-CT-2 BUNDLE

The fuel rods and bundles suffered severe damage during the tests. The final state was characterised by fragmentation, formation of cracks and brittle failure of the Zr components. The bottom part of the fuel that was cooled by water, remained intact. The experience of handling of fuel after the test showed that the material was very brittle: even a small mechanical load lead to further fragmentation of the cladding and the shroud.

There were many corrosion product fragments originating from the steal heaters in the test section (see left side picture in Fig. 54). Probably their presence was the main cause of the formation of flow blockages during the test.

The CODEX-CT-2 bundle showed much more brittle picture than the CODEX-CT-1 bundle: the shroud was severely damaged, the fuel rods were fragmented and the fragments relocated to lower positions during the removal of bundle from the test section. (Figures 54 and 55) The bundle was handled together with the heaters in order to keep the original structure of the bundle. After putting the bundle in horizontal position a plastic tube was moved between the heaters and the shroud and the structure of the bundle was fixed by epoxy. Sampling of some small Zr fragments for post-test examination was carried out before filling the bundle with epoxy.

6.2. COMPLEX RADIOGRAPHY INSPECTIONS FOR THE CODEX-CT-2 BUNDLE

The complex radiography inspections were produced on the Radiography station of the Budapest research reactor where the gamma- and X-ray radiography were used to study the inner structure of the inspected, damaged CODEX sample. It was packed in a polivinil chloride (PVC) tube, its diameter was 62 mm and its length was 1050 mm. The inside of the tube was filled up by artificial resin to fix the position of the sample. The radiography pictures were exposed in horizontal position of the PVC tube. A lead marker system was used for the easier identification of the errors. Every five centimetres was marked by lead numbers from zero to 105 cm. The PVC tube is shown in the Fig. 56 with the marker system in the beam position. A step wedge etalon (from 5 to 50 mm, in 10 steps, made from iron) and FE1 type wire picture quality indicator were used to estimate the dimensions of the errors as it is visible in the middle in Fig. 56.

BAS 20 X 40 MS type imaging plate was used as detector both for gamma- and X-ray radiography. BAS 2500 type scanner was used to read the plates. The evaluation work was contributed by AIDA software. The sample was divided in three (A,B and C) bands. The “A”

band was from 0 to 350 mm-, “B” band was from 350 to 650 mm and “C” band was from 650 to 1020 mm. Every band was exposed in 0^o, 45^o and 90^o rotations.

The energy of the gamma radiation was 8,2 MeV from the reactor and its dose rate was 8,3 Gy/h, 10 sec was the exposure time with 50 mm led filter. The weak contrast of the gamma radiography pictures was not available for the high level evaluation work. The source of the X-ray radiation was MXR 300 type portable, industrial generator. The applied power was 275 kV and 3 mA. The focus distance was 1250 mm. The exposure time was 60 sec.

The high resolution X-ray radiography pictures showed the fragmentation of the fuel elements and the relocation of some rod segments (Fig. 57a,b,c.). The Fig. 57a shows the X-ray radiography picture of the whole CODEX-C-2 bundle in PVC tube. On the left side of the figure is visible the arrangement of the “A”, “B” and “C” bands. The longitudinal dimensions of the tube are given by the numbers in centimetre on the right side of Figure 57a for the coordination of the interesting places. The Figure 57b shows two typical damages. The lower three parts of the figure contain of details of the debris material in the tube. The upper two parts of the figure give the position of the cracks in the artificial resin. The original places of the damages are shown by the arrows to the whole CODEX-CT-2 bundle. The fields of the collapsed areas are shown in the Figure 57c. The most interesting parts are marked by white “1”, “2” and “3” in the figure.

6.3. HYDROGEN ABSORBTION IN THE CODEX-CT-2 TEST

Several pieces of shroud, cladding, cladding tube plug and spacer grid were investigated after CODEX-CT-2 test in order to determine the amount of hydrogen absorbed in the Zr components. Sampling was carried out in two steps:

- After the tests the bundle was heavily damaged and it was possible to remove some small fragments from the bundle. Such sampling was carried out between elevations 690-890 mm, where the fragments were accessible.
- 3 mm thick cross sections were prepared from the bundle after its fixation by epoxy in a plastic tube. In these cases the epoxy had to be removed from the samples before the determination of hydrogen content.

The original position of some samples could not be identified exactly, since the fragments relocated from upper positions during the quench phase and the later handling of the bundle. In the following description those positions are indicated from where the samples were taken. At some selected elevations parallel measurements were performed for different samples. For this reason there are different values given in those elevations.

High temperature extraction was applied to determine the hydrogen content in the samples. The typical mass of samples was 0.01 g. The hydrogen content was expressed in weight ppm unit. The mass of samples was measured with high precision. The spalling oxide layers caused some accuracy problems during the weighting of samples.

The shroud had about 150 ppm hydrogen content at the elevation of the water level. The hydrogen distribution along the shroud was similar to the profile observed in the preliminary test, but the absolute values were lower and showed larger scatter in the

CODEX-CT-2 test. The maximum hydrogen content in the shroud was measured at 900 mm. The low values at the top of the shroud can be explained by the lower temperature.

The cladding had a profile with three maximums at the bottom, in the central section and top (Fig. 58). The maximum hydrogen content in the cladding was 6000 ppm. The end plug of the cladding tube had 9000 ppm, while the spacer grid at 100 mm had 1000 ppm hydrogen content.

Using the hydrogen distributions along the length of cladding and shroud the total mass of hydrogen absorbed in them can be estimated as 6.77 g.

The total mass of hydrogen produced during CODEX-CT-2 test can be determined as the sum of hydrogen released from the cleaning tank and absorbed in the metallic Zr. It gives 80+81=161 l hydrogen at room temperature (13.4 g).

6.4. METALLOGRAPHIC EXAMINATIONS

18 cross sections were cut from the bundle. The surfaces were polished and ground for metallographic examinations. The samples were etched with 0.5% HF in order to improve the observation of fine structures (Figures 62-65). The positions of cross sections are shown in Table 11 The first cross section was cut from the bottom and the last from the top of the bundle.

No. of cross section	Elevation (mm)	No. of cross section	Elevation (mm)
1	150	10	600
2	200	11	650
3	250	12	700
4	300	13	750
5	350	14	800
6	400	15	850
7	450	16	900
8	500	17	950
9	550	18	995

Table 11. Positions of cross sections

Cross sections of the CODEX-CT-2 bundle are shown in Fig. 59. The fuel rod were numbered counter-clockwise from the rod in the right corner. The central rod has No. 7.

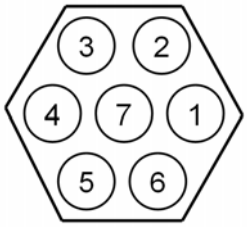

The main observation done on the cross sections can be summarised as follows:

- The cross section at 150 mm elevation of the bundle shows intact structure, but there is a pellet that fell down from an upper elevation. This section was covered by water during the test, so there are no sings of oxidation or ballooning.

- In the cross section at 200 mm an additional cladding tube was found that was relocated from an upper elevation (Fig. 59). Two fuel rods in the bottom of the picture show some gap between the pellet and cladding. It is obviously the result of clad ballooning.
- In the third and fourth cross sections at 250 and 300 mm even more ballooning can be observed.
- Debris of zirconium cladding was accumulated at the elevation of 350 mm cross section (Fig. 61). Spacer grid was located below this elevation and that facilitated the accumulation.
- The cross section at 350 mm shows the first fragmentation of fuel cladding at original elevation: the cladding of rod No. 5 is broken at this elevation.
- At 450 mm elevation very large ballooned area can be seen around rod No. 3 (Fig. 60
- Accumulation of pellets and cladding fragments is typical in cross sections between 500-750 mm.
- In the top elevations most of the fuel rods are missing, since they relocated to lower positions.

Elevation (mm)	Oxide layer on shroud		Oxide layer on cladding		Remaining metal layer (μm)
	external (μm)	internal (μm)	minimum (μm)	maximum (μm)	
150	7.9	7.9	7.9	7.9	
200	22.1	18.9	20.5	22.1	
250	33.2	30.8	13.4	32.4	480
300	44.3	41.9	62.4	109.9	503
350	83.8	83	47.5	72.7	470
400	117	64.8	25.3	62.4	452
450	170.7	165.2	60.9	80.6	490
500	102	21.3	37.1	78.2	400
550	278.2	64	37.9	150.2	470
600	210.9	110.9	30	37.1	450
650	261.6	86.9	122.5	156.5	520
700	306.7	83.8	51.4	86.9	450
750	268.7	111.4	12.7	124.9	546
800	205.5	98	81.4	100	596
850	162	62.4	94	98.7	546
900	96.4	92.5	72.7	85.4	575

Table 12. Measured oxide and metal layers in the CODEX-CT-2 bundle

The oxide layer thicknesses were measured in several positions on each fuel rod and on the wall of shroud in each cross section. The oxide scale on the fuel rods had layered structure (Fig. 63) and the external oxide scales were spalling from the cladding (Fig. 62). The oxide scale on both internal and external surfaces of the shroud had more compact structure without layers (Figs. 64 and 65, Table 12). The axial oxidation profiles are shown in Figures 66 and 67. The maximum oxide layer was observed on the external surface of the shroud, where 300 μm thickness was measured at 700 mm elevation. On the internal surface of the shroud and on the external surface of the cladding tubes the oxide layer thickness was

less, the maximum values reached only 150-160 μm. Furthermore the oxidation profiles were similar on the internal surface of the shroud and the external surface of the tubes.

Since significant part of the external oxide scale fell down before fixation of the bundle, it was necessary to measure the thickness of the remaining metal phase of Zr (Table 12). It can help in the better estimation of the degree of oxidation. The metal layer thickness profile is shown in Fig. 68. During the evaluation of the metal layer thickness it must be considered that the decrease of tube thickness was a common result of two processes: ballooning and oxidation.

Eleva-tion (mm)	External diameter (mm)						
	Rod No. 1	Rod No. 2	Rod No. 3	Rod No. 4	Rod No. 5	Rod No. 6	Rod No. 7
0	9.1	9.1	9.1	9.1	9.1	9.1	9.1
150	10.49	10.4	10.4	10.5	10.4	10.2	10.2
200	11.11	10.1	10.9	11.07	12.2	11.67	11.1
250	10.72	10.55	10.73	10.59	11.1	10.64	10.43
300	10.3	11.09	11.57	10.74	12.12	10.87	10.54
350	11.11	10.46	11.71	10.4	12.27	10.9	11.09
400	11.33	11.33	13.15	9.89	13.71	11.4	10.97
450	11.11	10.89	14.77	10.54	13.72	11.5	11.5
500	11.91	12.44	18.45	10.96	13.75	11.91	11.24
550	12.3	12.57	19.3	10.97	14.7	11	11.45
600	12.54	12.7	20.6	10.9	15.9	10.2	12.2
650	12.9	12.8	20.17	10.73	17.1	10.3	12.36
700	11.69	12.88	12.01	10.73	14.59	10.4	12.4
750	11.62	12.01	10.72	10.3	12.3	10.5	12.3
800	11.25	11.13	10.5	10.6	10.49	10.5	12.03
850	10.6	10.6	10.4	10.51	10.6	10.5	11.4
900	10.5	9.7	11	12.1	10.5	10.5	10.7
950	10.1	9.2	11.37	11.5	11.51	10.1	10.45
995	9.5	9.15	9.1	10.1	10	10.3	10.4
1000	9.1	9.1	9.1	9.1	9.1	9.1	9.1

Table 13. Measured external diameter fuel rods

Long ballooned sections were observed in the post-test examinations. The diameter change was a common result of plastic deformation and oxidation, but the oxidation effect was much less in the diameter increase than that of ballooning. The ballooning profiles are shown in Figs. 69 and 70. The axial distribution of cladding diameter was determined using the final state of the bundle and considering the cladding sections in each elevation (Table 13). In case of intact cladding the diameter was determined as an average value for the given tube. If the cladding was fragmented the diameter was determined by extrapolation from the available cladding fragments. For this reason the measured external diameter exceeded 20 mm in some positions, but the maximum intact cladding was only about 15 mm diameter.

6.5. SEM ANALYSES

Table 14 summarises some data of samples selected for SEM + EDX studies. The morphological features of them were examined by a Philips SEM 505 type scanning electron microscope (SEM) working at 20 kV accelerating voltage and with a few times 10^{-10} A specimen current. EDX studies were done mainly with an Oxford ISIS 200 type energy dispersive X-ray microanalyser (EDX) attached to a JEOL 733 type electron microprobe (EPMA). For EDX studies 20 kV accelerating voltage, 4-5 nA specimen current and standardless quantitative analyses were used.

Mark of the samples	Elevation (cm)	Notes
CT-2-100	100	Shroud and small tube piece
CT-2-60	60	One piece of shroud and small piece of cladding
CT-2-30	30	One Al_2O_3 pellet with 2/3 part cladding, one piece of shroud
CT-2-965	96.5	Small pieces collected from the given elevation
CT-2-901	90.1	Cladding tube
CT-2-565	56.5	Shroud pieces
CT-2-545	54.5	Cladding tube

Table 14. Samples selected for SEM + EDX studies

The last four samples summarised in Table 14 were put onto SEM sample holders covered with double sided carbon tape and were sputtered with a thin carbon layer to decrease electrical charging. Samples containing pellet and some pieces of the cladding were embedded and ground; then the selected pieces was broken out from the relatively thin cross sectional samples. Their surfaces were made electrical conductive by means of a thin sputtered carbon layer. Shroud pieces were embedded, ground, polished and sputtered for SEM + EDX studies.

Figures 71 and 72 show typical backscattered electron images (BEI) for the shroud and tube taken from 100 cm elevation. On the shroud the thickness of the oxide was changing between 30 and 60 μm, while at the tube relatively it was relatively thick (about 120 μm), a little larger than half of it had circumferential cracks and probably a lot of hydride. There was a large difference between the hydrogen content of the shroud and the tube: 1200-1400 ppm was measured for the shroud, while 8500-9000 ppm for the tube. Table 15 shows results of the EDX analyses performed at different parts of the shroud and the tube. Figure 72 contains BEI images from the oxide and the metallic parts of the shroud sample taken from 100 cm elevation. Large cracks starting from the oxide and penetrating to the metallic part can be seen together with some grain boundaries.

Shroud with 4100 ppm hydrogen content and almost maximum amount of hydrogen content for the cladding was found for samples taken at 60 cm elevation. Figures 73 and 74 show the different oxide thicknesses and the microstructure of the metallic part of the shroud further two BEI images from a piece of the cladding. The thicknesses of the oxide layers of

the shroud are about 90 and 280 μm, respectively. Large cracks seem to be started from the interface between the oxide and the metallic part and they are larger on the side with thicker oxide layer. The grain size of the metallic part of the shroud is between 15 and 40 μm. Non uniform oxide layer ranging from about 40 to 130 μm thickness can be seen at one side of the cladding. Almost half of the cladding is very fragmented. EDX analysis performed on different parts of the oxides and the metal of the shroud and the cladding shows almost stochiometric ZrO_2 composition on the oxide and 2-3 mass % oxygen on the metallic part.

Place of the analysis	O content (mass %)	Zr content (mass %)
Oxide on the shroud	16.43	83.57
Metallic part of the shroud*	4.08	85.37
Other oxide layer on the shroud	22.19	77.81
1.layer on the tube	13.32	86.68
2.layer on the tube	15.71	84.29
3.layer on the tube	16.08	83.92
4.layer on the tube	16.03	83.97
5.layer on the tube	16.95	83.05
6.layer on the tube	15.64	84.36
7.layer on the tube	15.57	84.43
Metallic part of the tube*	3.81	88.17

Table 15. Some EDX results for sample pieces taken from 100 cm elevation
Note:* A few percent of boron was detected in the metallic parts.

Figure 75 shows BEI images of the cladding and that of the shroud taken from 30 cm elevation (sample CT-2-30). The thickness of the oxide on the cladding is between 35 and 65 μm, while on the shroud it is about 50 μm. At the interface between the oxide and the metallic part of the cladding there are cracks and broken parts. In case of the shroud there are also some cracks, but their number and sizes seem to be smaller. These finding are probably in correlation with the different hydrogen contents of the shroud (about 800 ppm) and the cladding (1800-1900 ppm). Microstructure of the cladding and that of its oxide can be seen in Figure 76. The microstructure of the cladding shows intertwining crystallites (probably β-phase) and a few larger crystals (probably α-phase). Large and smaller cracks and opening of the oxide layer can be recognised. Microstructure of the cladding shows the effect of the hydrogen and also the relatively high temperature. EDX analysis of the oxide and metallic part of the cladding and that of the shroud shows a few mass % oxygen in the metal and 16.4 – 17.6 mass % in the oxide layers.

In the samples collected from the particulate material at various elevations, mostly zirconium oxide was detected and other elements, such as Cr, Fe, Si and Al were also found. Fe was detected mostly in the sample taken from 56.5 cm, while Al and smaller amounts of Si were detected at elevation 54.5 cm. Figures 77 and 78 show typical SEM images for the four samples. In samples taken from 90.1 and 56.5 cm elevations columnar oxide layers and large sized metallic grains can be seen. The thickest oxide layer is on sample taken from 56.5 cm elevation, the thickness is about 500-600 μm, while for sample taken from 90.1 cm, it is

about 250 μm. At 96.5 cm elevation the sample consists of grains with a few μm sizes, except some needle like crystals with 15-20 μm. At 54.5 cm elevation zirconium grains ranging from a few μm to 15-25 μm are covered with fine sized oxide.

7. EXPERIMENTAL DATABASE

The experimental data were collected for code validation purposes into a database, which cover 36530 s time period with 1 s^{-1} frequency. The parameters are listed in Table 16 and plotted in Figs. 13-52 for the period of 0-29094 s. (Part of the preparatory work is also covered in the database before "0" time.)

The database is presented in a large ASCII type file. The first column of the matrix contains the time. The "0" experimental time was set to real time 9:00:00, 18th December 2007. Each variable listed in Table 16 is given in a separate column in the file. The order of variables is the same as listed in the table.

Name	Unit	Definition
TFR136	°C	Fuel rod No. 1 temperature at 360 mm
TFR183	°C	Fuel rod No. 1 temperature at 830 mm
TFR229	°C	Fuel rod No. 2 temperature at 290 mm
TFR276	°C	Fuel rod No. 2 temperature at 760 mm
TFR322	°C	Fuel rod No. 3 temperature at 220 mm
TFR355	°C	Fuel rod No. 3 temperature at 550 mm
TFR415	°C	Fuel rod No. 4 temperature at 150 mm
TFR462	°C	Fuel rod No. 4 temperature at 620 mm
TFR536	°C	Fuel rod No. 5 temperature at 365 mm
TFR583	°C	Fuel rod No. 5 temperature at 825 mm
TFR690	°C	Fuel rod No. 6 temperature at 900 mm
TFR755	°C	Fuel rod No. 7 temperature at 550 mm
TSH8	°C	Shroud temperature at 80 mm
TSH27	°C	Shroud temperature at 270 mm
TSH70	°C	Shroud temperature at 700 mm
TSH75	°C	Shroud temperature at 750 mm
THR70	°C	Heater temperature at 700 mm
TG5	°C	Gap temperature at 50 mm
TG27	°C	Gap temperature at 270 mm
TG74	°C	Gap temperature at 740 mm
TG97	°C	Gap temperature at 970 mm

TCIN	°C	Coolant inlet temperature in the intlet junction
TCOUT	°C	Coolant outlet temperature in the outlet junction
TXT	°C	Temperature in the expansion tank
PYROM	°C	Temperature measured by pyrometer
PFR1	bar	Fuel rod No.1 pressure
PFR2	bar	Fuel rod No.2 pressure
PFR3	bar	Fuel rod No. 3 pressure
PFR4	bar	Fuel rod No. 4 pressure
PFR5	bar	Fuel rod No. 5 pressure
PFR6	bar	Fuel rod No. 6 pressure
PFR7	bar	Fuel rod No.7 pressure
PSYS	bar	System pressure
LTS	cm	Water level in the test section
LXT	cm	Water level in the expansion tank
FLOW	g/s	Coolant flowrate
H2	l	Volume of released hydrogen from the cleaning tank model
TCD1	-	Molar fraction of hydrogen above the bundle
TCD2	-	Molar fraction of hydrogen at 760 mm elevation
POWER	W	Electrical power

Table 16. List of measured parameters available in the CODEX-CT-2 database

The database includes also the pictures of post-test examination. There are 432 pictures in 18 subdirectories. The subdirectories are named after the elevation of cross section (see Table 10).

Each subdirectory includes the following pictures:

- View of the bundle.
  - The names of the files are N-0.bmp,
    - where N is the number of cross section.

- View of each fuel rod at the given elevation.
  - The names of the files are: N-R.bmp,
    - where N is the number of cross section and
    - R is the number of rod.
  - The magnification in these pictures was 6.5x.

- Close view of cladding and shroud segments.

- The names of the files are N-R-MX.bmp,
  - where N is the number of cross section,
  - M indicates magnification with the following values: M=10 means 10x, M=16 means 16x,
  - R is the number of rod, R=0 is the shroud,
  - X=A,B,C,Ap.... shows that there are several pictures from the same cladding.

8. SUMMARY AND CONCLUSIONS

Fuel assembly damage took place in the cleaning tank under specific conditions during the Paks-2 incident. The fuel was oxidised in large stagnant steam volume that had high hydrogen content. The fragmentation of brittle fuel happened during the quenching of heavily oxidised assemblies. This incident was beyond the LOCA type accidents, since the oxidation took place for a very long time.

The main conditions of the incident were reproduced in the CODEX-CT experiments. In spite of the different scenarios the final state of the bundles was rather similar in terms of mechanical load bearing capabilities. There was no reliable information on the hydrogen release through the air letdown line during the incident. The comparison of the CODEX-CT-1 and CT-2 test made clear that both large hydrogen release and no hydrogen release cases could have lead to the very brittle final state of the fuel assemblies.

After the tests the fuel bundle rods showed similar view to the samples observed at the Paks NPP after the incident. The upper part of the rods was almost fully oxidized, while the bottom part – cooled by water during the experiment – remained intact. The middle and upper sections were broken into several pieces. The material was very brittle, further fragmentation took place during the handling of fuel rods. The post-test examination indicated very high hydrogen content (several thousands weight ppm) in the Zr components (cladding and shroud). Many similarities were found between the damaged Paks-2 fuel and the rods tested in the CODEX-CT experiments. This fact allowed us to draw conclusions on the similarities between measured test parameters and the unknown parameters of the incident.

The simulation of the cleaning tank incident provided detailed information on the probable scenario of the real incident. The data will be used for model development purposes to improve the predictive capabilities of fuel behaviour codes.

ACKNOWLEDGMENTS

The CODEX-CT-2 experiment was performed in the framework of the Economic Competitiveness Operational Programme of Hungary (contract number GVOP-3.1.1.-2004-05-0020/3.0) with the financial support of the National Office for Research and Technology (NKTH).

REFERENCES

[1] Perez-Feró, E, Vasáros, L., Győri, Cs., Windberg, P., Hózer, Z., Horváth, M. (2005). Effects of oxidation and hydrogen uptake of E110 cladding oxidized in hydrogen rich steam atmosphere, *QUENCH-11 Workshop*, October 2005, Karlsruhe.

[2] Hózer, Z., Maróti, L., Windberg, P., Matus, L., Nagy, I., Gyenes, Gy., Horváth, M., Pintér, A., Balaskó, M., Czitrovszky., A., Jani, P., Nagy, A., Prokopiev, O., Tóth, B. (2006). Behaviour of VVER fuel rods tested under severe accident conditions in the CODEX facility, *Nuclear Technology*, vol.154, pp. 302-317.

[3] Hózer, Z., Windberg, P., Nagy, I., Maróti, L., Matus, L., Horváth, M., Pintér, A, Balaskó, M., Czitrovszky, A., Jani P. (2003) 'Interaction of failed fuel rods under air ingress conditions', *Nuclear Technology*, vol. 141, pp. 244-256

[4] C.R. Wilke: A viscosity equation for gas mixtures. J. Chem. Phys. 18. 617 (1950)

[5] L. Maróti: Chemical Interaction between VVER Core Components under Accidental Conditions, *Nucl. Eng. Des.*, **172**, p. 73 (1997).

[6] Pintér Csordás A, Matus L, Czitrovszky A, Jani P, Maróti L, Hózer Z, Windberg P, Hummel R: Investigation of aerosols released at high temperature from nuclear core models, J. Nucl. Materials, vol 282, Iss 2-3, pp. 205-215

[7] Trambauer K, Haste T J, Adroguer B, Hózer Z, Magallon D, Zurita A: In-Vessel Core Degradation Code Validation Matrix, Update 1996-1999, NEA/CSNI/R(2000)21

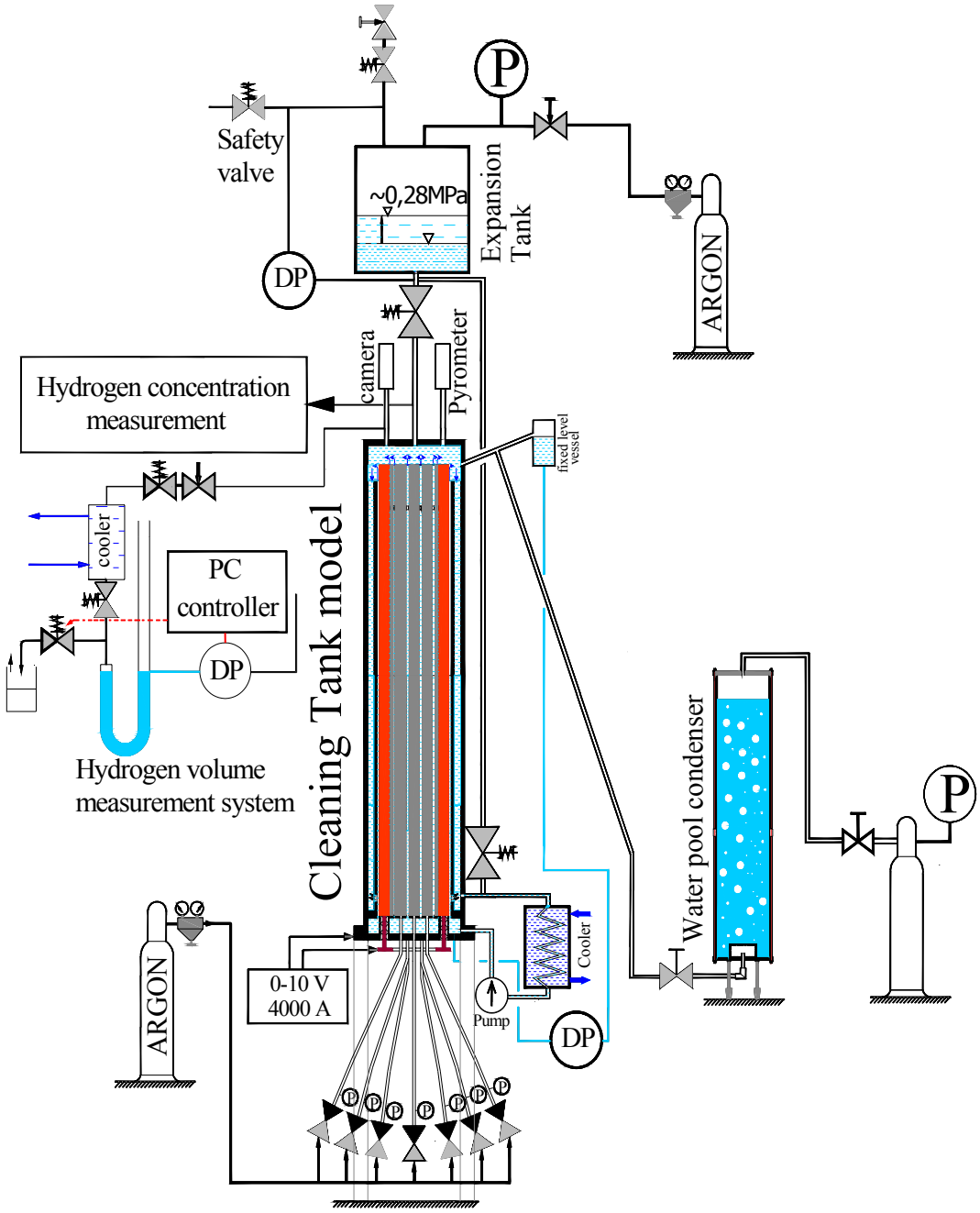

Fig. 1. Scheme and main components of the CODEX-CT facility

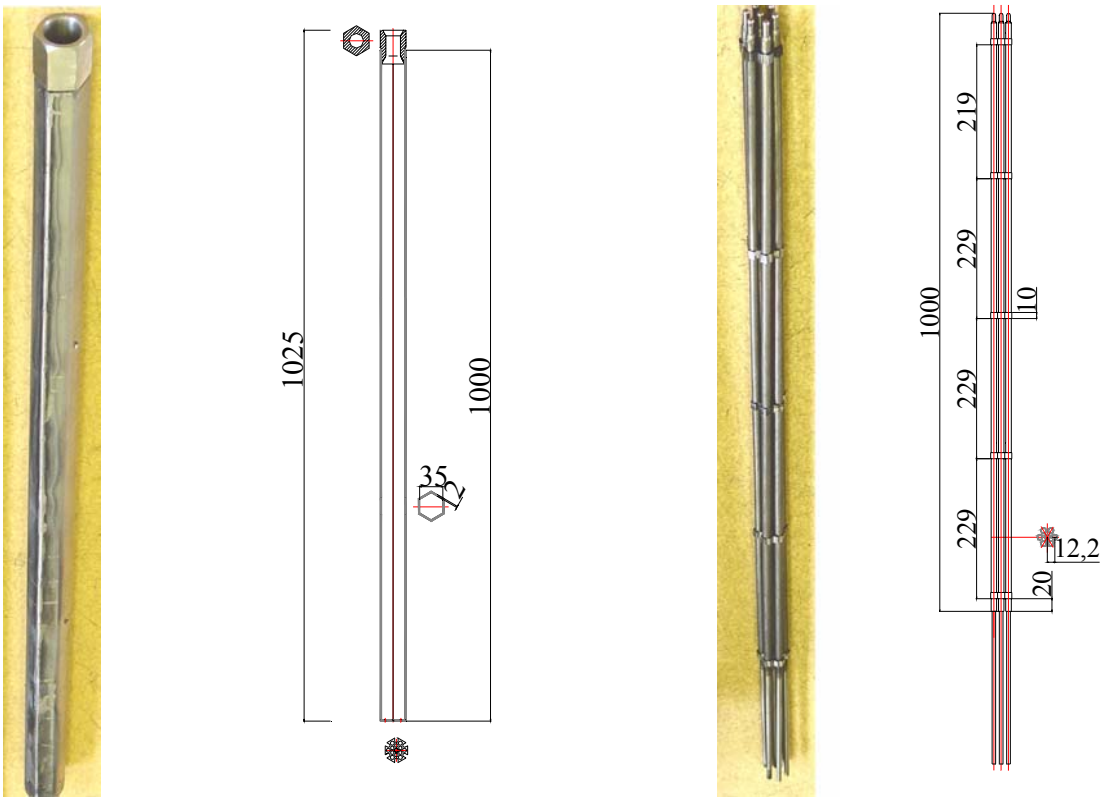

Fig. 2. Design and view of the shroud (left) and bundle (right)

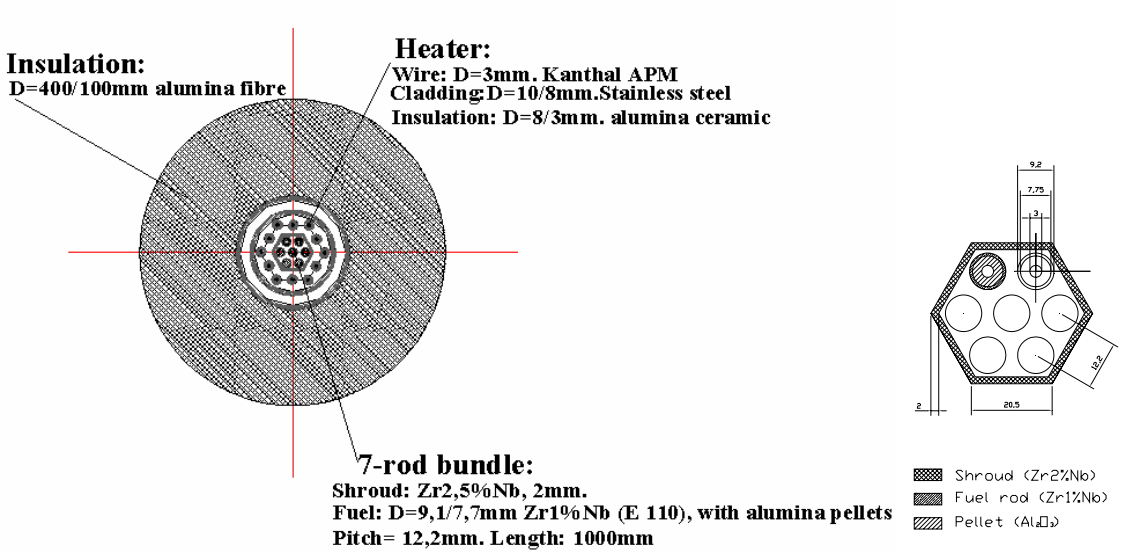

Fig. 3. Horizontals cross sections of the cleaning tank model (left) and of the bundle (right)

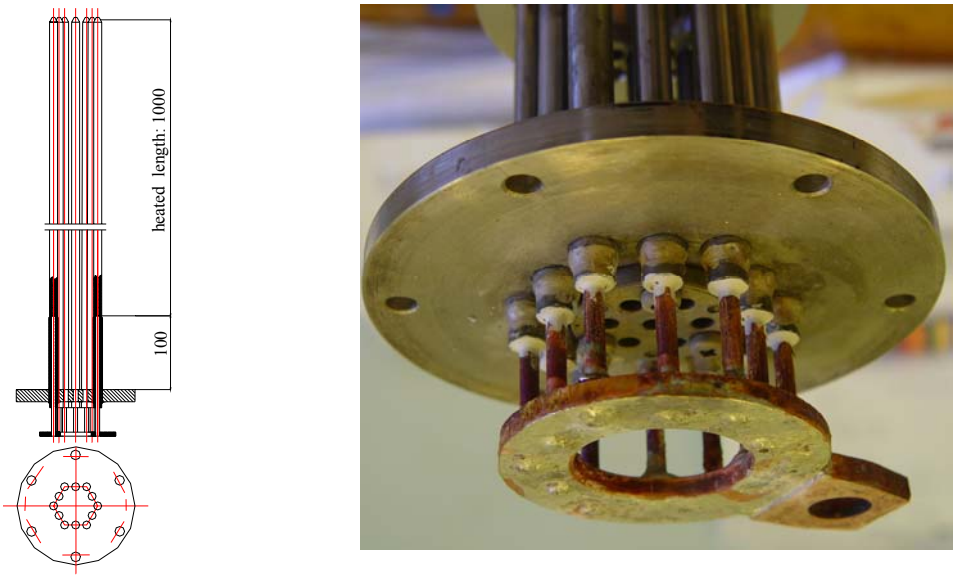

Fig. 4. Scheme (left) and view (right) of the heaters

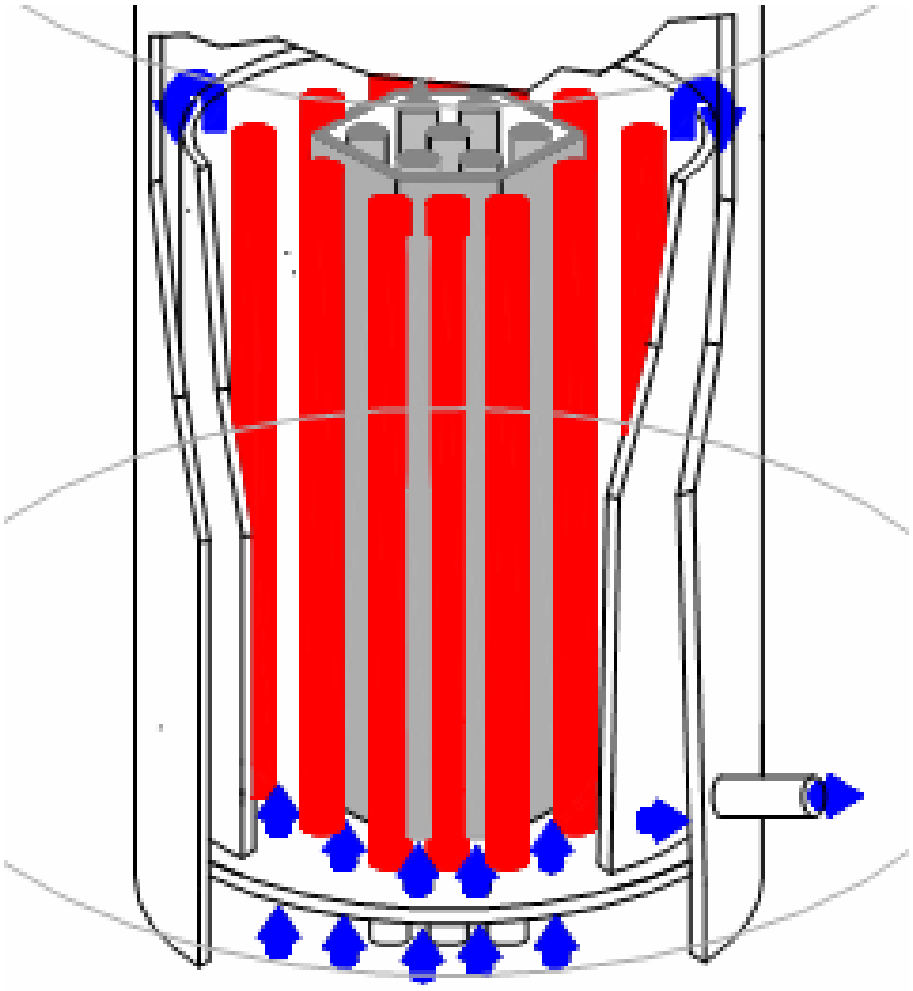

Fig. 5. Flow path in the test section of the CODEX-CT facility

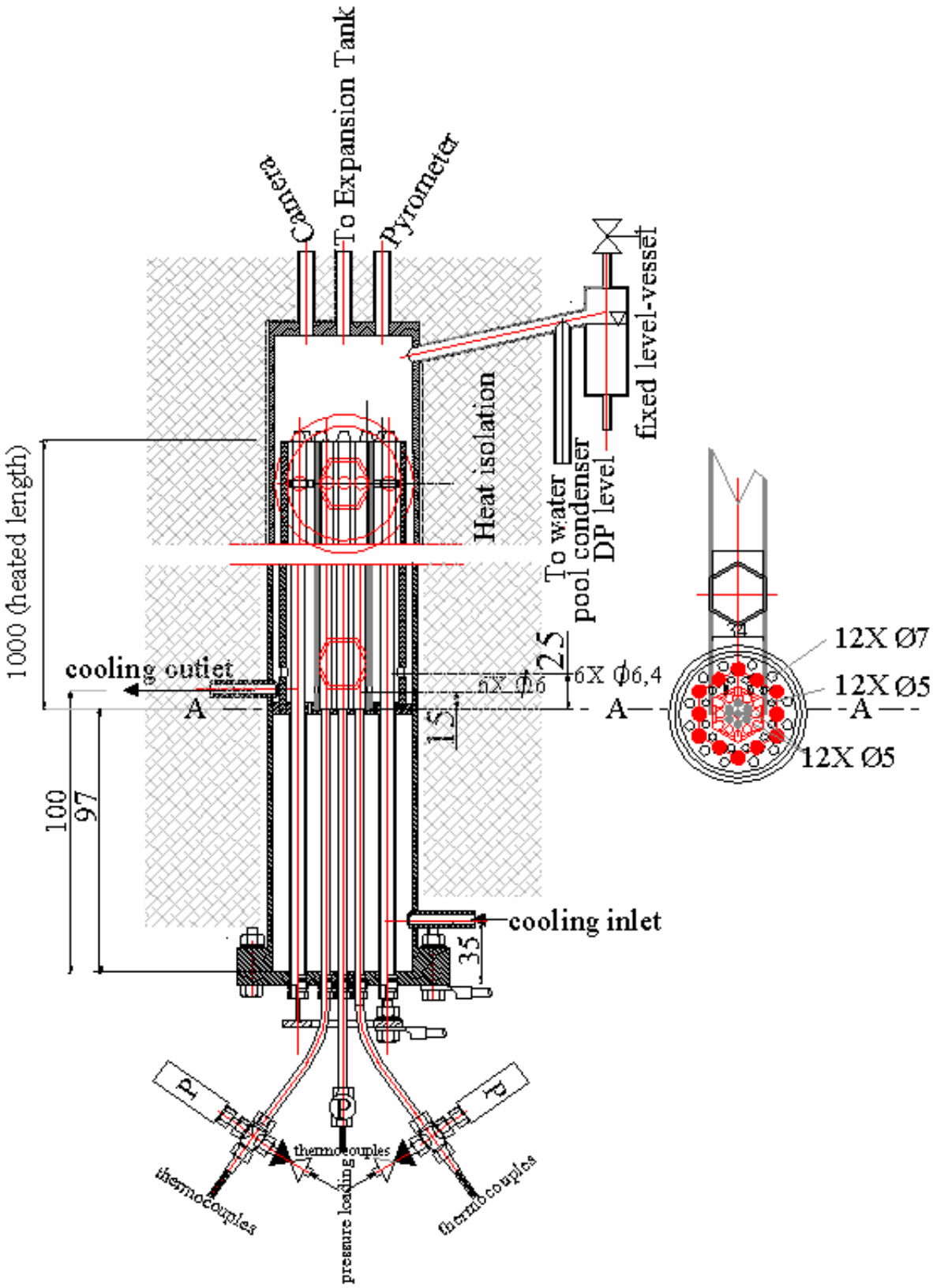

Fig. 6. Scheme of the CODEX-CT cleaning tank model

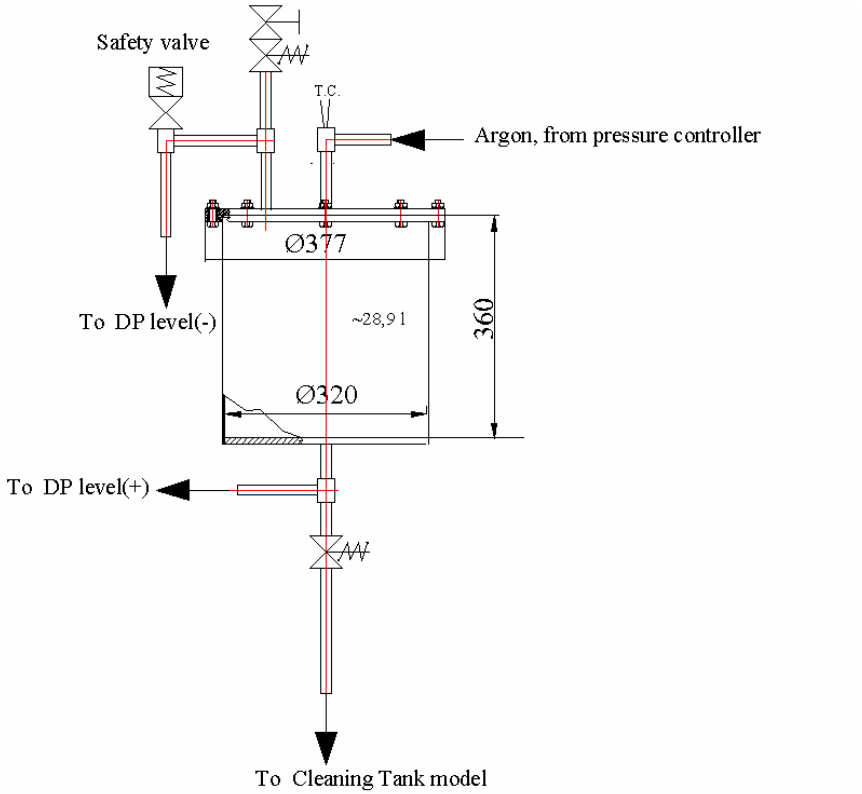

Fig. 7. Scheme of the expansion tank

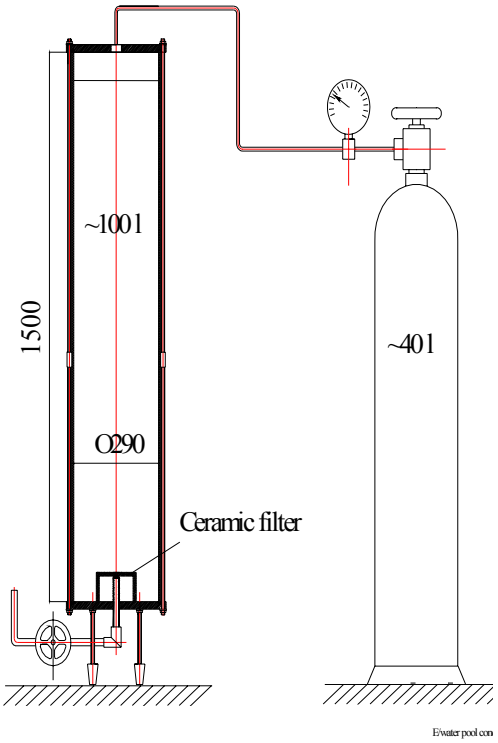

Fig. 8. Scheme of the condenser tank

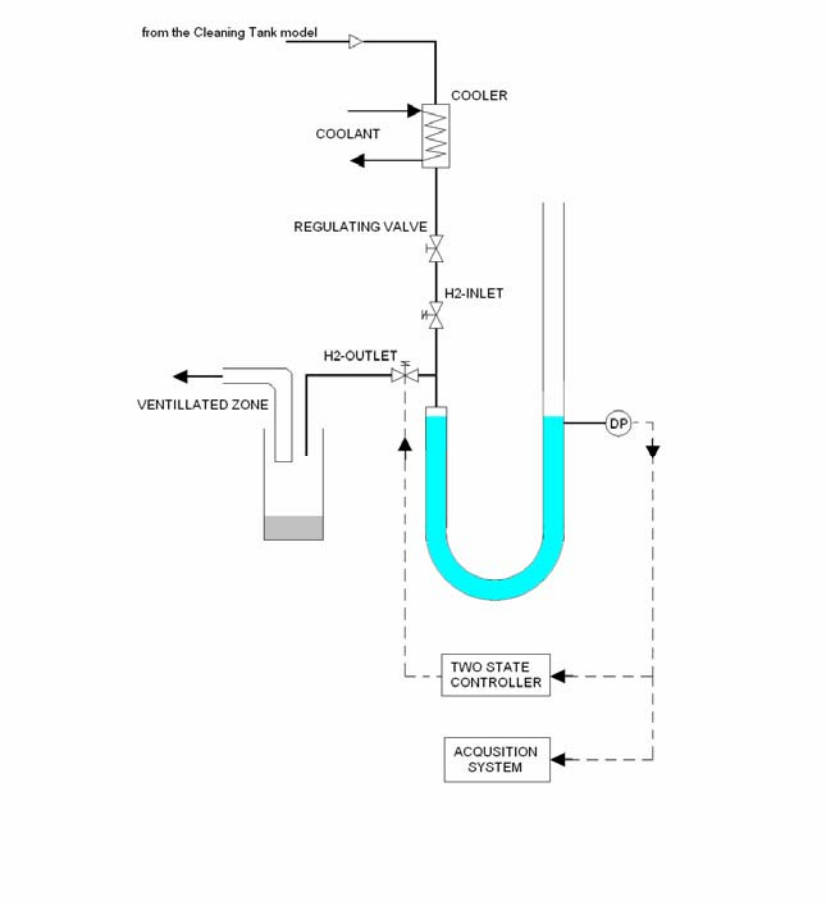

Fig. 9. Hydrogen flowrate measurement system

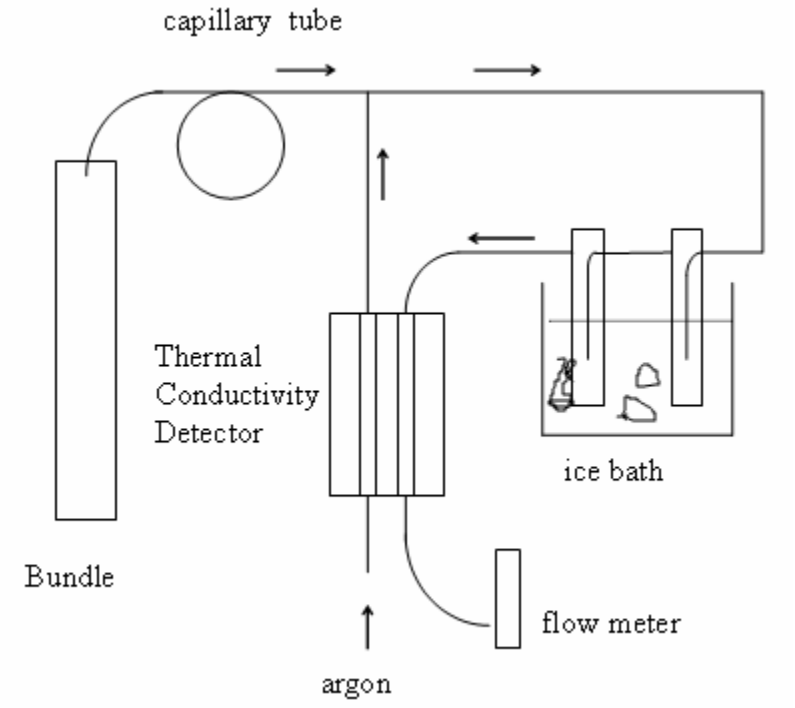

Fig. 10. Scheme of hydrogen concentration measurement

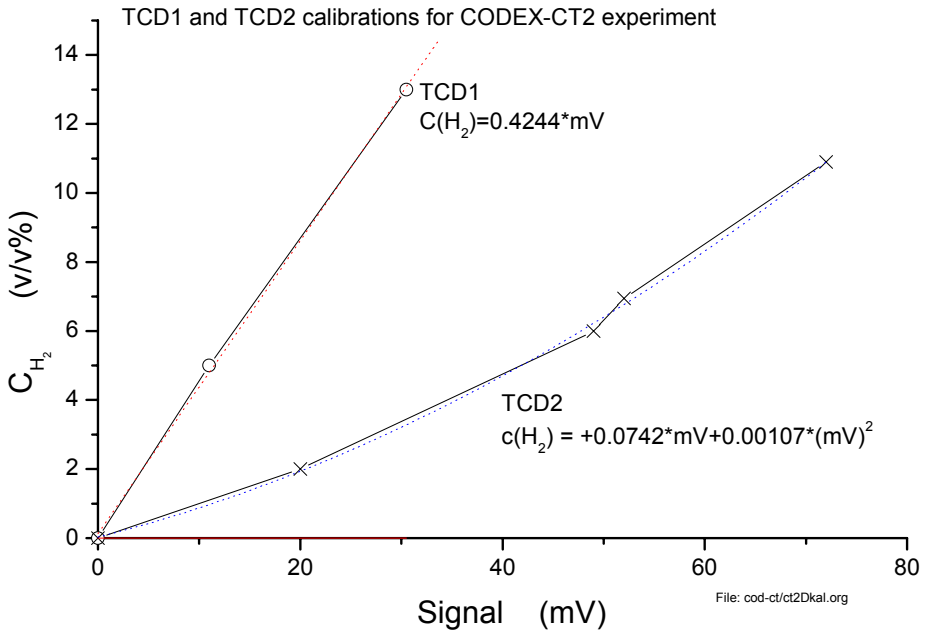

Fig. 11. Calibration curves, H_2 concentration as function of TCD signals

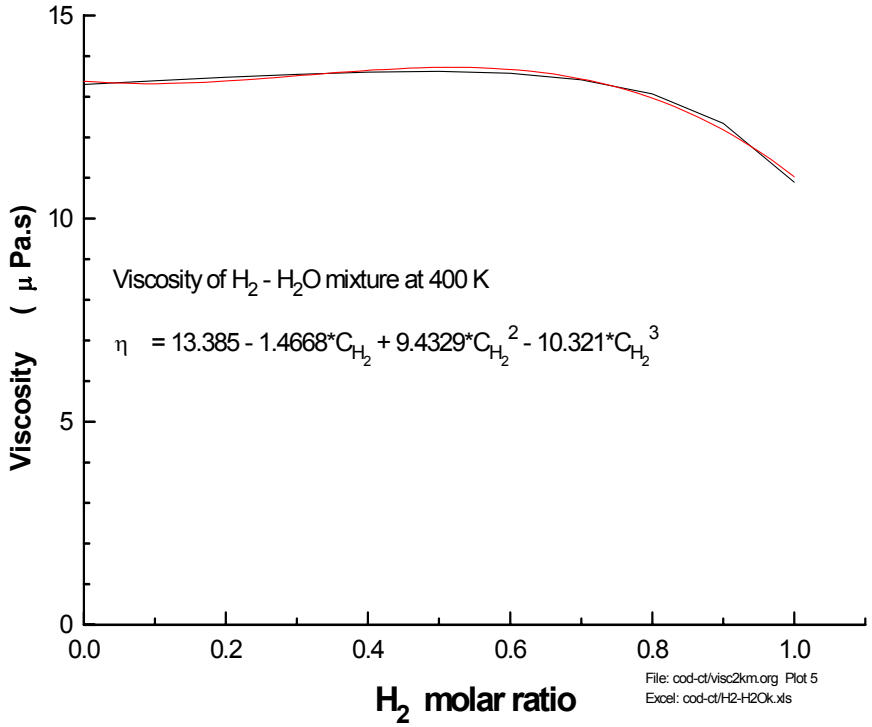

Fig. 12. Viscosity of H_2 - H_2O gas mixture at 400 K
(solid line calculated by [4], dotted line fitted curve)

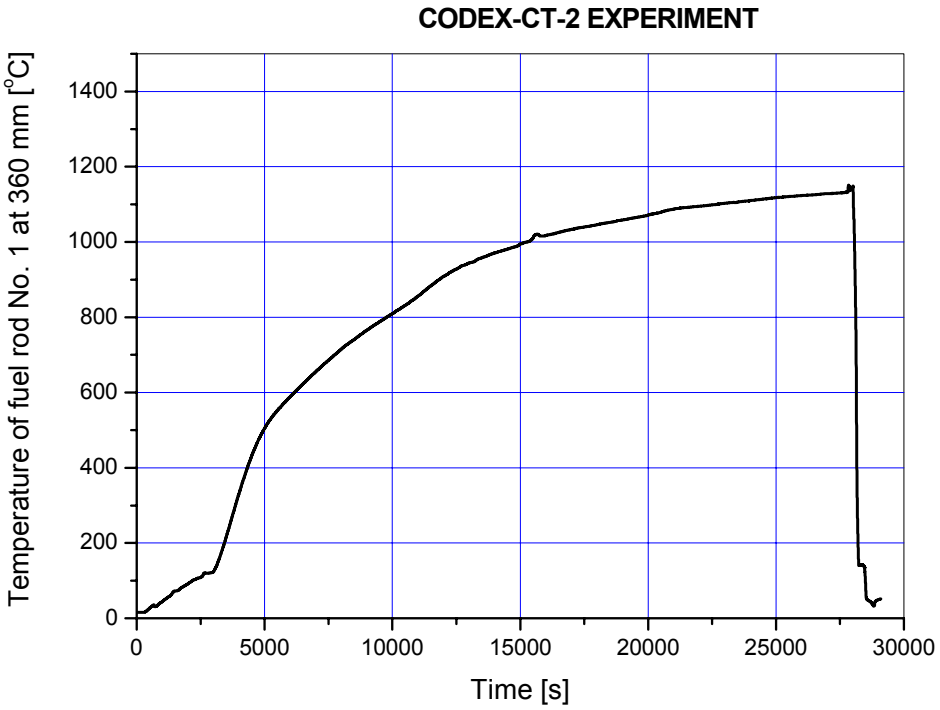

Fig. 13. TFR136: Temperature of fuel rod No. 1 at 360 mm elevation

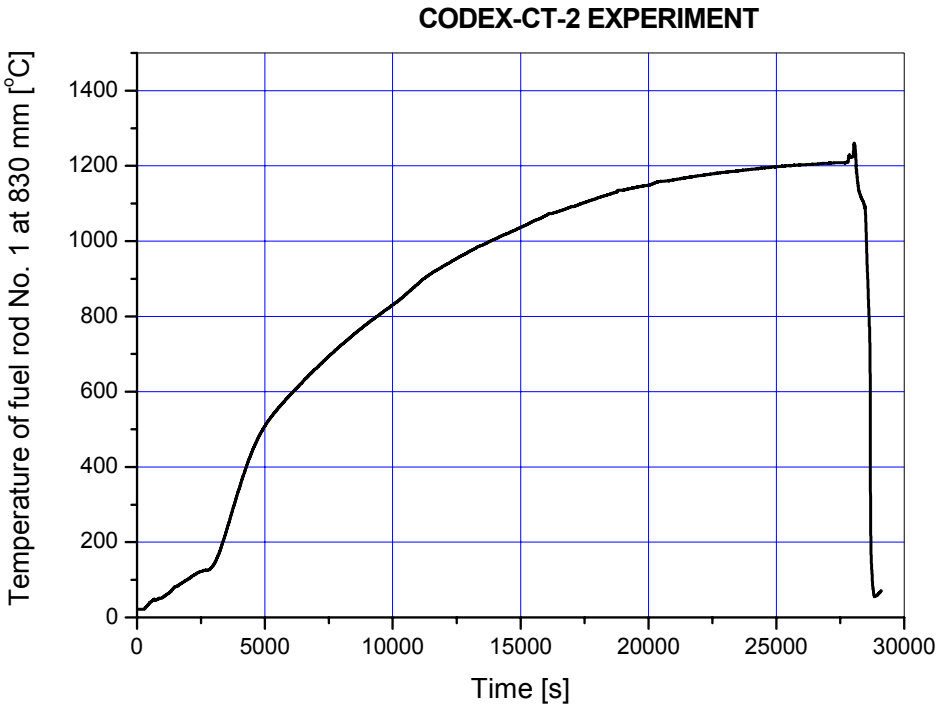

Fig. 14. TFR183: Temperature of fuel rod No. 1 at 830 mm elevation

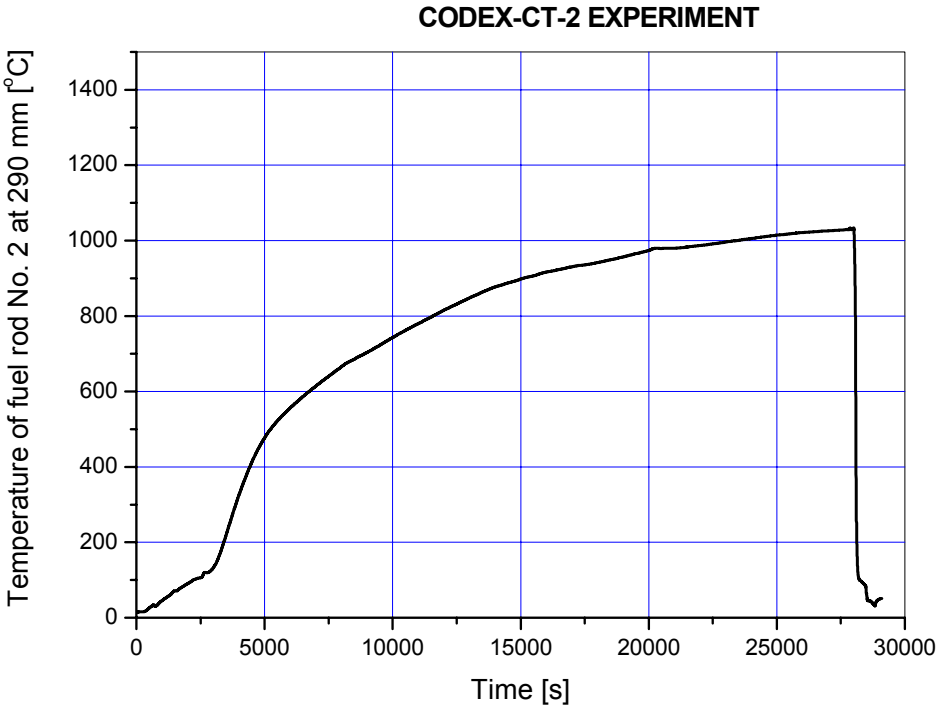

Fig. 15. TFR229: Temperature of fuel rod No. 2 at 290 mm elevation

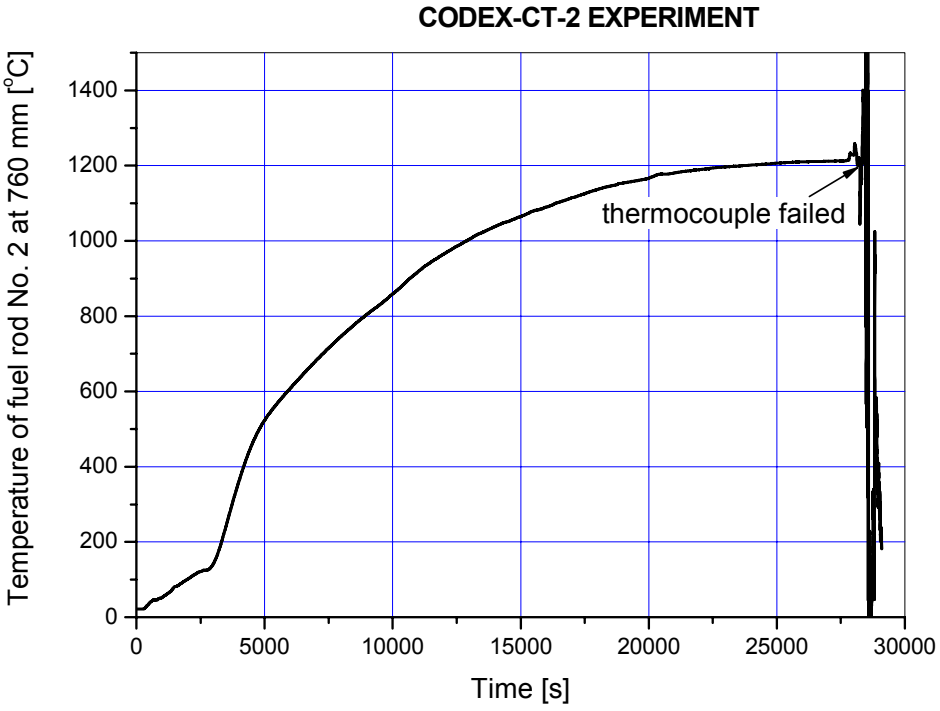

Fig. 16. TFR276: Temperature of fuel rod No. 2 at 760 mm elevation

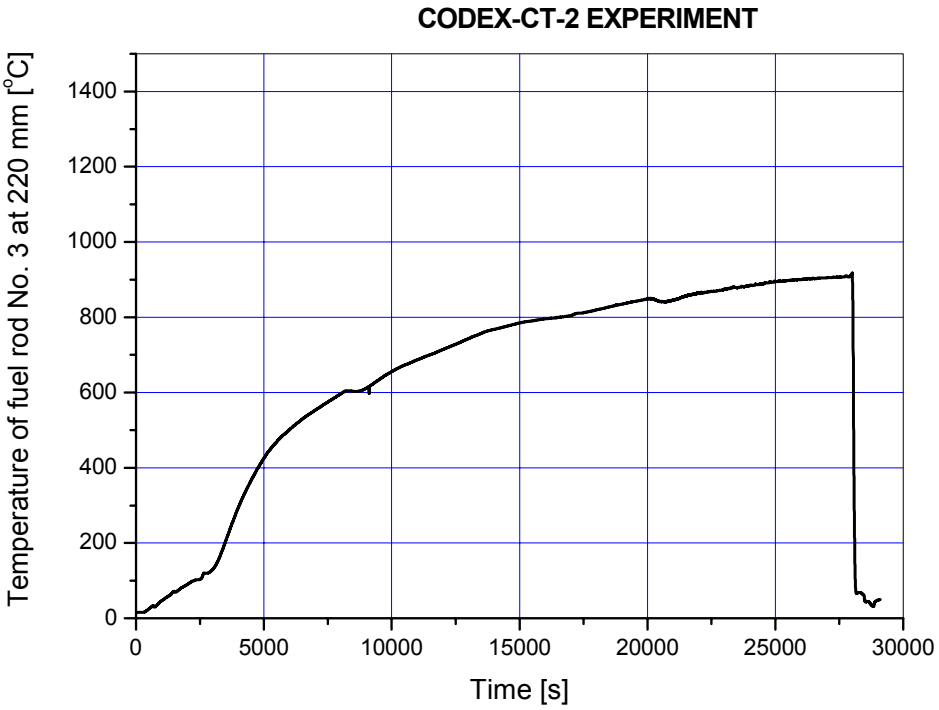

Fig. 17. TFR322: Temperature of fuel rod No. 3 at 220 mm elevation

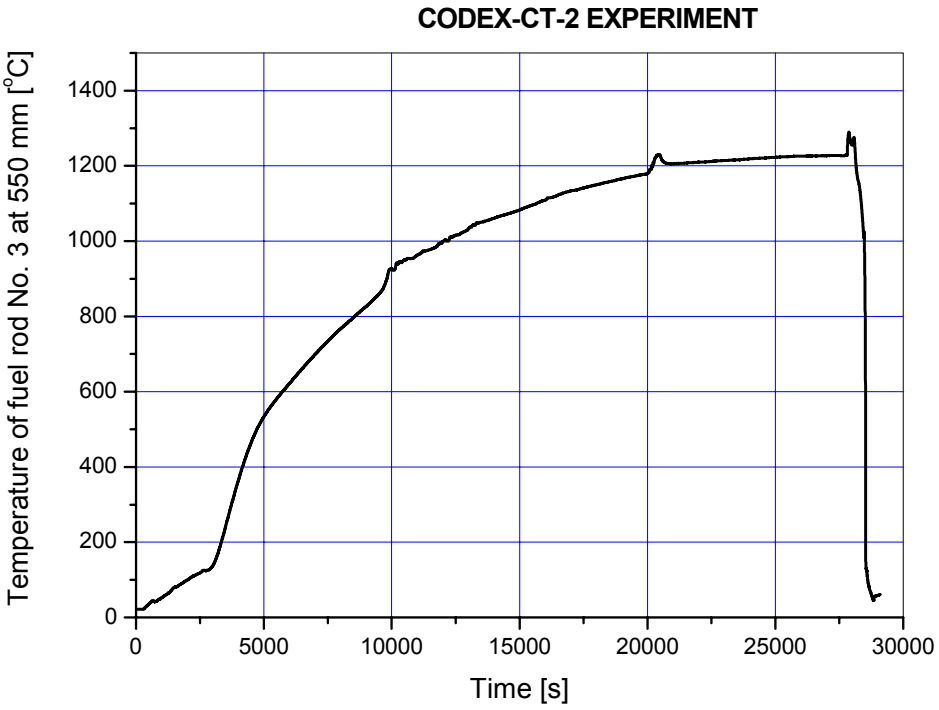

Fig. 18. TFR355: Temperature of fuel rod No. 3 at 550 mm elevation

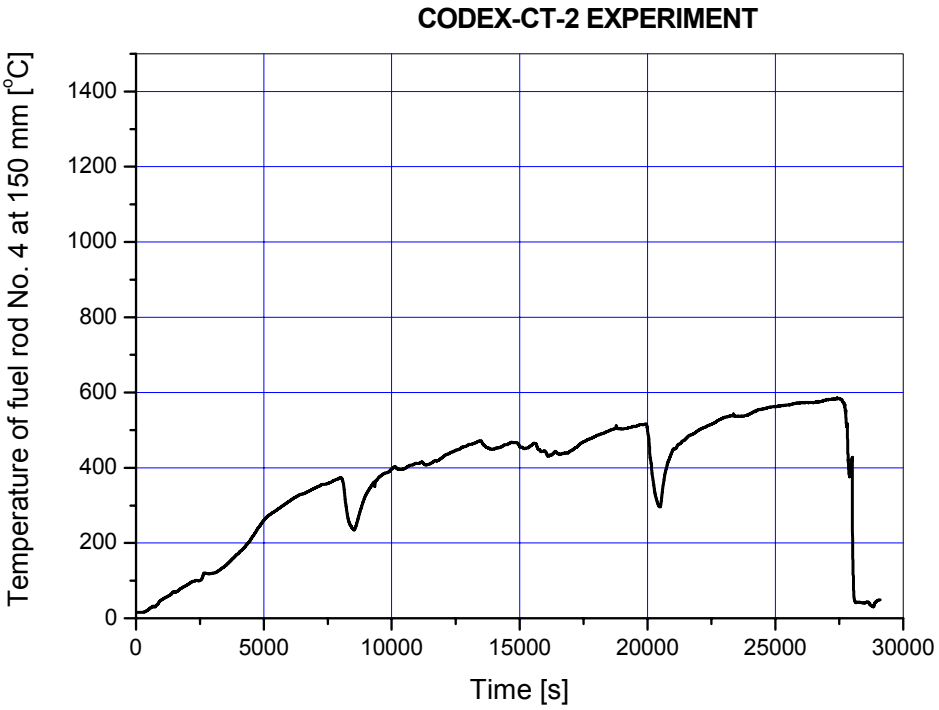

Fig. 19. TFR415: Temperature of fuel rod No. 4 at 150 mm elevation

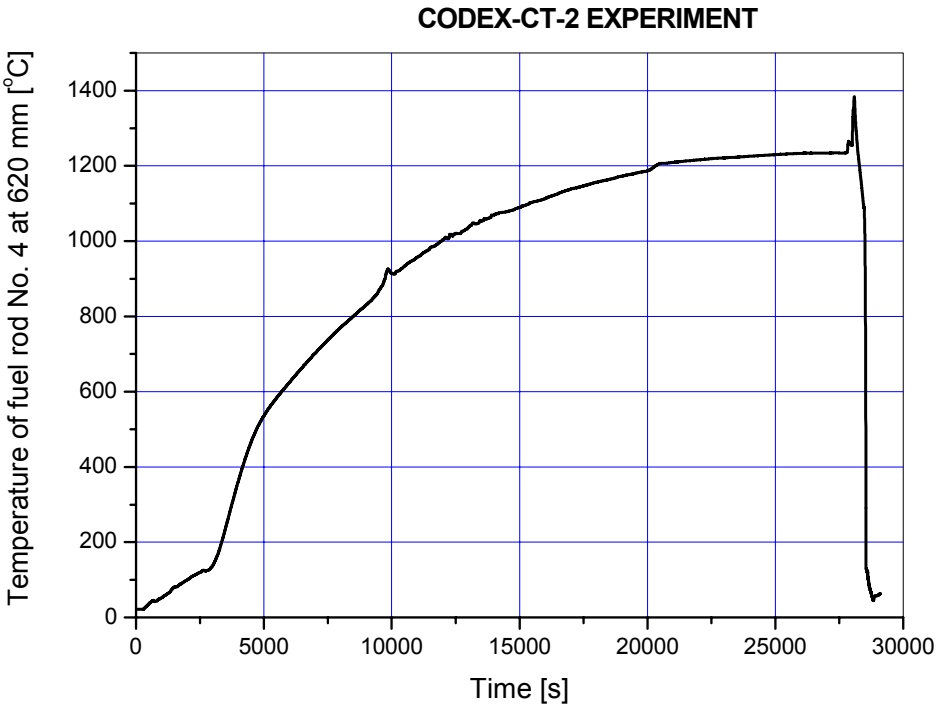

Fig. 20. TFR462: Temperature of fuel rod No. 4 at 620 mm elevation

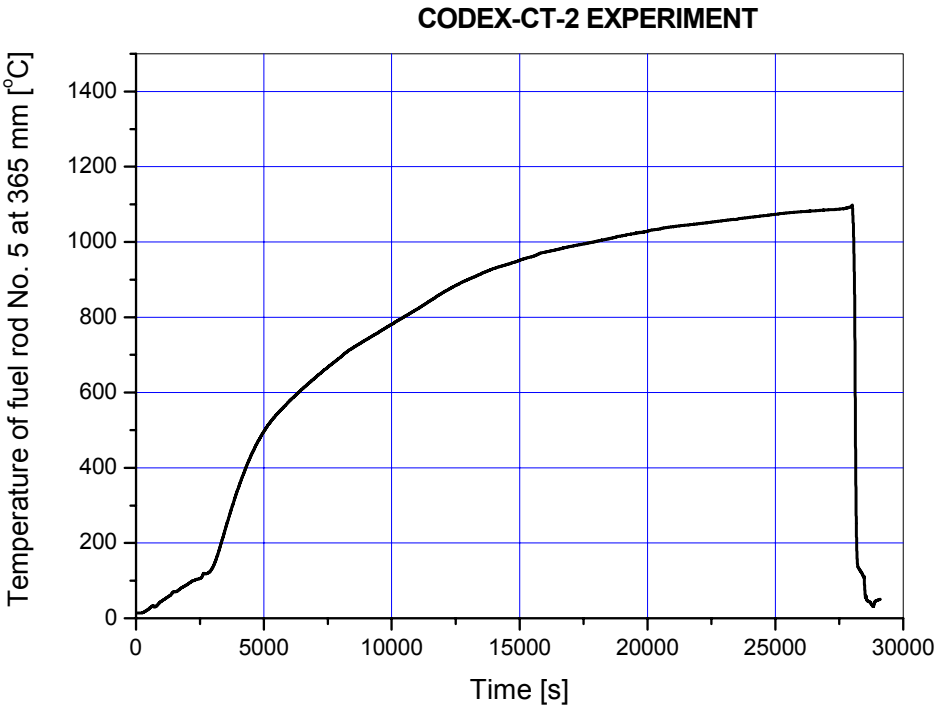

Fig. 21. TFR536: Temperature of fuel rod No. 5 at 365 mm elevation

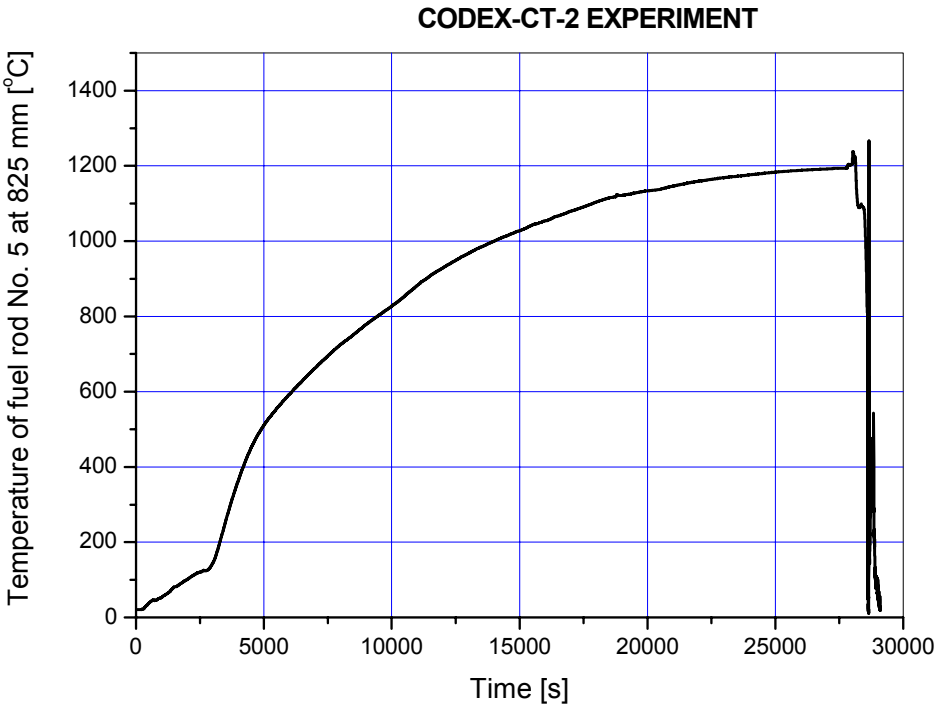

Fig. 22. TFR583: Temperature of fuel rod No. 5 at 825 mm elevation

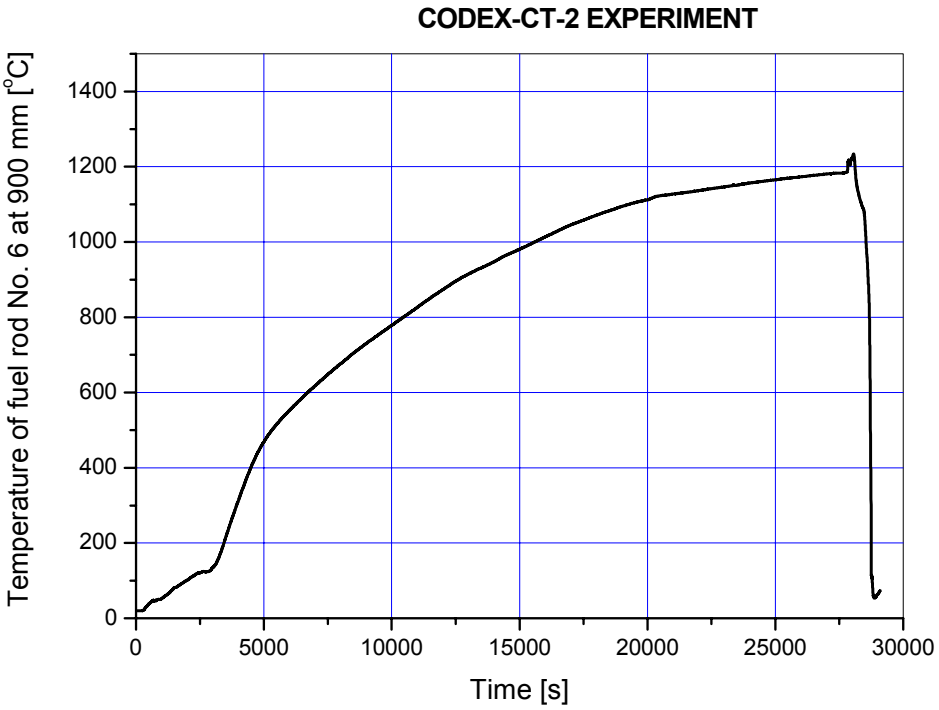

Fig. 23. TFR690: Temperature of fuel rod No. 6 at 900 mm elevation

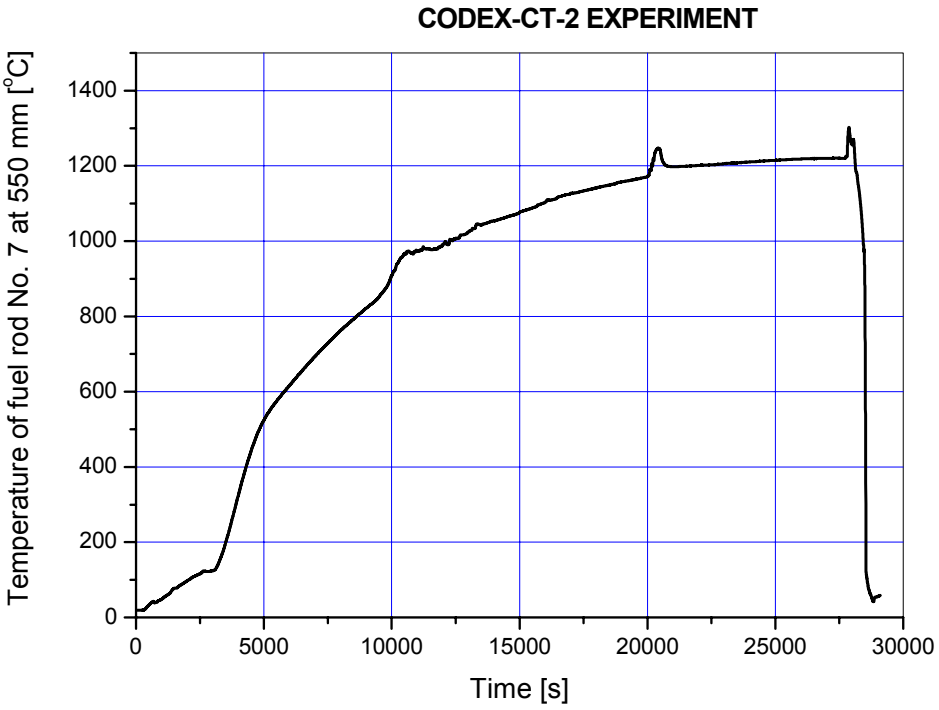

Fig. 24. TFR755: Temperature of fuel rod No. 7 at 550 mm elevation

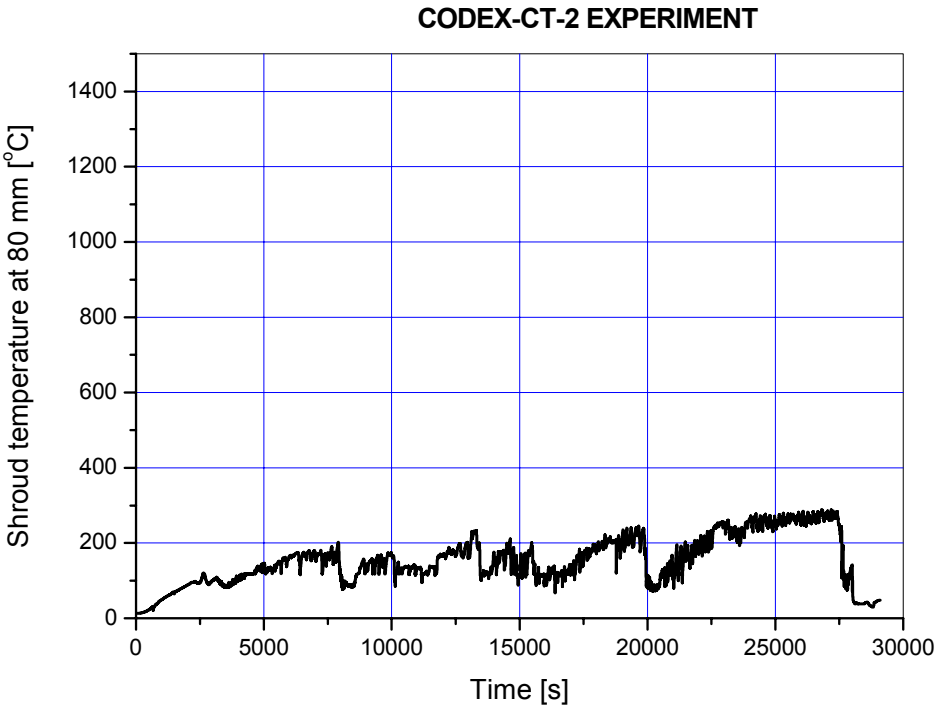

Fig. 25. TSH8: Temperature of shroud at 80 mm elevation

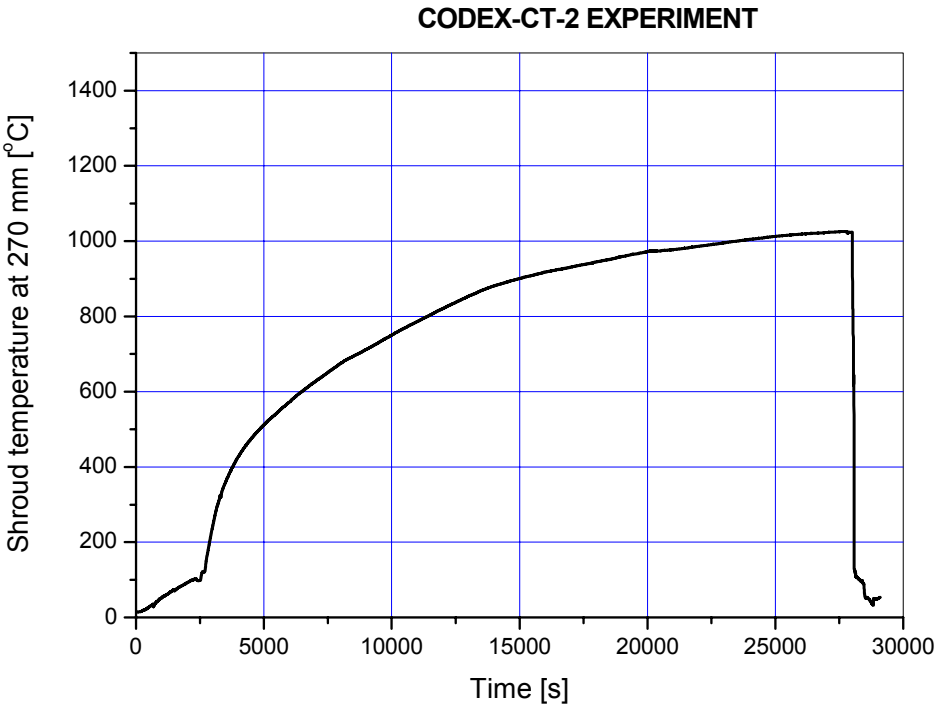

Fig. 26. TSH27: Temperature of shroud at 270 mm elevation

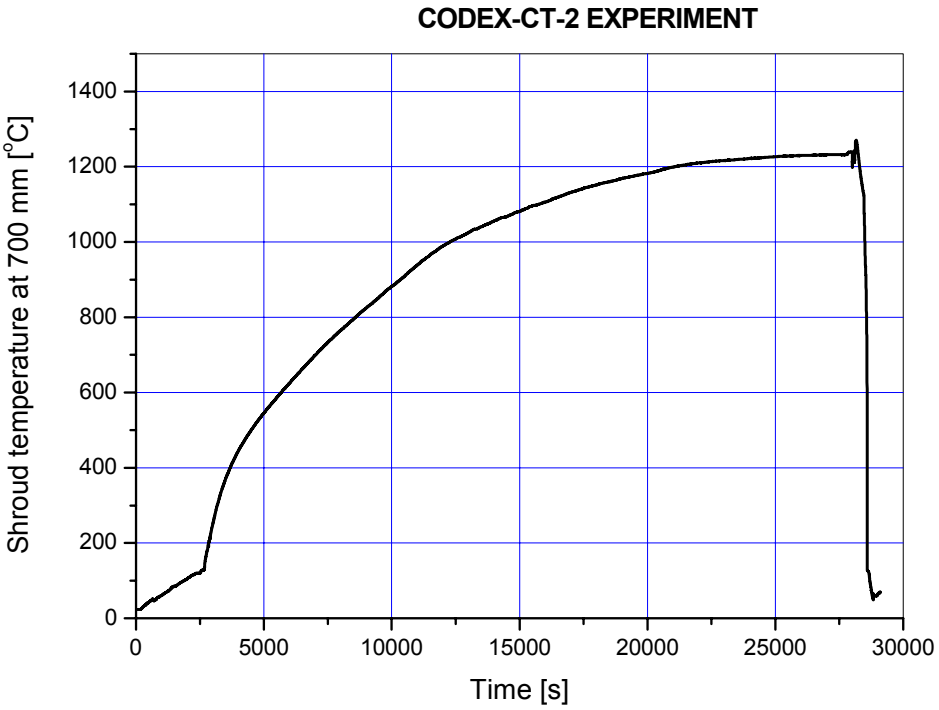

Fig. 27. TSH70: Temperature of shroud at 700 mm elevation

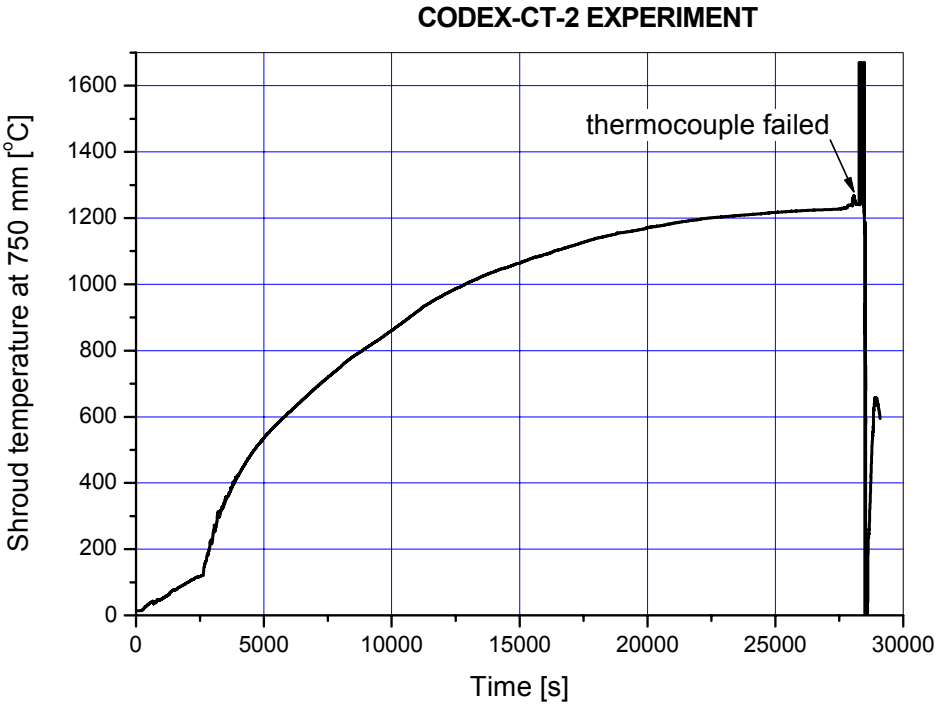

Fig. 28. TSH75: Temperature of shroud at 750 mm elevation

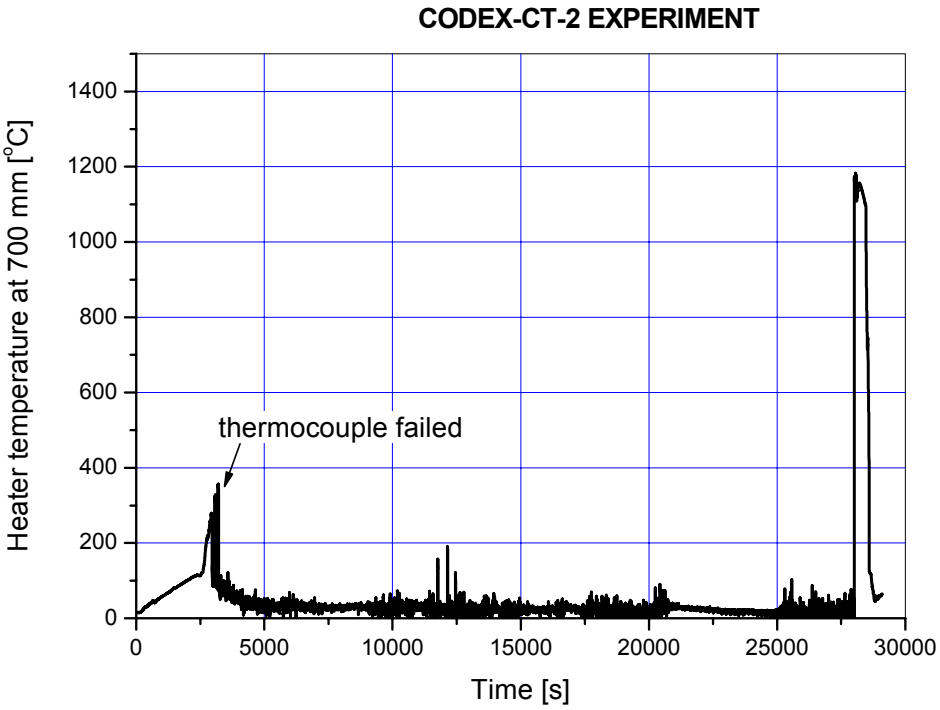

Fig. 29. THR70: Temperature of heaters at 700 mm elevation

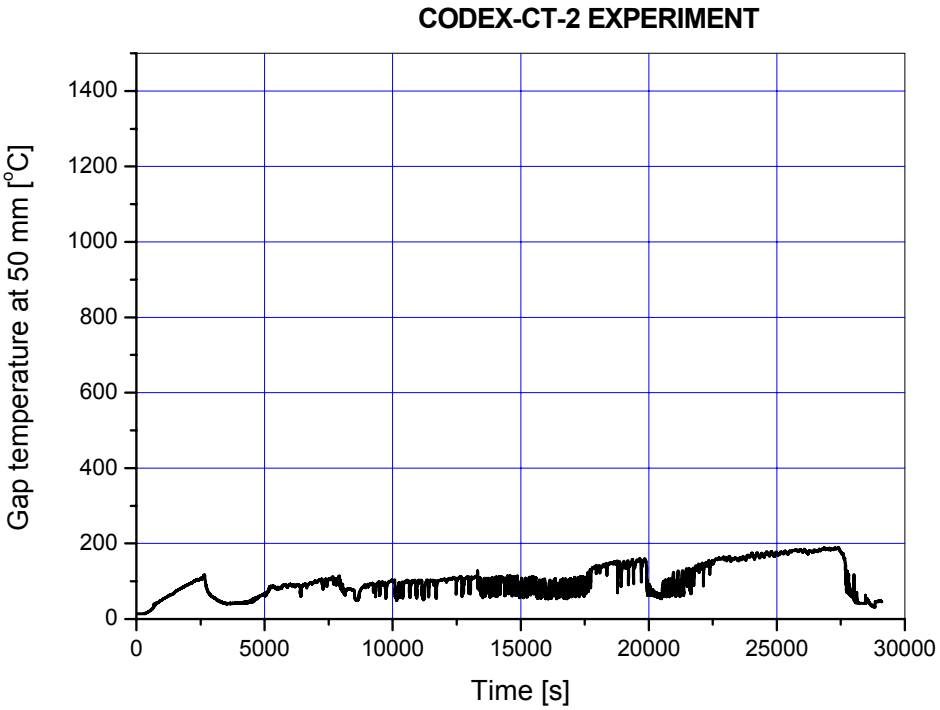

Fig. 30. TG5: Temperature in the gap at 50 mm elevation

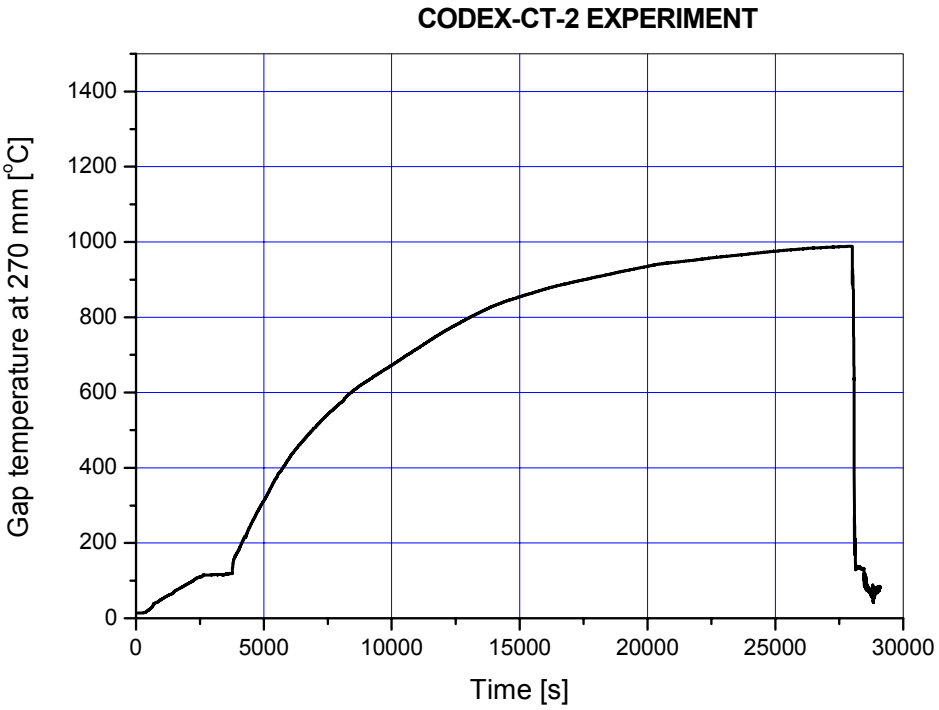

Fig. 31. TG27: Temperature in the gap at 270 mm elevation

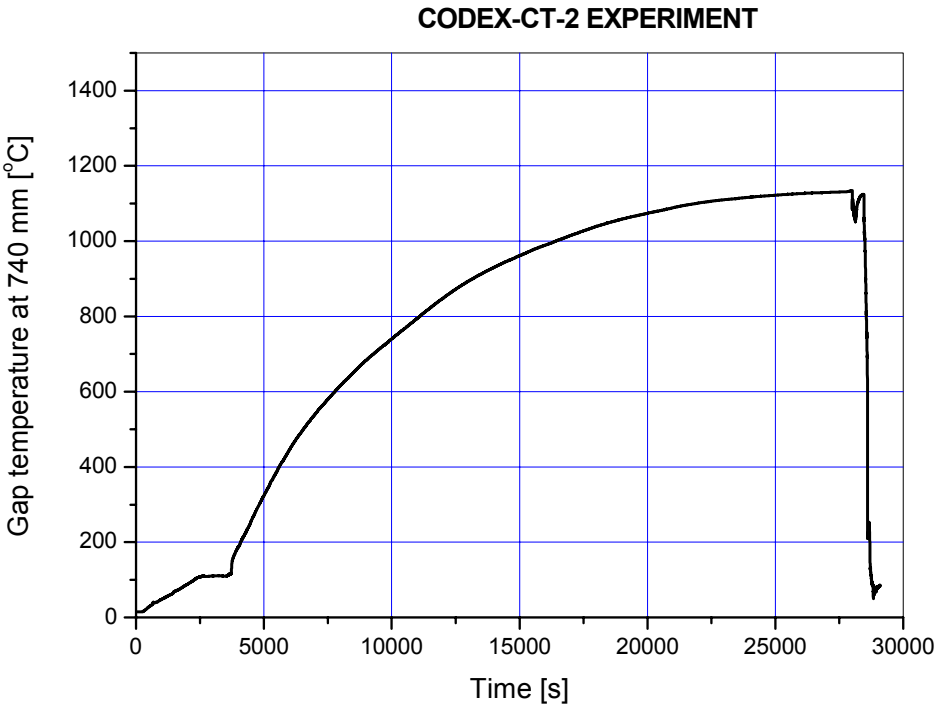

Fig. 32. TG74: Temperature in the gap at 740 mm elevation

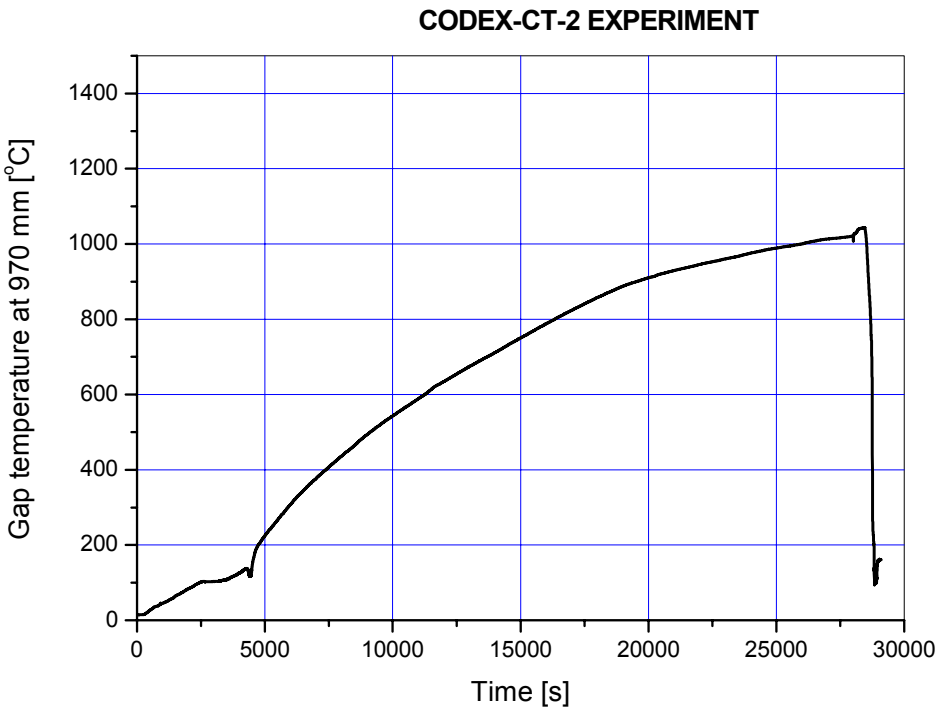

Fig. 33. TG97: Temperature in the gap at 970 mm elevation

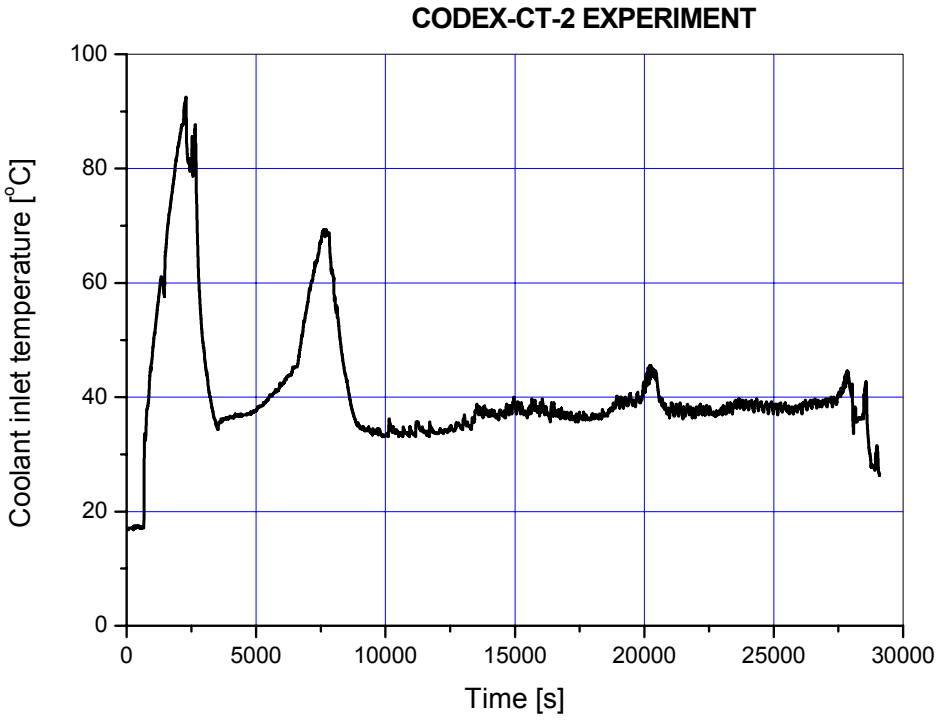

Fig. 34. TCIN: Coolant inlet temperature

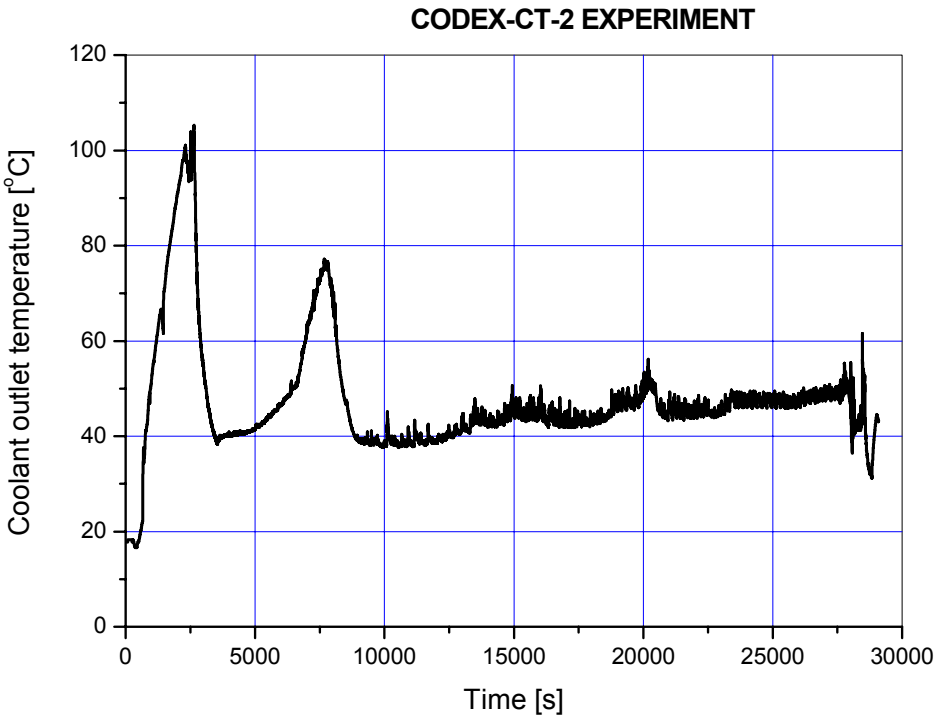

Fig. 35. TCOUT: Coolant outlet temperature

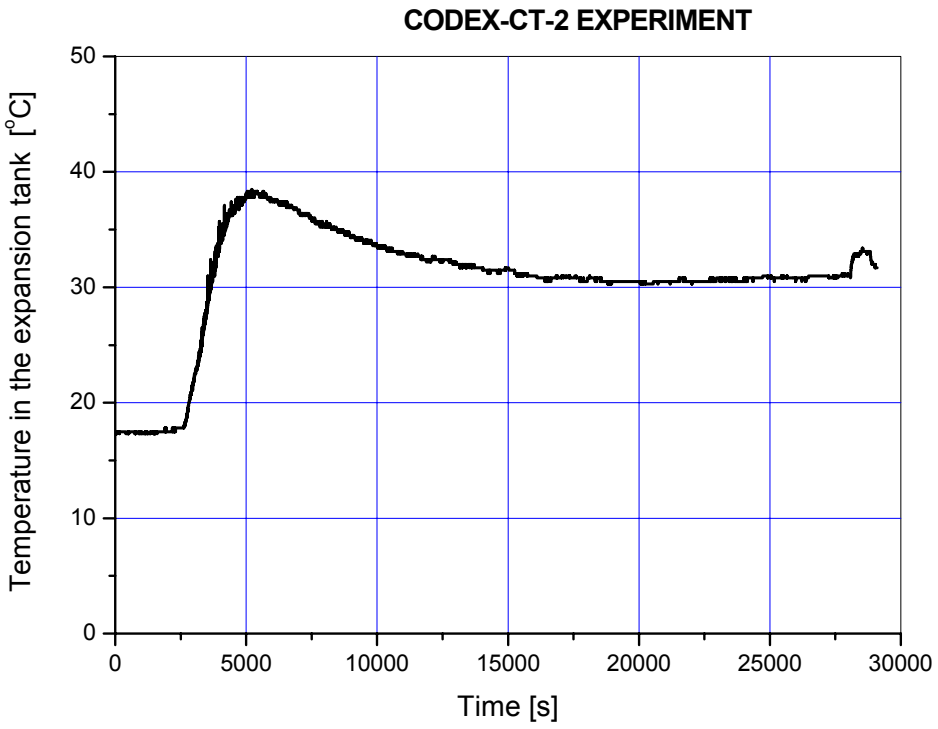

Fig. 36. TXT: Temperature in the expansion tank

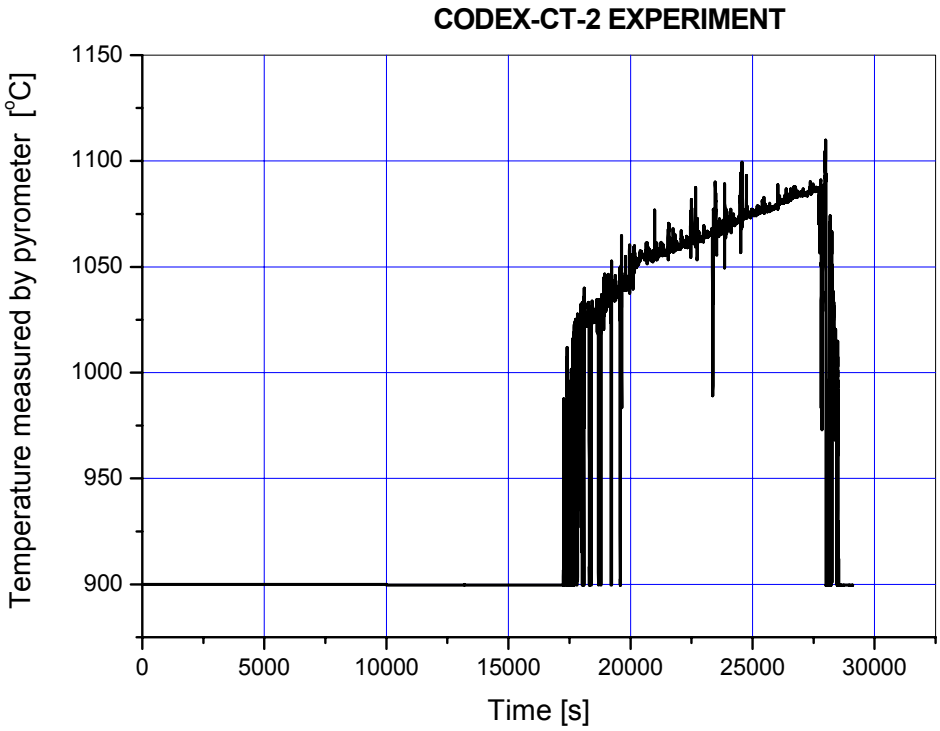

Fig. 37. PYROM: Temperature measured by pyrometer at the top of the bundle

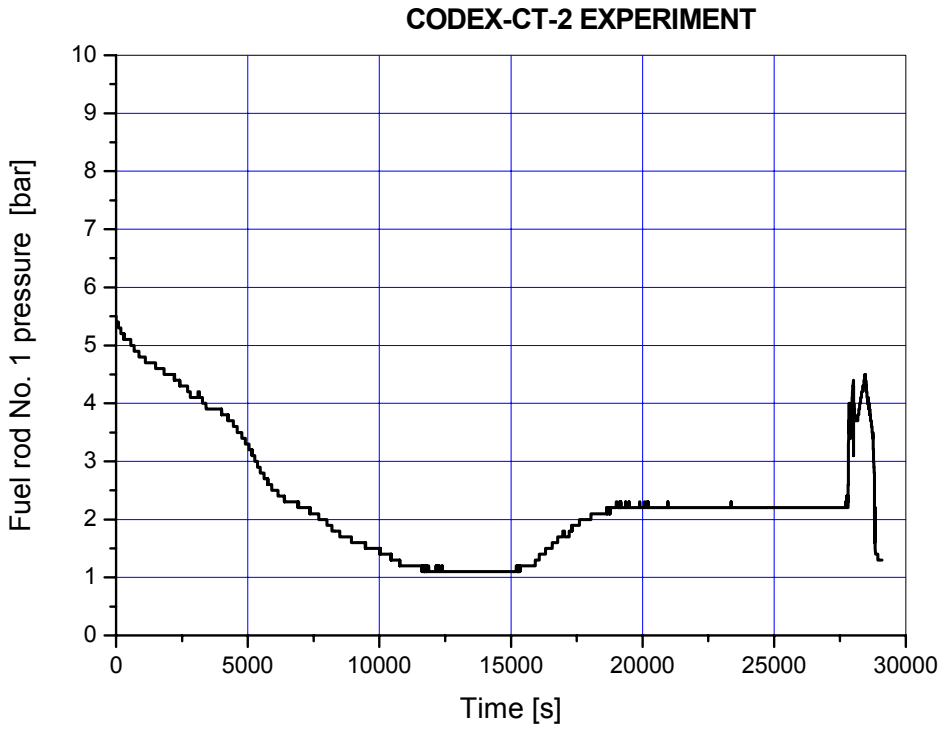

Fig. 38. PFR1: Pressure in fuel rod No. 1

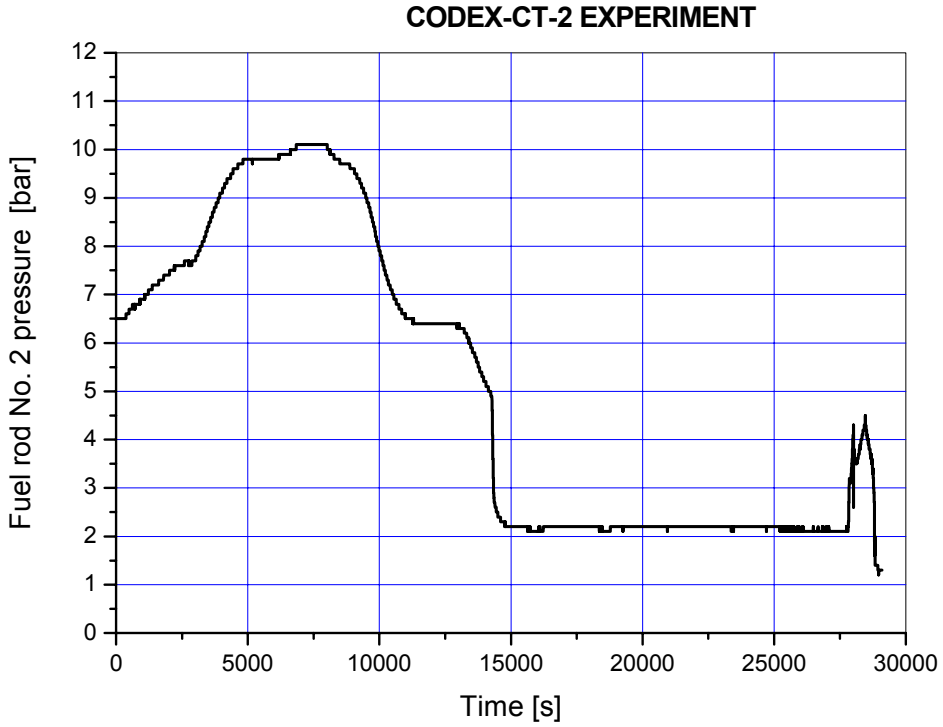

Fig. 39. PFR2: Pressure in fuel rod No. 2

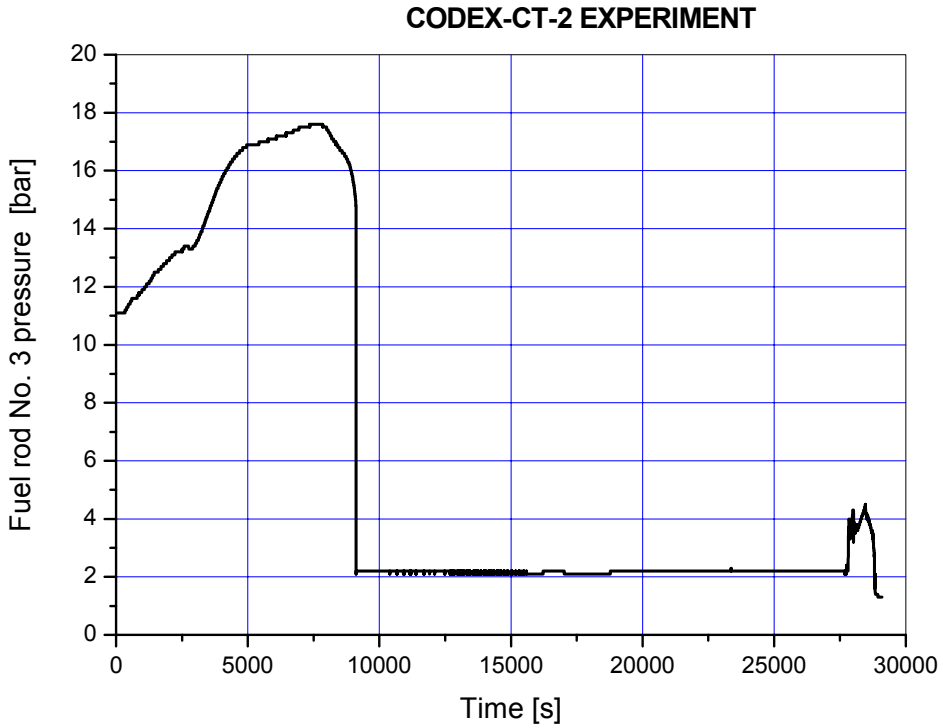

Fig. 40. PFR3: Pressure in fuel rod No. 3

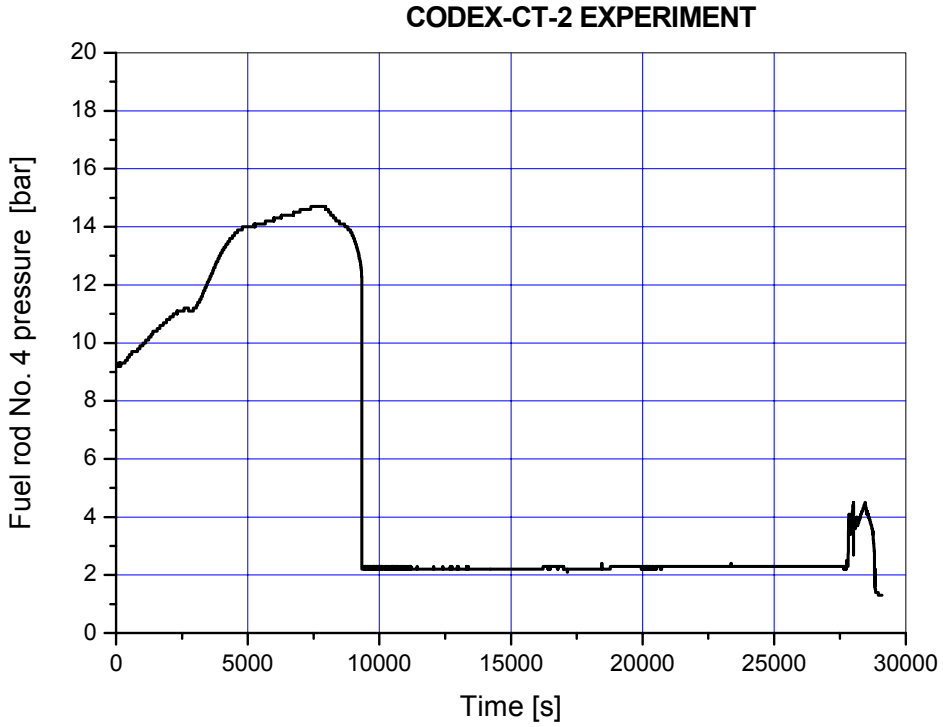

Fig. 41. PFR4: Pressure in fuel rod No. 4

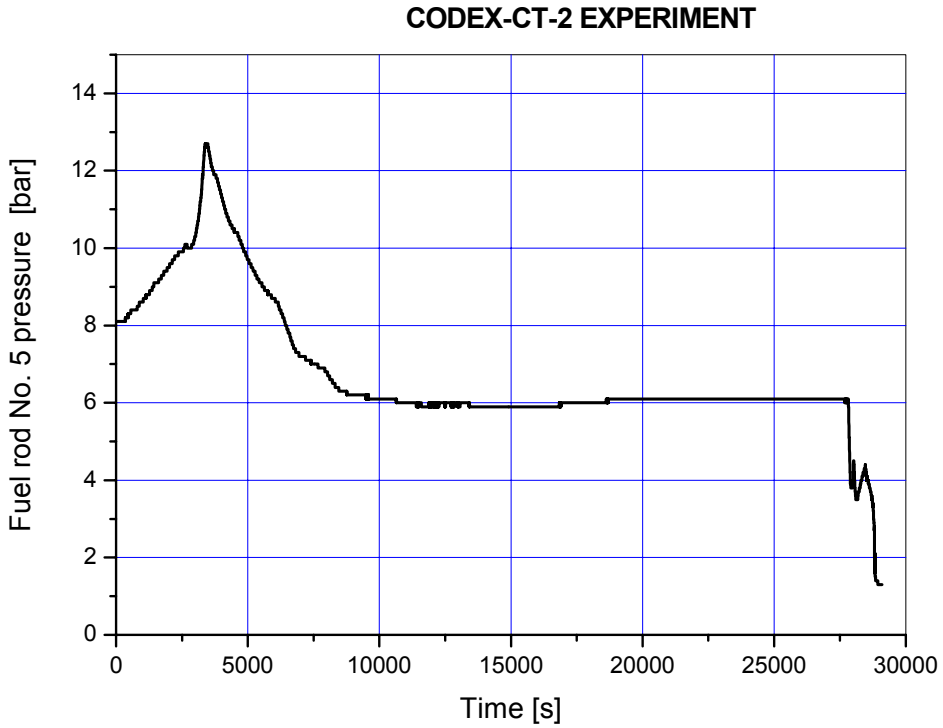

Fig. 42. PFR5: Pressure in fuel rod No. 5

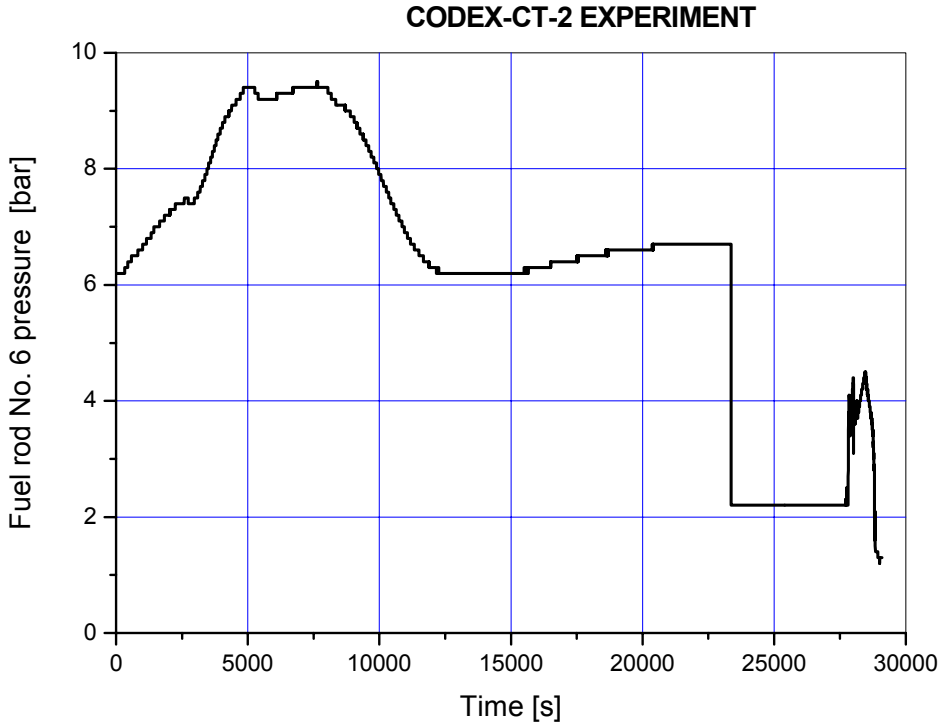

Fig. 43. PFR6: Pressure in fuel rod No. 6

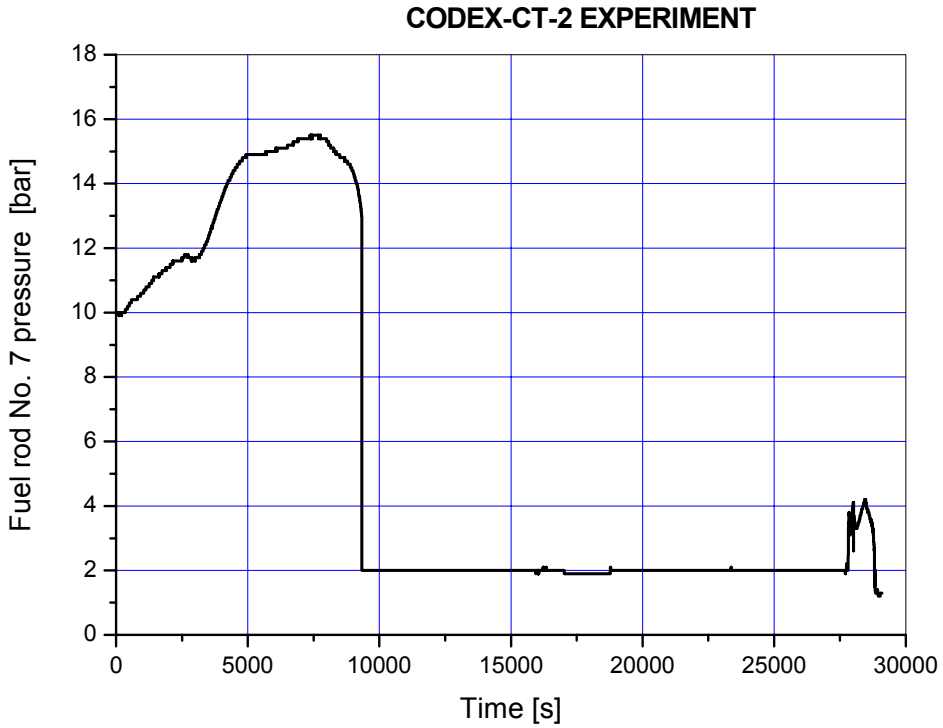

Fig. 44. PFR7: Pressure in fuel rod No. 7

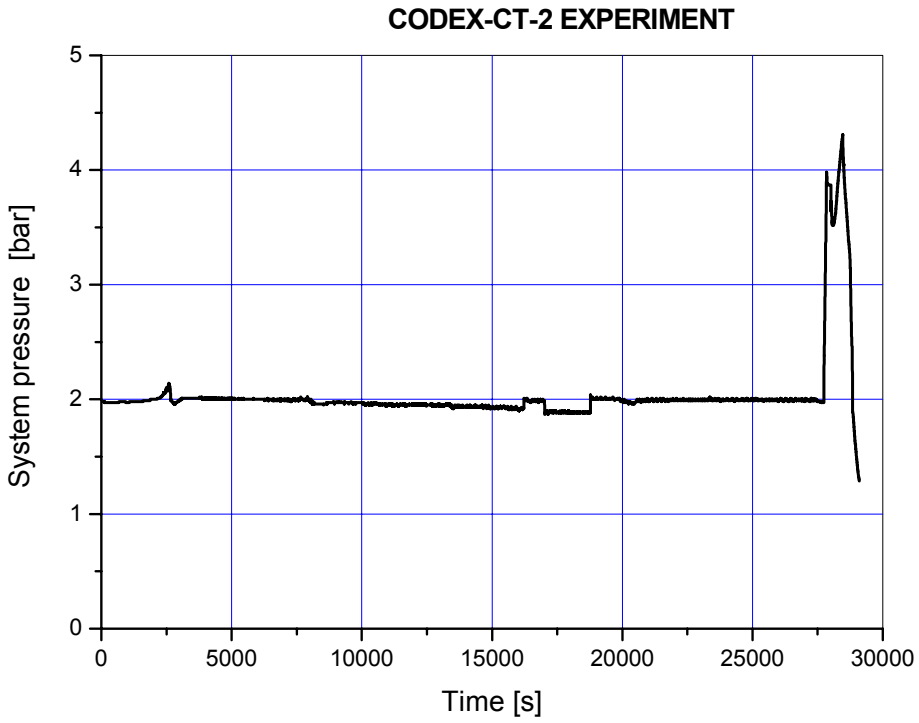

Fig. 45. PSYS: System pressure

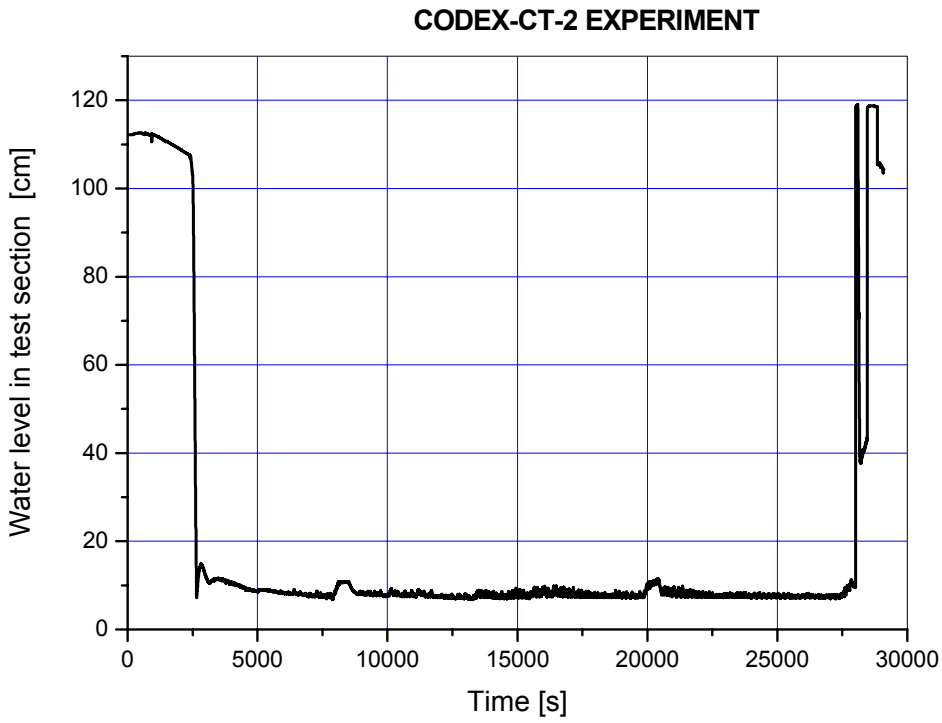

Fig. 46. LTS: Water level in the test section

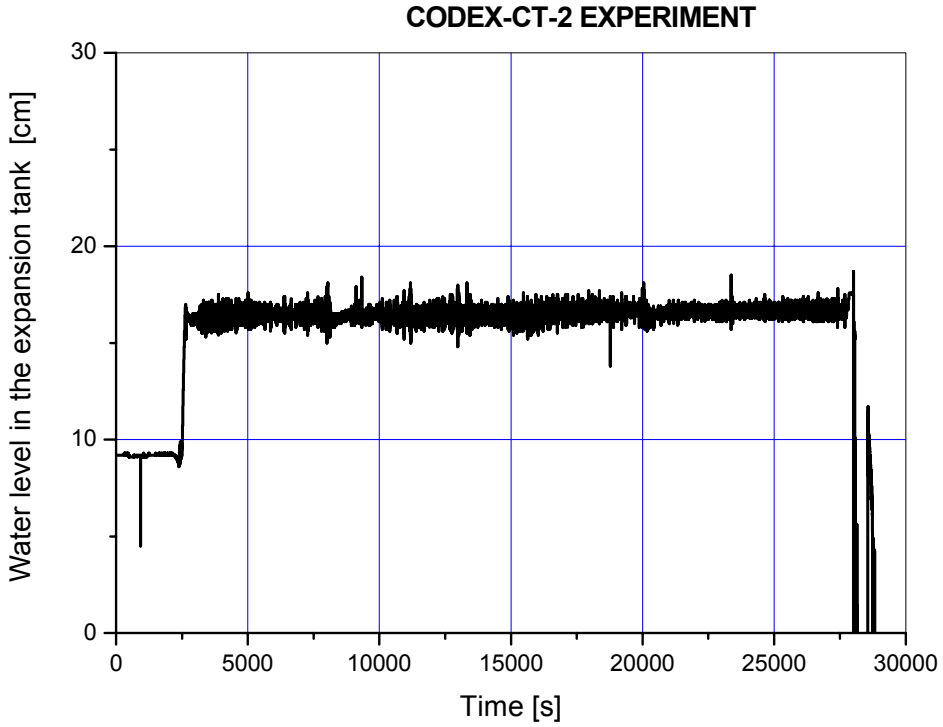

Fig. 47. LXT: Water level in the expansion tank

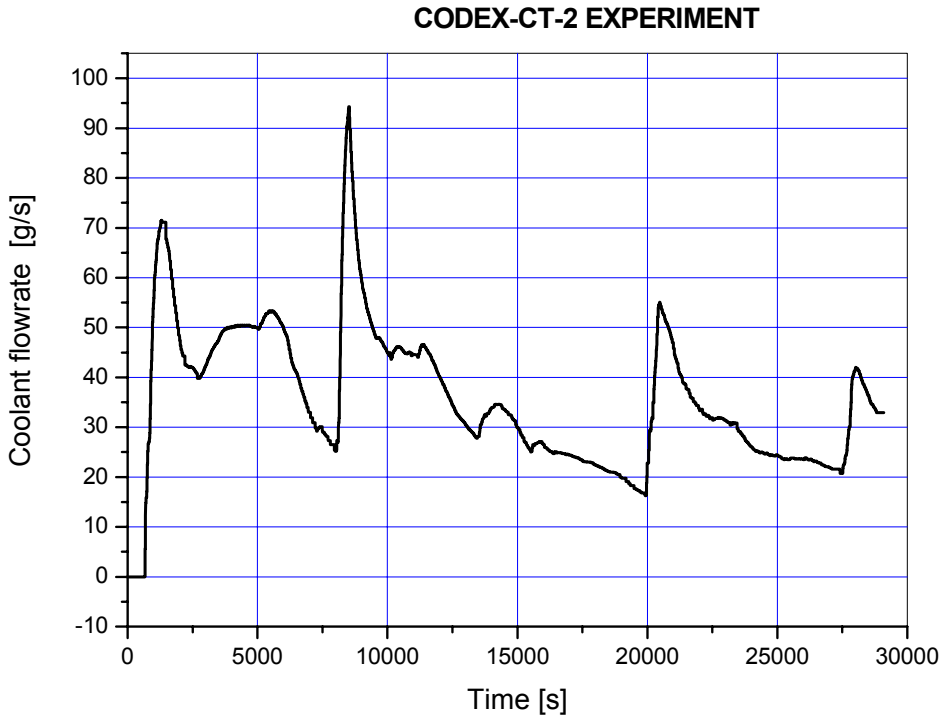

Fig. 48. FLOW: Coolant flowrate

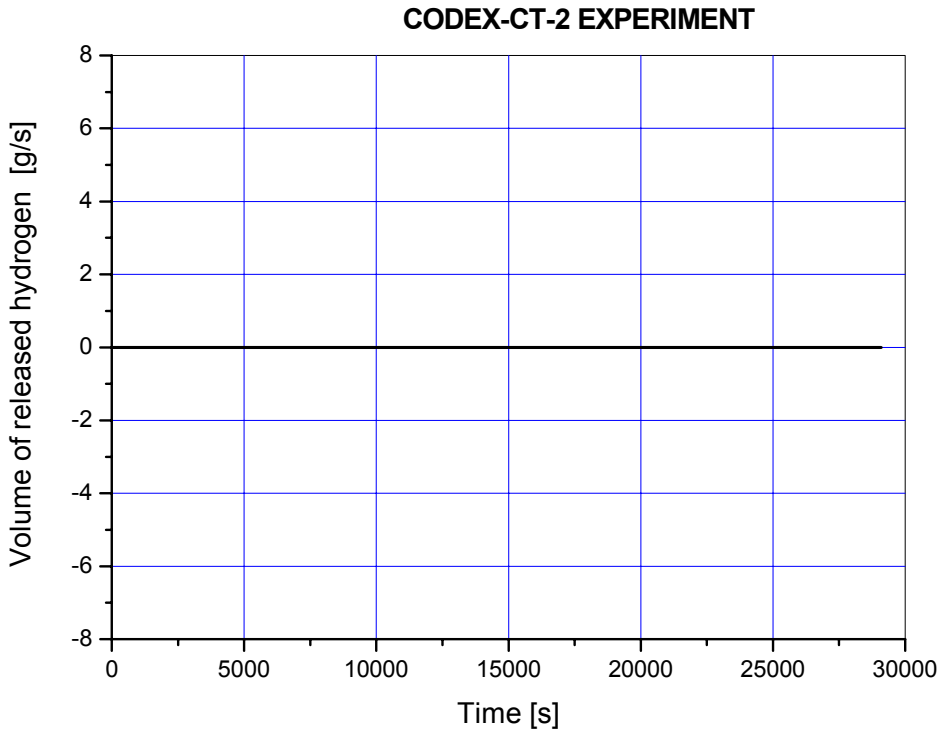

Fig. 49. H2: Volume of hydrogen released from the cleaning tank model

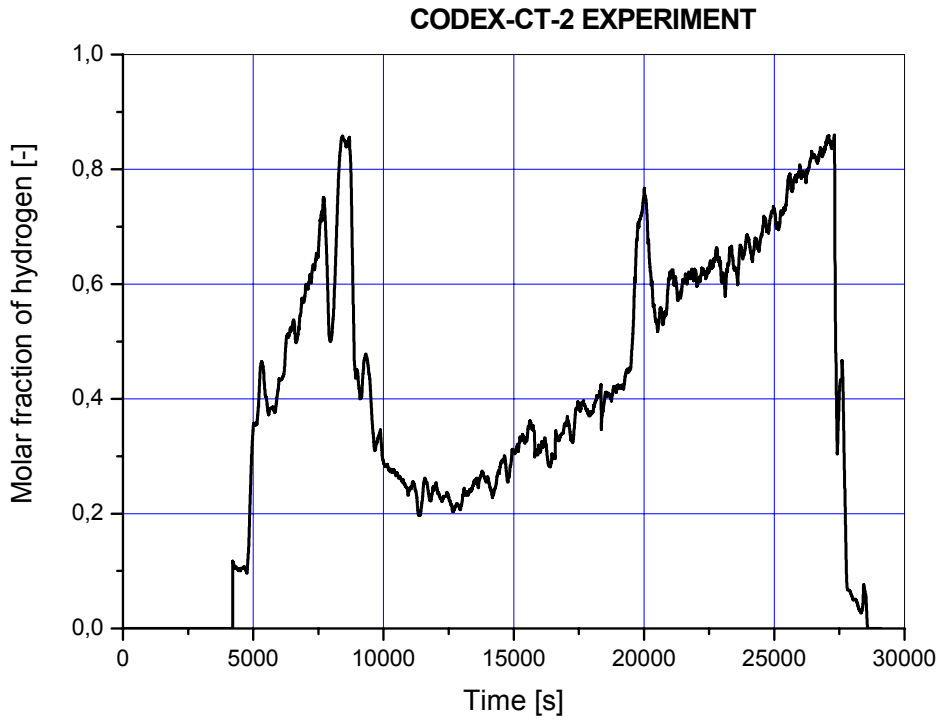

Fig. 50. TCD1: Hydrogen concentration above the bundle

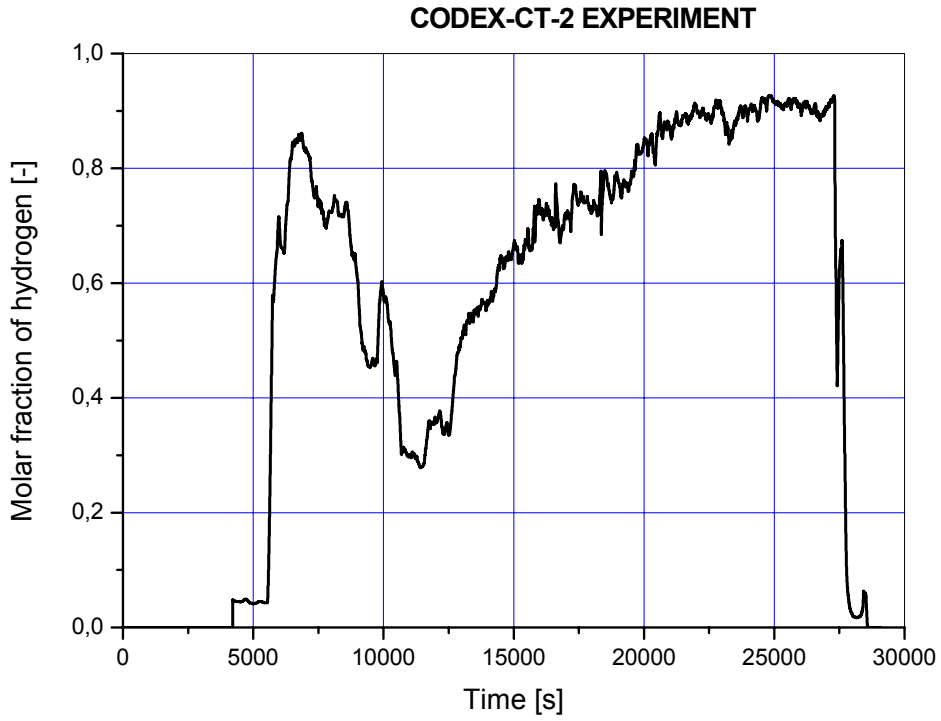

Fig. 51. TCD2: Hydrogen concentration between the shroud and heaters at 760 mm elevation

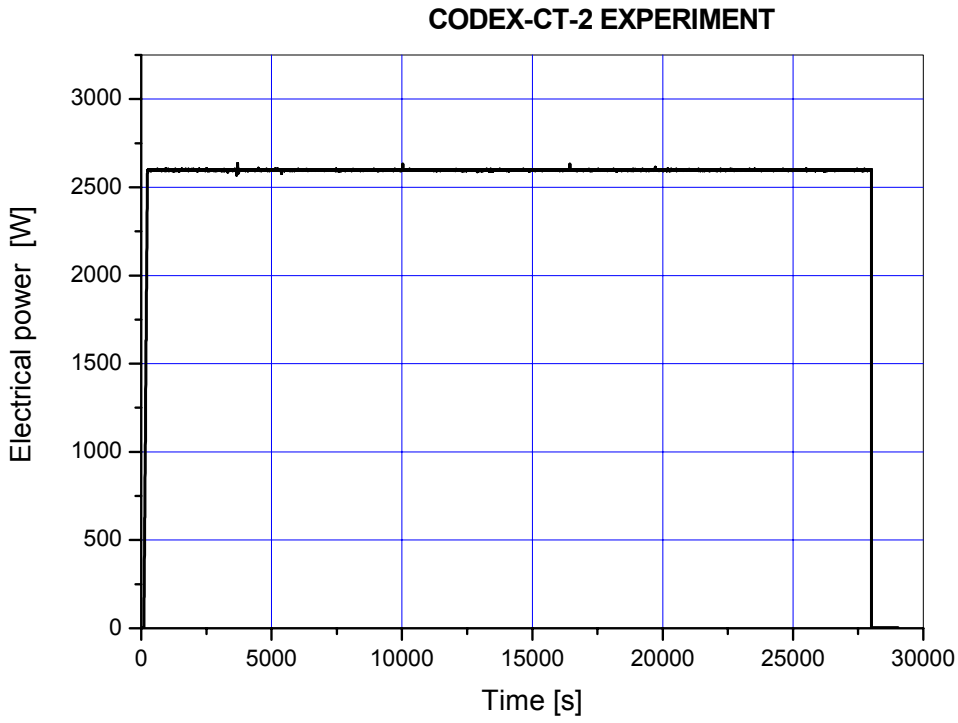

Fig. 52. POWER: Electrical power

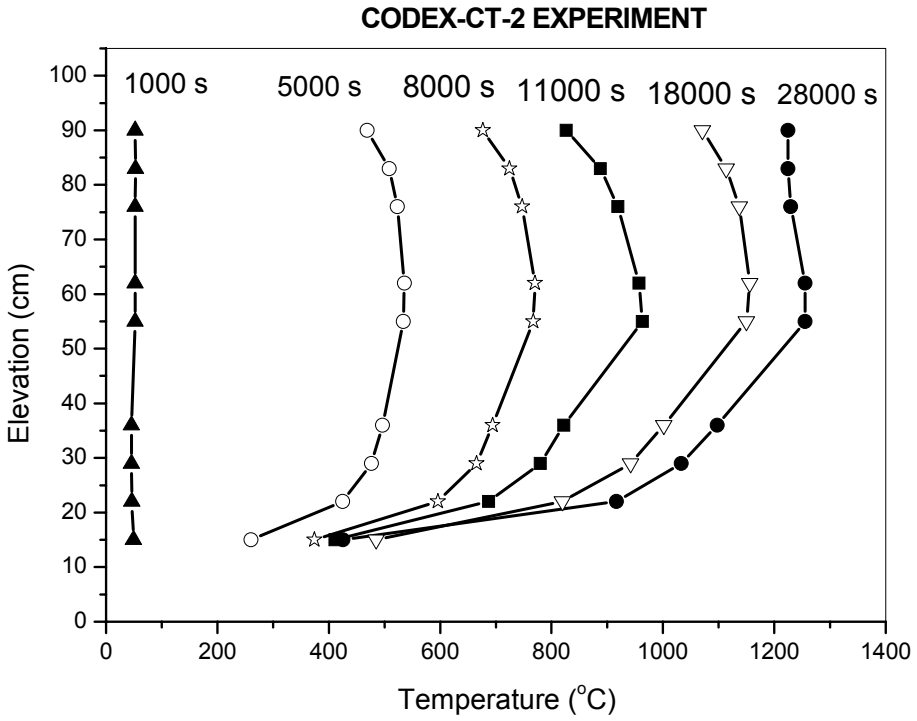

Fig. 53. Change of temperature profile during the CODEX-CT-2 test

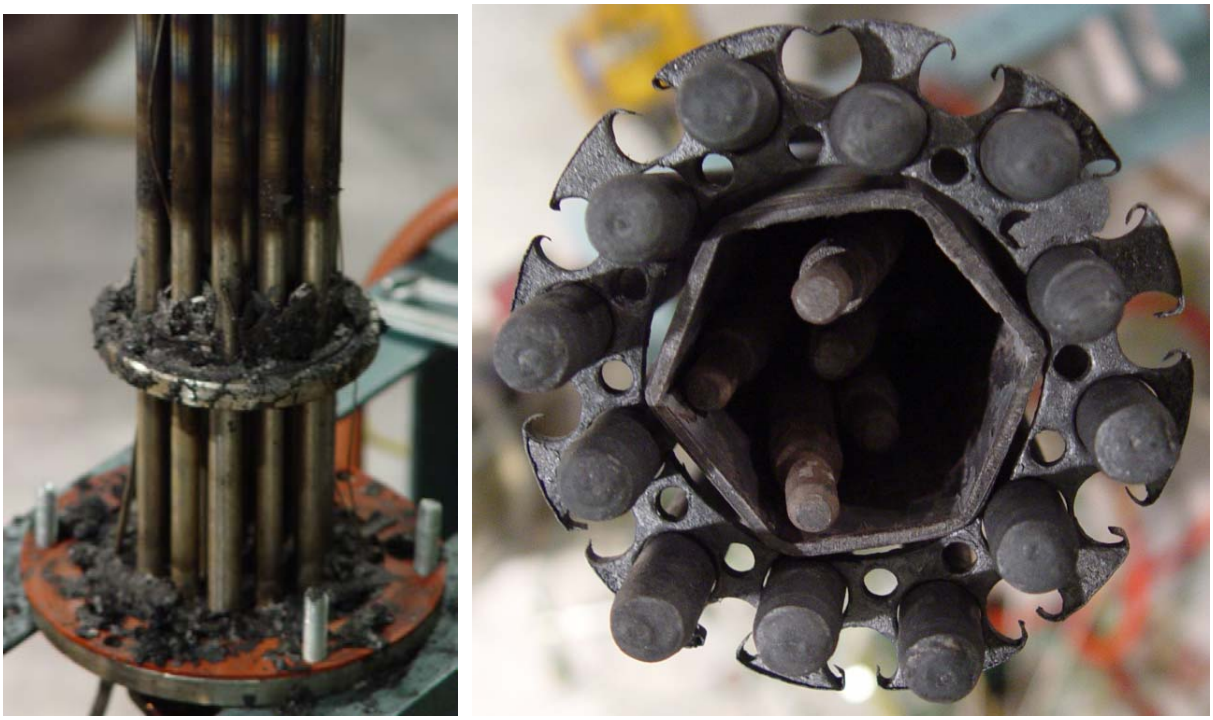

Fig. 54. View of the CODEX-CT-2 test section after the experiment
(The bottom part is shown in the left picture and
view from the top is in the right picture.)

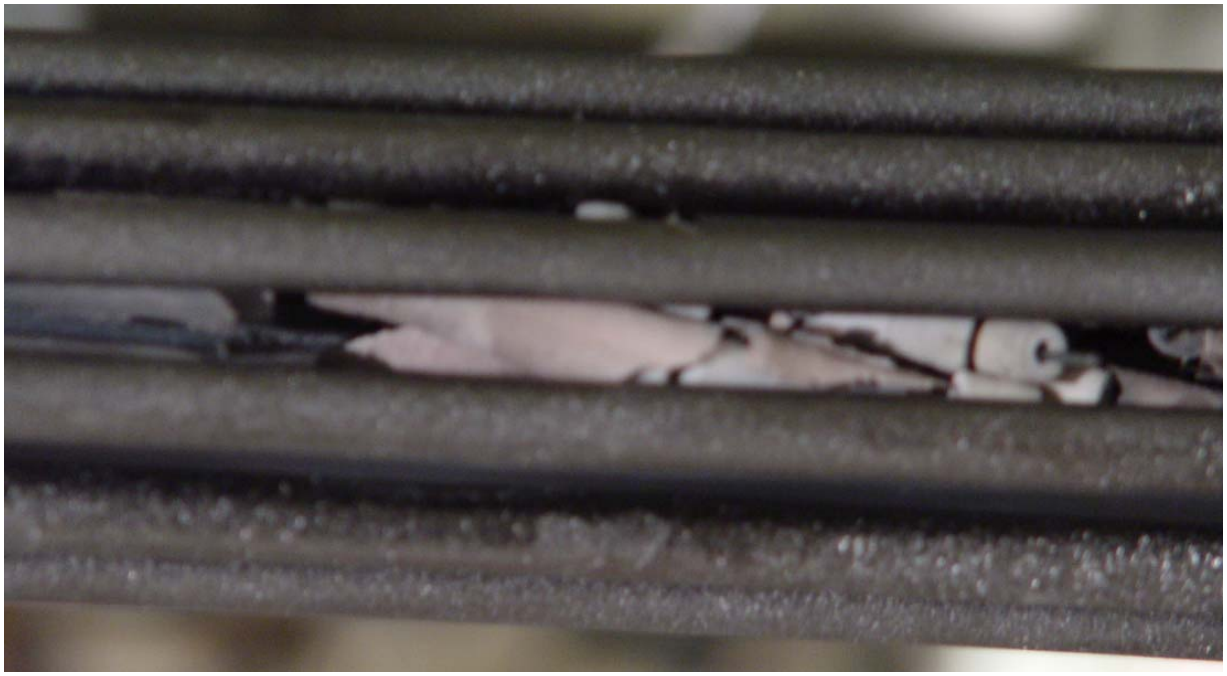

Fig. 55. Broken fragments of the CODEX-CT-2 bundle between the heater rods

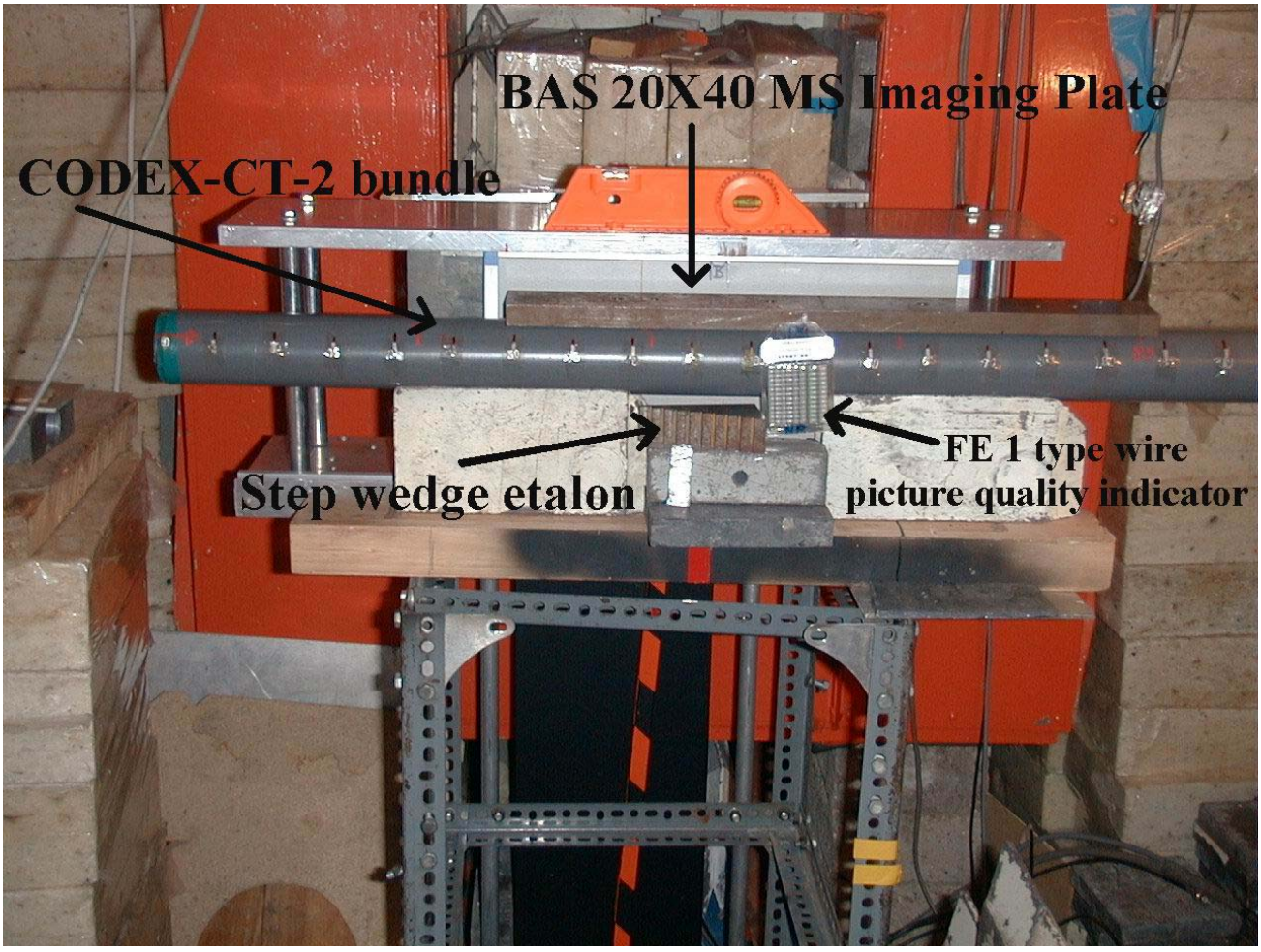

Fig. 56. X-Ray radiographic examination of the CODEX-CT-2 bundle

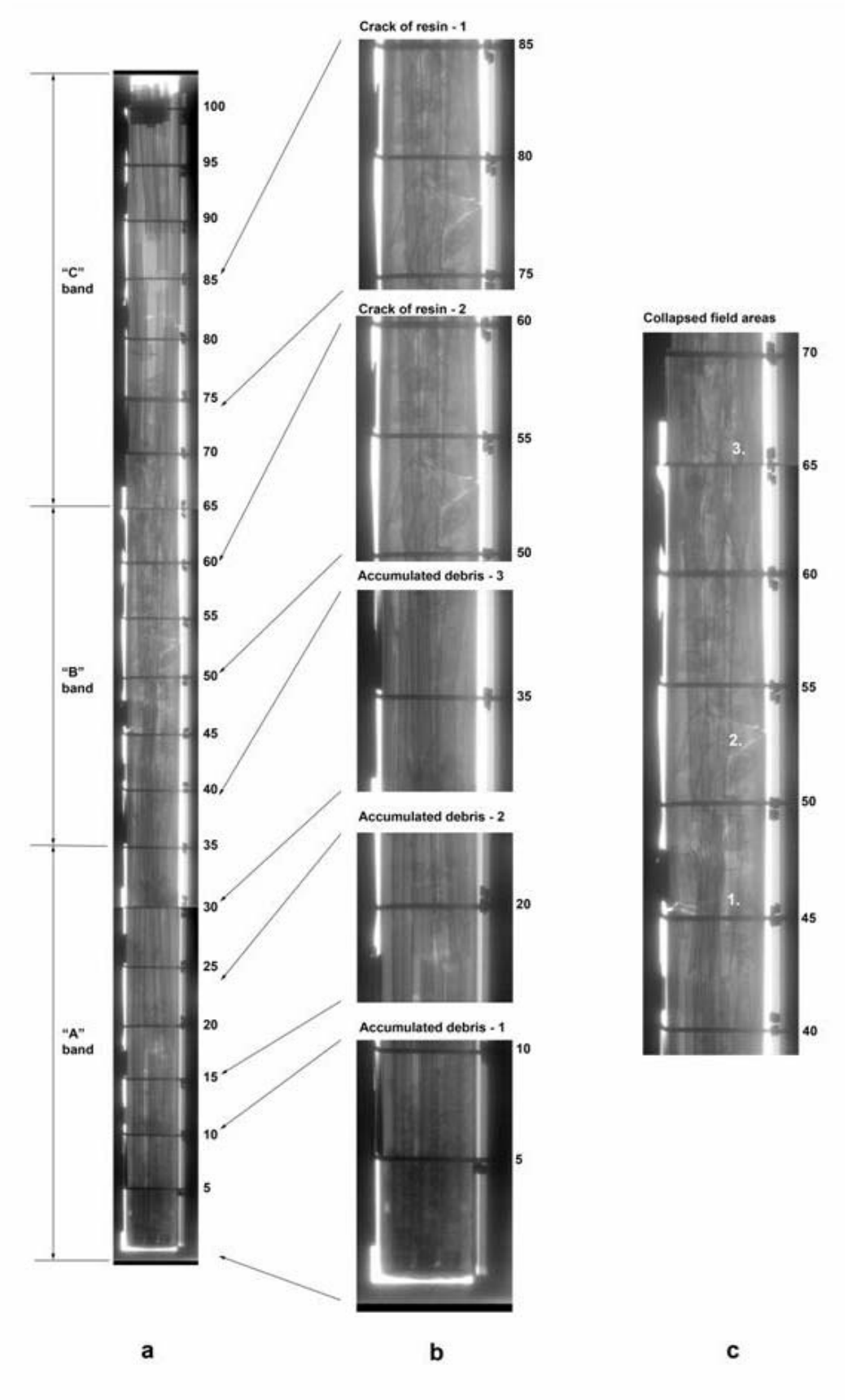

Fig. 57. X-ray radiography of the CODEX-CT-2 bundle

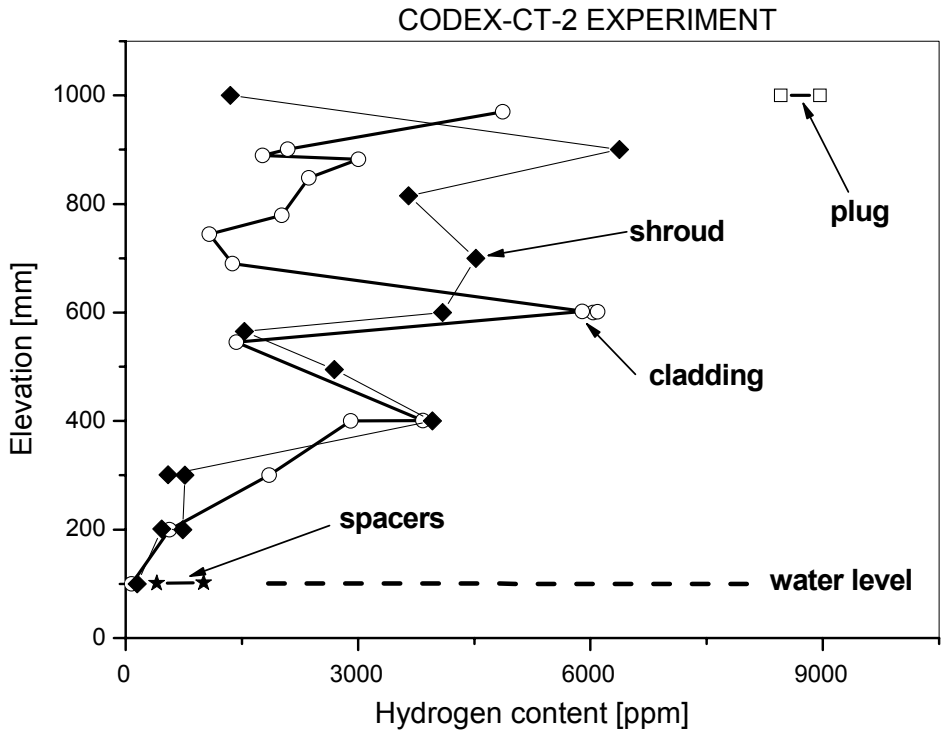

Fig. 58. Hydrogen content in the Zr components of CODEX-CT-2 bundle

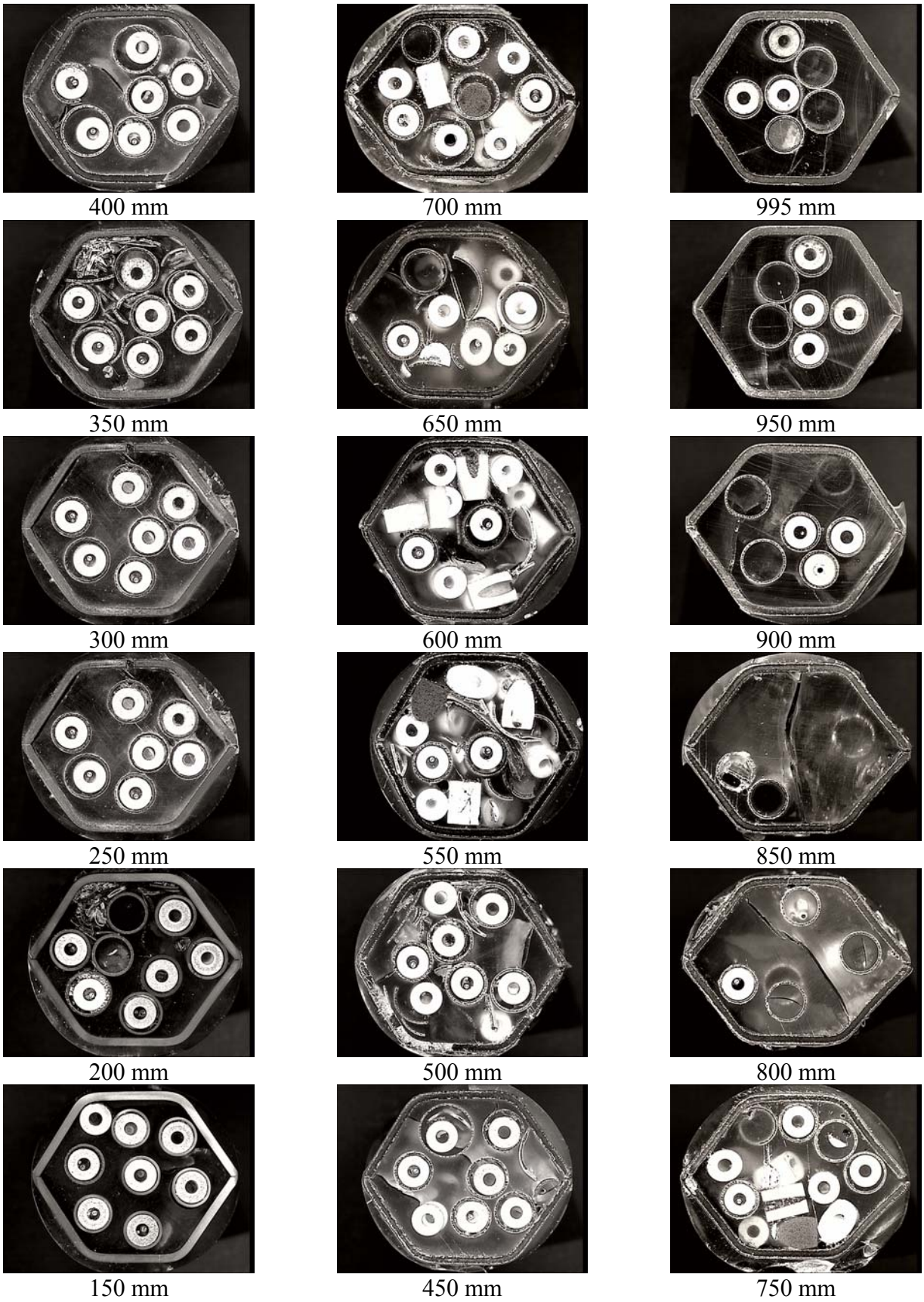

Fig. 59. Cross sections of the CODEX-CT-2 bundle

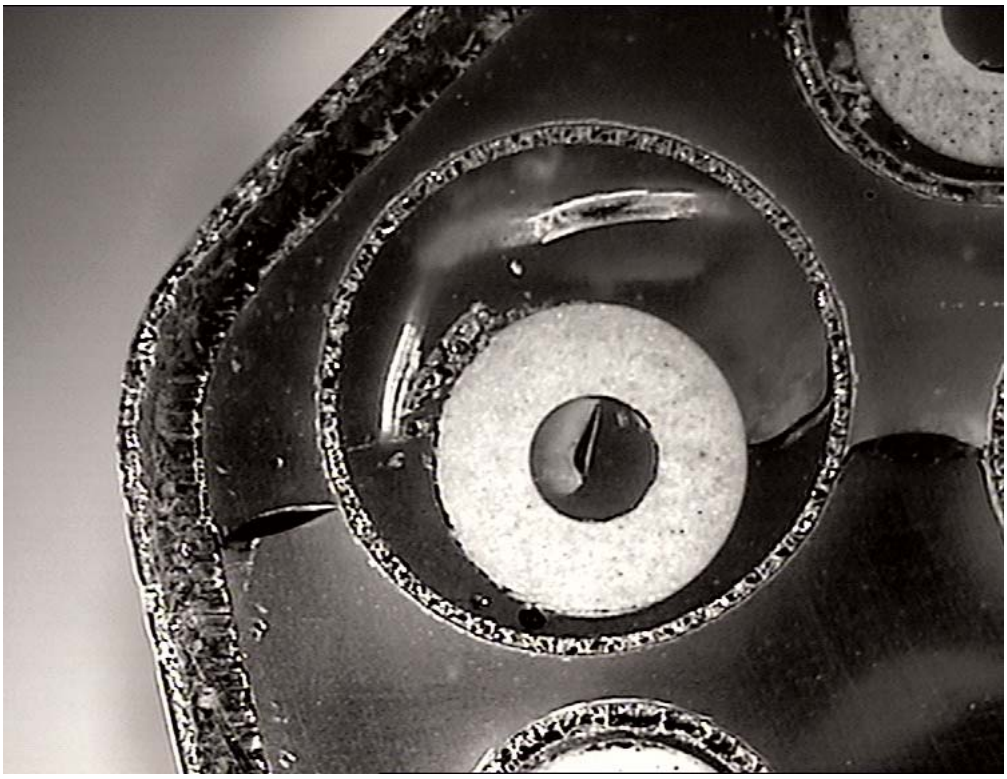

Fig. 60. Rod No. 3 at 450 mm elevation showing large ballooned cladding area

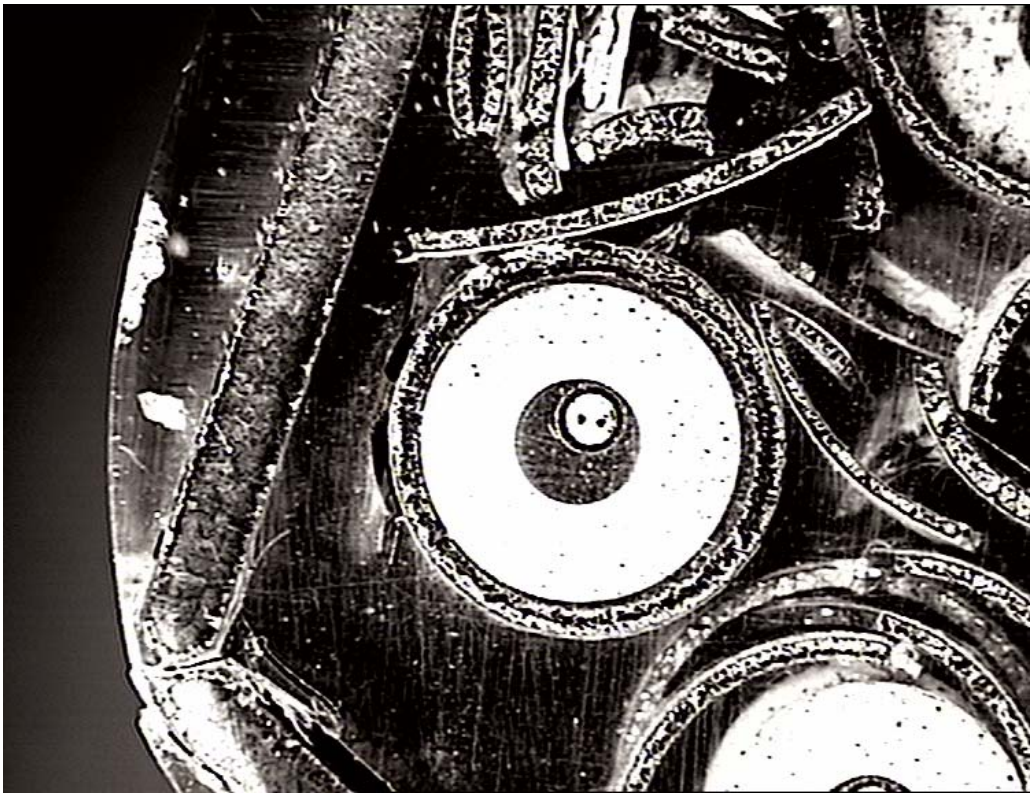

Fig. 61. Accumulated debris of Zr cladding around rod No. 4 at 350 mm elevation

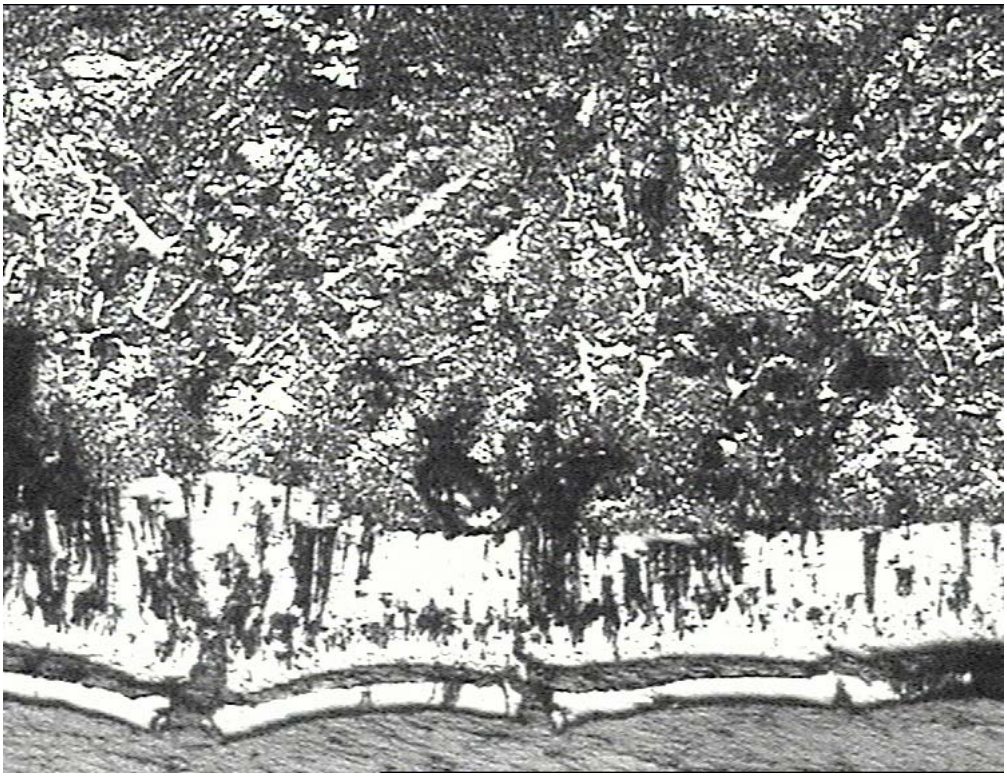

Fig. 62. Spalling oxide scale on rod No. 1 at 350 mm elevation

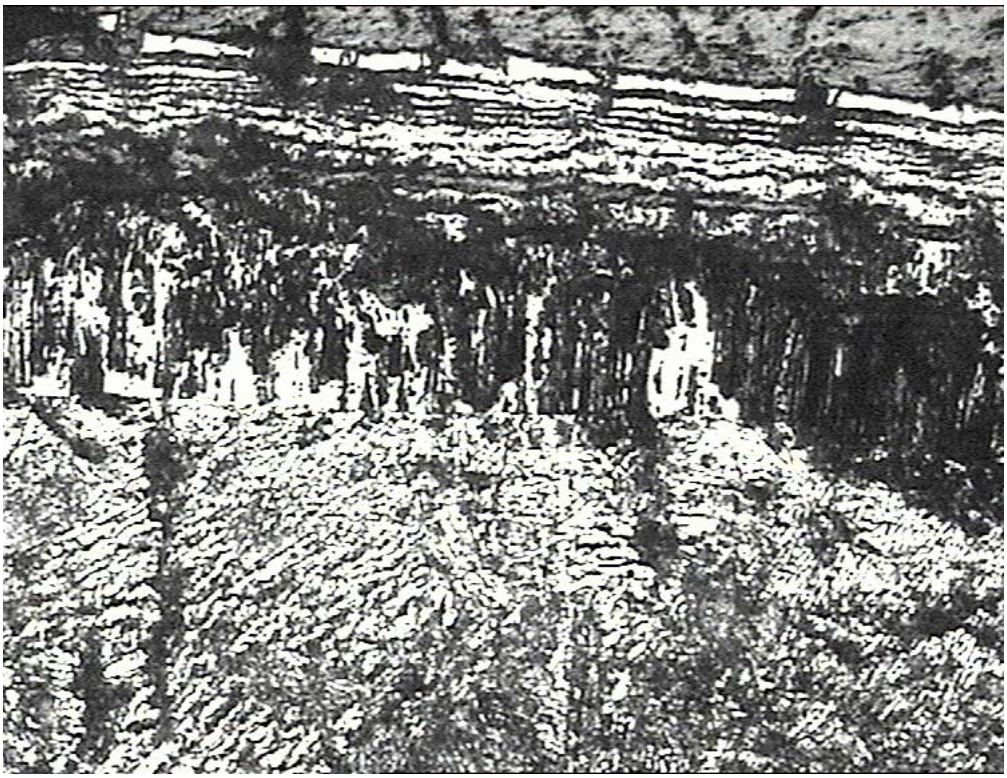

Fig. 63. Layered oxide scale on rod No. 7 at 350 mm elevation

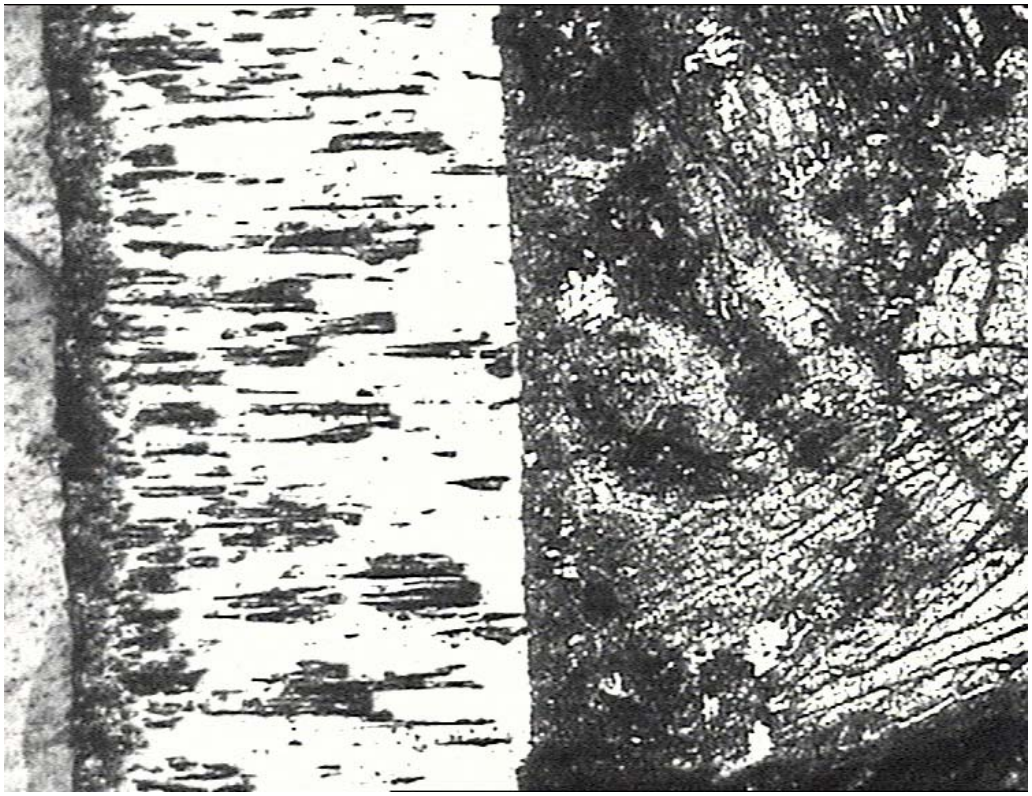

Fig. 64. External oxide scale on the shroud at 750 mm elevation

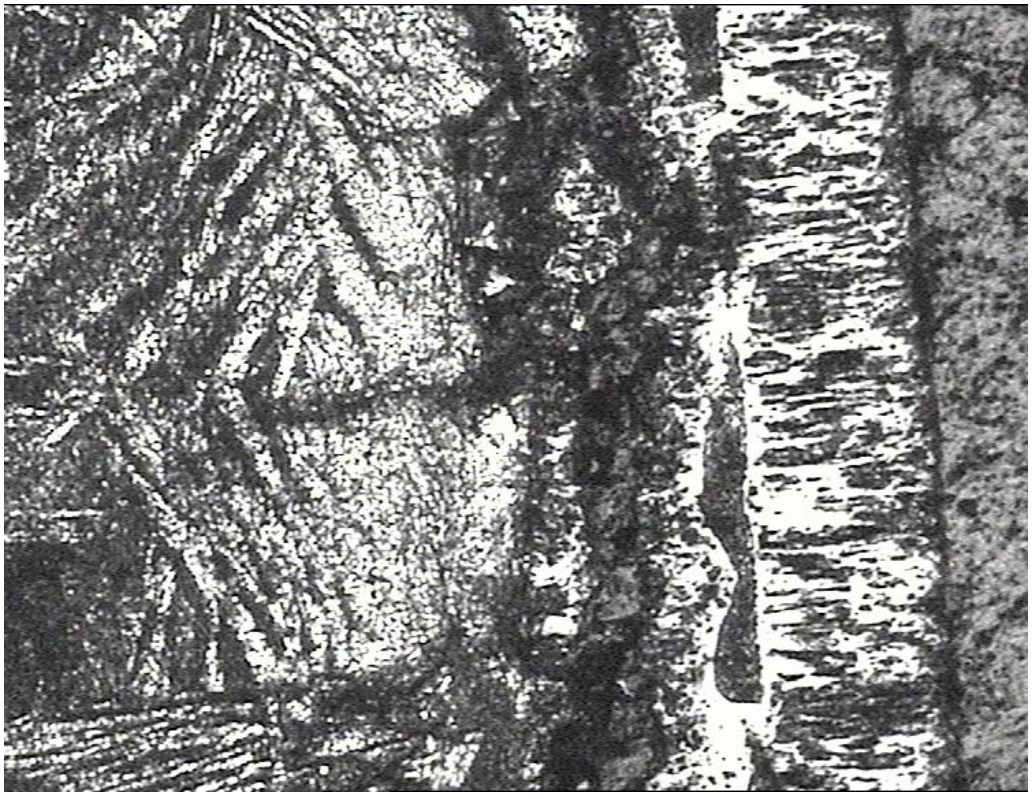

Fig. 65. Internal oxide scale on the shroud at 750 mm elevation

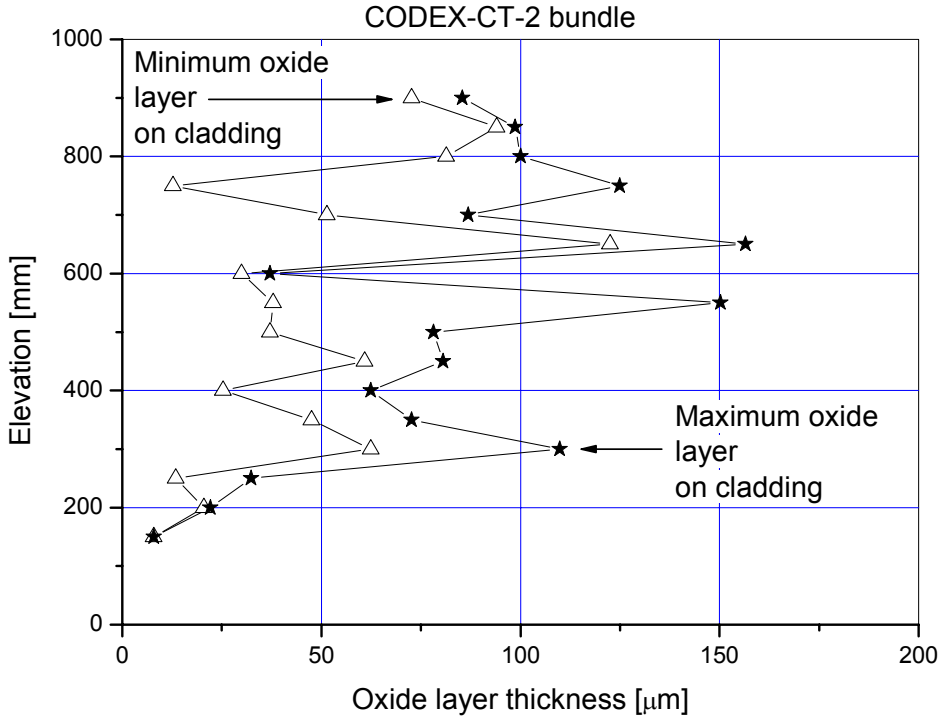

Fig. 66. External oxide layer thickness on cladding tubes

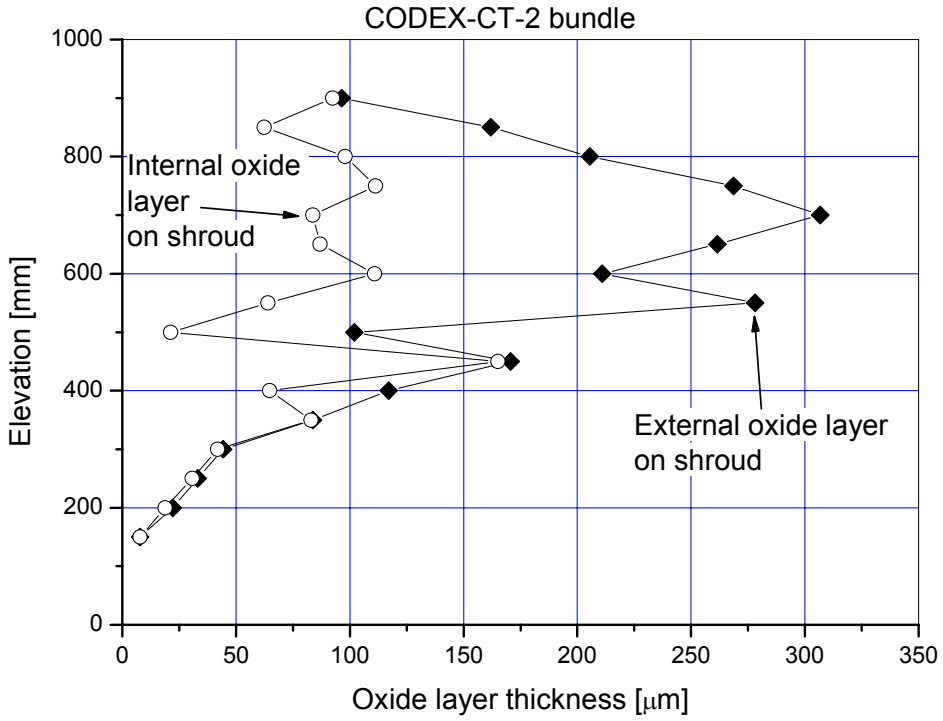

Fig. 67. Oxide layer thickness on shroud

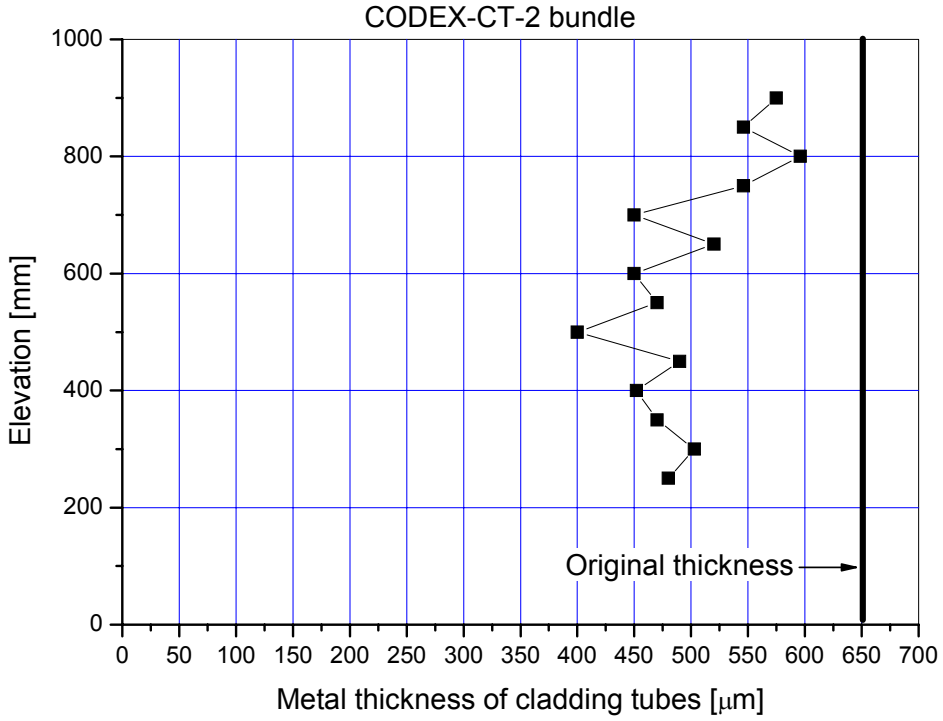

Fig. 68. Remaining metal layer thickness in the cladding tubes

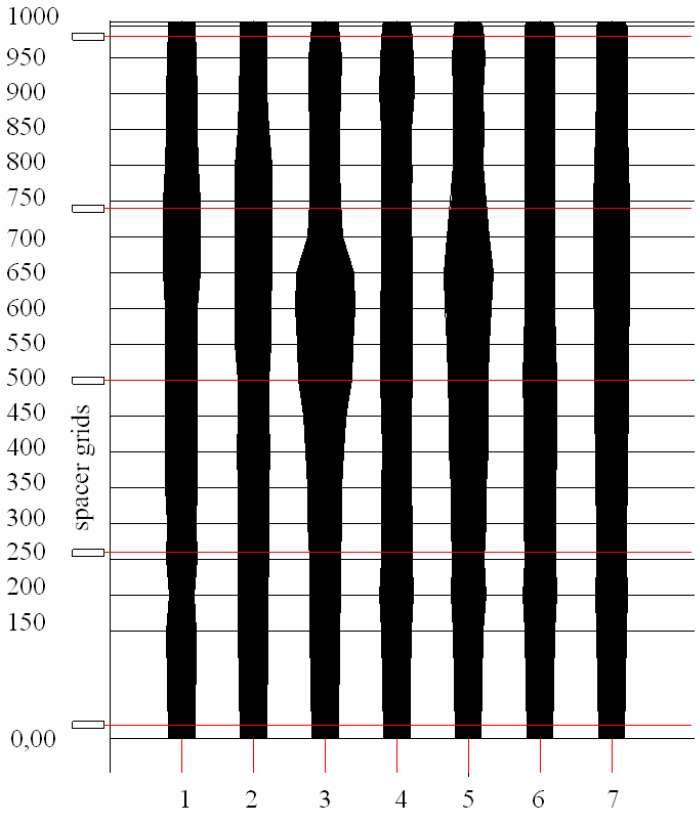

Fig. 69. Ballooning of fuel rods (based of metallographic examination)

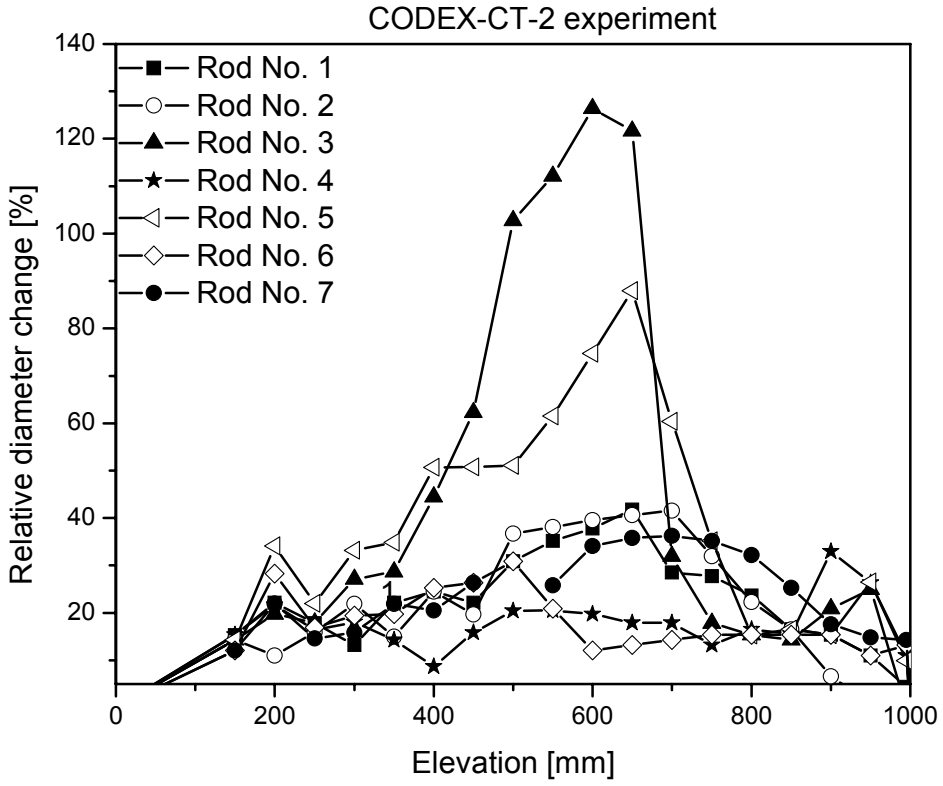

Fig. 70. Relative diameter change profile of fuel rods

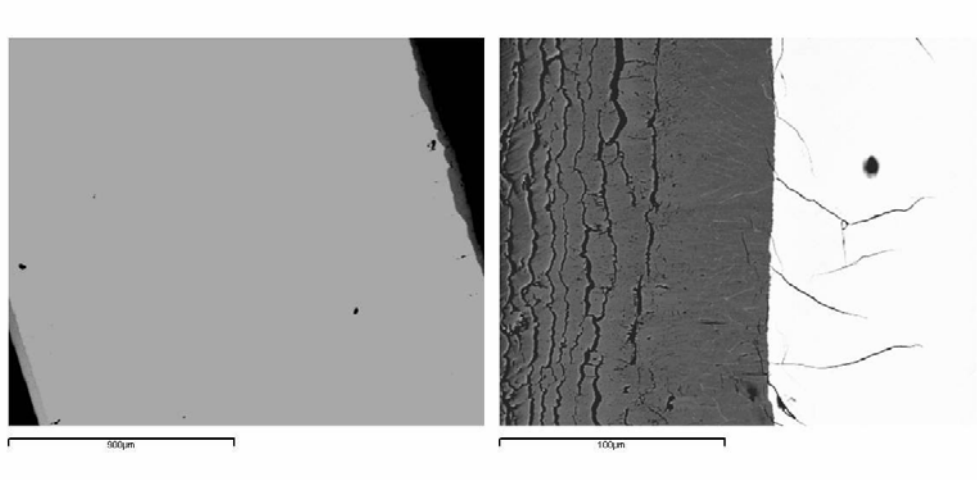

Fig. 71. BEI images for the shroud and the tube taken from sample CT-2-100

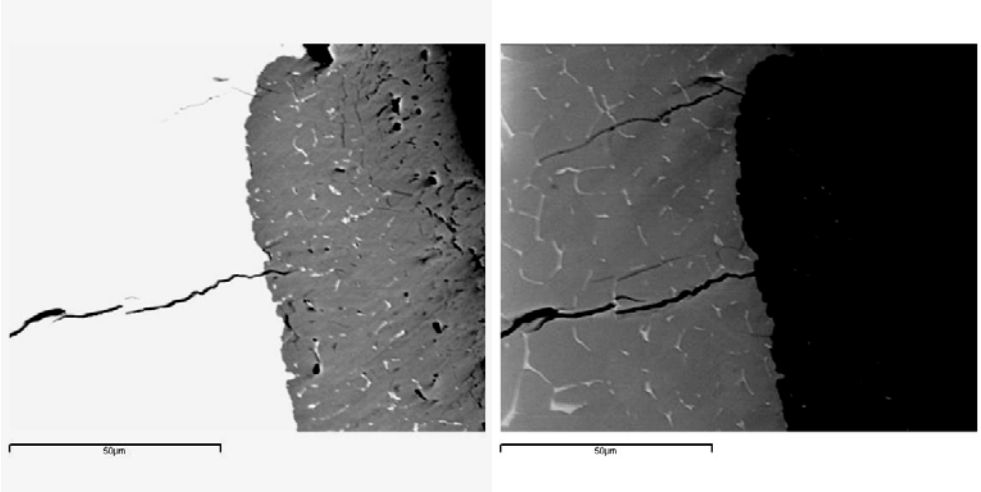

Fig. 72. BEI image pair of the oxide and metallic part of the shroud in sample CT-2-100

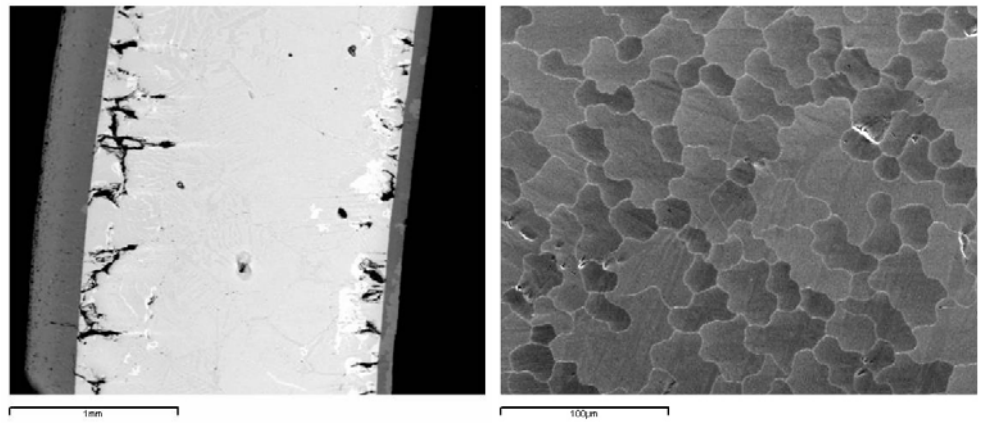

Fig. 73. SEM images from the shroud of sample CT-2- 60

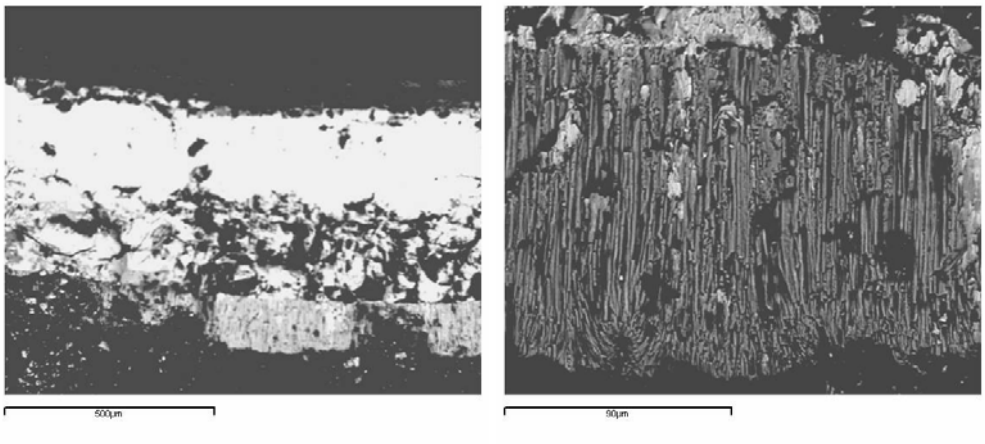

Fig. 74. SEM images from the cladding of sample CT-2- 60

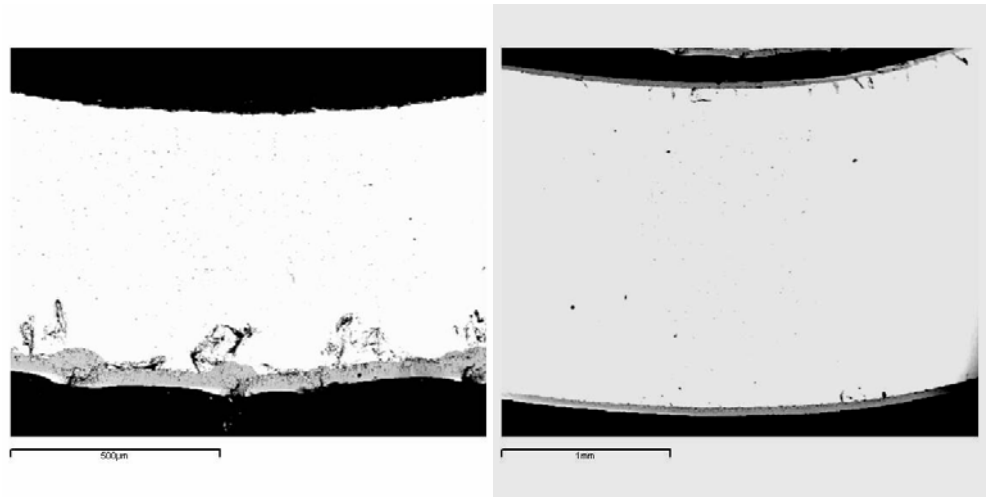

Fig. 75. BEI images of the cladding and the shroud taken from sample CT-2-30

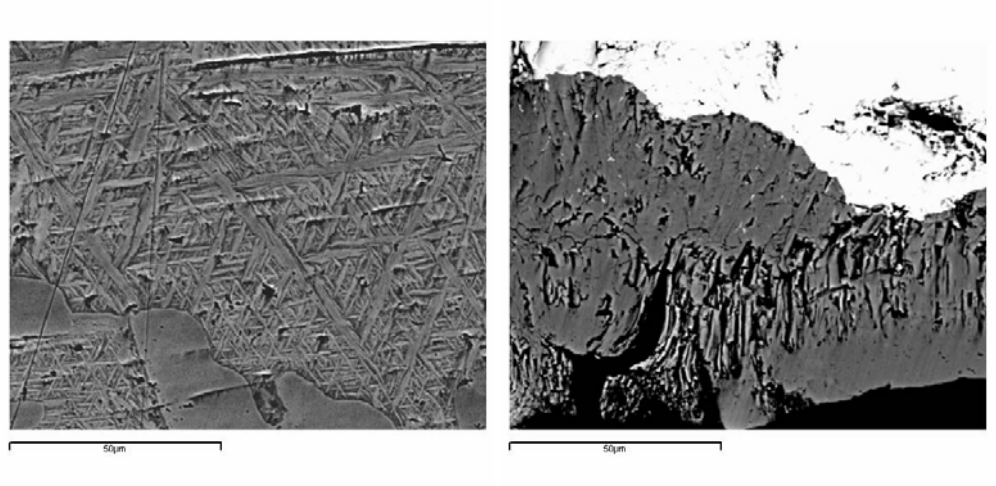

Fig. 76. BEI images taken from the metallic part and the oxide of the cladding in sample CT-2-30

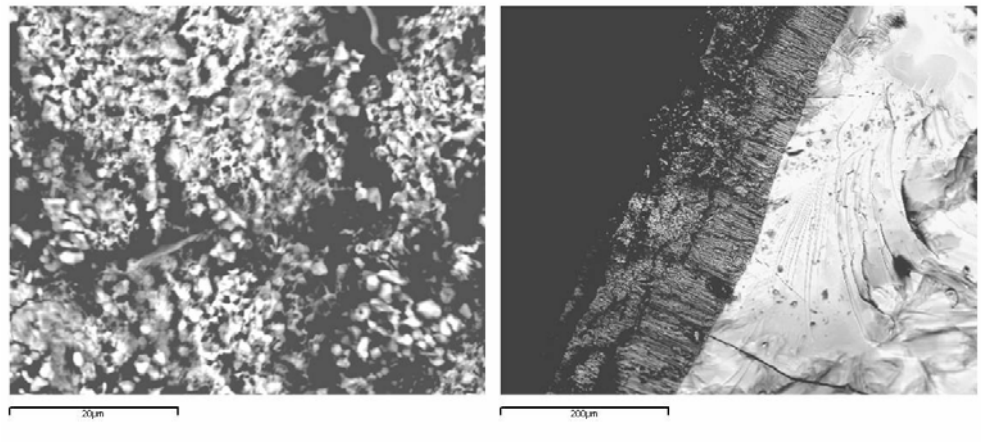

96.5 cm elevation 90.1 cm elevation

Fig. 77. Typical SEM images for samples taken from the top of the bundle

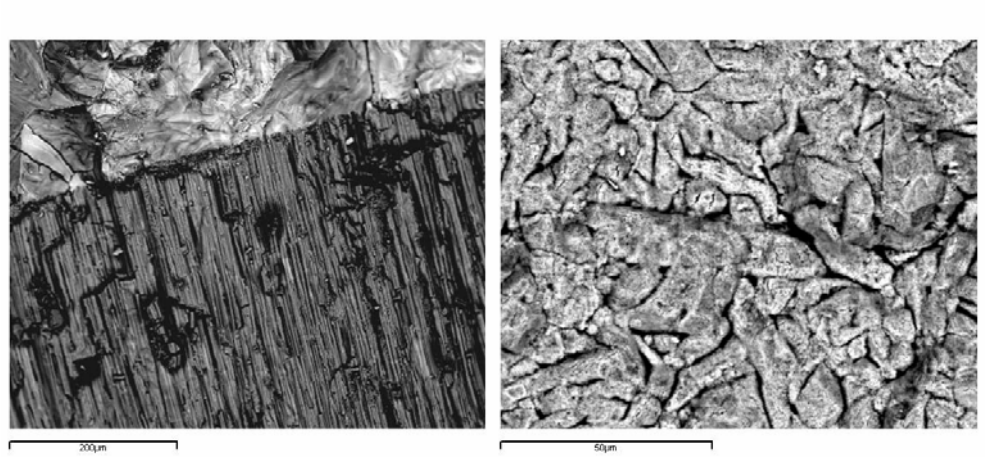

56.5 cm elevation 54.5 cm elevation

Fig. 78. Typical SEM images for samples taken from the middle section of the bundle